

Report No. CG-D-01-95

Wide Area DGPS Design Issues Study

Tysen Mueller
Peter Loomis
Len Sheynblat

TAU Corporation
485 Alberto Way
Los Gatos, CA 95032-5405



FINAL REPORT
JANUARY 1995

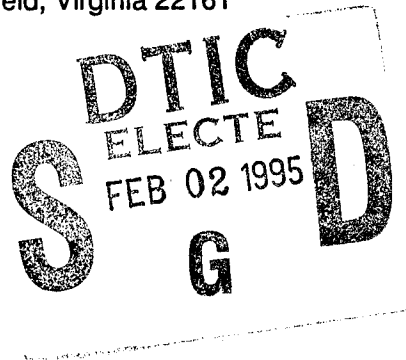
This document is available to the U.S. public through the
National Technical Information Service, Springfield, Virginia 22161

Prepared for:

U.S. Coast Guard
Research and Development Center
1082 Shennecossett Road
Groton, Connecticut 06340-6096

and

U.S. Department of Transportation
United States Coast Guard
Office of Engineering, Logistics, and Development
Washington, DC 20593-0001



19950131 027

NOTICE

This document is disseminated under the sponsorship of the Department of Transportation in the interest of information exchange. The United States Government assumes no liability for its contents or use thereof.

The United States Government does not endorse products or manufacturers. Trade or manufacturers' names appear herein solely because they are considered essential to the object of this report.

The contents of this report reflect the views of the Coast Guard Research & Development Center. This report does not constitute a standard, specification, or regulation.



D. L. Motherway
D. L. Motherway
Technical Director, Acting
United States Coast Guard
Research & Development Center
1082 Shennecossett Road
Groton, CT 06340-6096

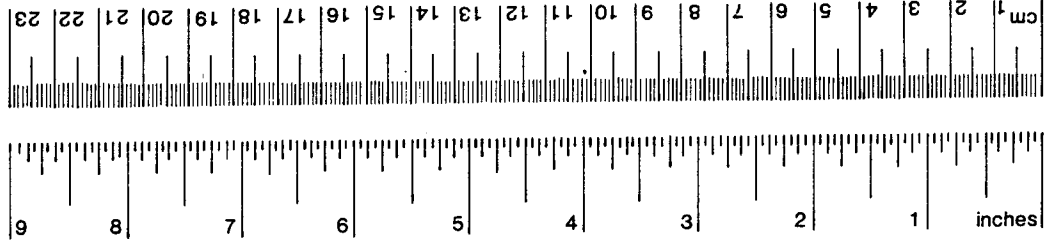
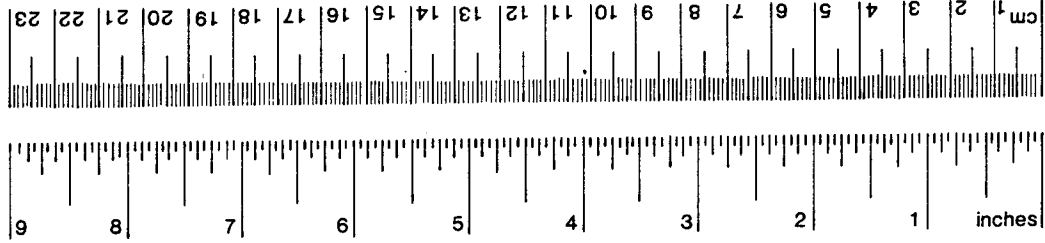
1. Report No. CG-D-01-95	2. Government Accession No.	3. Recipient's Catalog No.	
4. Title and Subtitle Wide Area DGPS Design Issues Study		5. Report Date January 1995	
		6. Performing Organization Code	
7. Author(s) T. Mueller, P. Loomis, L. Sheynblat		8. Performing Organization Report No. R&DC 21/94	
9. Performing Organization Name and Address TAU Corporation 485 Alberto Way Los Gatos, CA 95032-5405		10. Work Unit No. (TRAIS)	
		11. Contract or Grant No.	
12. Sponsoring Agency Name and Address U.S. Coast Guard Department of Transportation Research and Development Center U.S. Coast Guard 1082 Shennecossett Road Office of Engineering, Logistics, Groton, Connecticut 06340-6096 and Development Washington, D.C. 20593-0001		13. Type of Report and Period Covered Final Report September 1992-April 1993	
		14. Sponsoring Agency Code	
15. Supplementary Notes U.S. Coast Guard R&D Center contact: J. Spalding, (203) 441-2687.			
16. Abstract The U.S. Coast Guard will deploy a network of 50 DGPS reference stations by 1996 using the existing marine beacon network to transmit differential GPS corrections to marine users as part of a marine user DGPS service. The stations will provide coverage on the East, Gulf, and West Coasts, as well as the Great Lakes, Alaska, Hawaii, and Puerto Rico. Under this study, the authors postulated and evaluated three candidate Wide Area DGPS (WADGPS) network architectures. These architectures would extend the DGPS service architecture to a proposed WADGPS service architecture. This report presents results in broad areas of WADGPS network technology: network architectures and network software. One of the new concepts introduced is that of a fault-tolerant network. This concept incorporates flexible architecture which can reconfigure itself in the event of a failure of any of its components-such as the loss of some of the reference stations in the network. The Model Assessment section examines the error mechanisms which contribute to Differential GPS errors, both for the DGPS (single reference station) service and each of the three WADGPS (multiple reference station) networks. This leads into a presentation of various candidate network algorithms for these three WADGPS networks. In particular, a new algorithm, developed under this contract, is presented which offers improved performance for two of the three WADGPS network architectures over existing algorithms in the literature.			
17. Key Words Differential GPS (DGPS), Wide Area DGPS (WADGPS), Performance, Algorithms, Reliability, Networks, Architectures, Software, Error Models, Fault-Tolerant Networks		18. Distribution Statement Document is available to the U.S. public through the National Technical Information Service, Springfield, Virginia 22161	
19. Security Classif. (of this report) UNCLASSIFIED	20. SECURITY CLASSIF. (of this page) UNCLASSIFIED	21. No. of Pages	22. Price

METRIC CONVERSION FACTORS

Approximate Conversions to Metric Measures

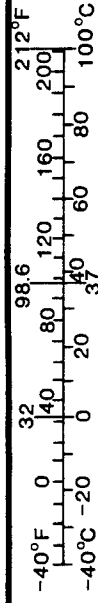
Symbol	When You Know	Multiply By	To Find	Symbol
LENGTH				
in	inches	* 2.5	centimeters	cm
ft	feet	30	centimeters	cm
yd	yards	0.9	meters	m
mi	miles	1.6	kilometers	km
AREA				
in ²	square inches	6.5	square centimeters	cm ²
ft ²	square feet	0.09	square meters	m ²
yd ²	square yards	0.8	square meters	m ²
mi ²	square miles	2.6	square kilometers	km ²
	acres	0.4	hectares	ha
MASS (WEIGHT)				
oz	ounces	28	grams	g
lb	pounds	0.45	kilograms	kg
	short tons (2000 lb)	0.9	tonnes	t
VOLUME				
tsp	teaspoons	5	milliliters	ml
tbsp	tablespoons	15	milliliters	ml
fl oz	fluid ounces	30	milliliters	ml
c	cups	0.24	liters	l
pt	pints	0.47	liters	l
qt	quarts	0.95	liters	l
gal	gallons	3.8	liters	l
ft ³	cubic feet	0.03	cubic meters	m ³
yd ³	cubic yards	0.76	cubic meters	m ³
TEMPERATURE (EXACT)				
°F	Fahrenheit temperature	5/9 (after subtracting 32)	Celsius temperature	°C

* 1 in = 2.54 (exactly).



Approximate Conversions from Metric Measures

Symbol	When You Know	Multiply By	To Find	Symbol
LENGTH				
mm	millimeters	0.04	inches	in
cm	centimeters	0.4	inches	in
m	meters	3.3	feet	ft
m	meters	1.1	yards	yd
km	kilometers	0.6	miles	mi
AREA				
cm ²	square centimeters	0.16	square inches	in ²
m ²	square meters	1.2	square yards	yd ²
km ²	square kilometers	0.4	square miles	mi ²
ha	hectares (10,000 m ²)	2.5	acres	
MASS (WEIGHT)				
g	grams	0.035	ounces	oz
kg	kilograms	2.2	pounds	lb
t	tonnes (1000 kg)	1.1	short tons	
VOLUME				
ml	milliliters	0.03	fluid ounces	fl oz
l	liters	0.125	cups	c
l	liters	2.1	pints	pt
l	liters	1.06	quarts	qt
l	liters	0.26	gallons	gal
m ³	cubic meters	35	cubic feet	ft ³
m ³	cubic meters	1.3	cubic yards	yd ³
TEMPERATURE (EXACT)				
°C	Celsius temperature	9/5 (then add 32)	Fahrenheit temperature	°F



PREFACE

The U.S. Coast Guard will deploy a network of 50 DGPS reference stations by 1996 using the existing marine beacon network to transmit Differential GPS corrections to marine users as part of a marine user DGPS service. The stations will provide coverage on the East, Gulf, and West Coasts, as well as the Great Lakes, Alaska, Hawaii, and Puerto Rico. Under this study, the authors postulated and evaluated three candidate Wide Area DGPS (WADGPS) network architectures. These architectures would extend the DGPS service architecture to a proposed WADGPS service architecture.

This report presents results in two broad areas of WADGPS network technology: network architectures and network software. One of the new concepts which is introduced is the concept of a fault-tolerant network. This concept incorporates a flexible architecture which can reconfigure itself in the event of a failure of any of its components -- such as the loss of some of the reference stations in the network.

The Model Assessment section examines the error mechanisms which contribute to Differential GPS errors, both for the DGPS (single reference station) service and each of the three WADGPS (multiple reference station) networks. This leads into a presentation of various candidate network algorithms for these three WADGPS networks. In particular, a new algorithm, developed under this contract, is presented which offers improved performance for two of the three WADGPS network architectures over existing algorithms in the literature.

The authors wish to acknowledge Mr. John H. Kraemer and Mr. Frank Castillo, Department of Transportation, John A. Volpe National Transportation Systems Center, and Mr. Joseph W. Spalding, Program Manager, Coast Guard R&D Center, for their invaluable direction, comments, and data provided to perform this study. Also, the excellent support provided by Ms. Janice Smith and Ms. Margie Hager, TAU Corporation, is acknowledged in making this report a reality.

Accession For	
NTIS	<input checked="checked" type="checkbox"/>
CRA&I	<input type="checkbox"/>
DTIC	<input type="checkbox"/>
TAB	<input type="checkbox"/>
Unannounced	<input type="checkbox"/>
Justification _____	
By _____	
Distribution /	
Availability Codes	
Dist	Avail and/or Special
A-1	

TABLE OF CONTENTS

<u>Section</u>	<u>Page</u>
1. INTRODUCTION	1
1.1 FAA INTERESTS	1
1.2 COAST GUARD INTERESTS	1
1.3 REPORT OVERVIEW	2
2. GENERAL	5
2.1 WADGPS NETWORK ARCHITECTURES	5
2.2 WADGPS MAJOR ISSUES	6
2.3 MODEL ASSESSMENT	8
2.4 RECOMMENDATIONS	9
3. OVERVIEW OF WADGPS	11
3.1 BASELINE DGPS ARCHITECTURE	11
3.1.1 System Architecture	13
3.1.1.1 Reference, Monitor, and Broadcast Station Locations	13
3.1.1.2 Communications Requirements	16
3.1.1.3 Equipment Requirements	17
3.1.1.4 System Operating Procedures	17
3.1.2 Component Architecture	18
3.1.2.1 Reference Station	20
3.1.2.2 Broadcast Transmitter	20
3.1.2.3 Integrity Monitor	20
3.1.2.4 Control Station	20
3.1.2.5 Marine User	20
3.1.3 System Performance	20
3.2 SYSTEM UPGRADE TO WADGPS ARCHITECTURE	22
3.2.1 Federated Local Area DGPS Network	24
3.2.2 East-Coast/West-Coast Area DGPS Network	26
3.2.3 CONUS DGPS Network	28
3.3 WADGPS ARCHITECTURE AUGMENTATION	34
3.3.1 AFSFC Near-Real-Time Ionospheric Effects Data	34
3.3.2 FAA Wide Area Differential Global Positioning System (WADGPS)	37
4. WADGPS MAJOR ISSUES	41
4.1 COST	41
4.2 PERFORMANCE	43
4.3 INTEGRITY	47
4.4 RELIABILITY	49
4.5 OTHER	50

TABLE OF CONTENTS (continued)

<u>Section</u>	<u>Page</u>
5. MODEL ASSESSMENT	53
5.1 WADGPS ERROR MODELS	53
5.1.1 WADGPS Network Models	53
5.1.2 Ionospheric Model	61
5.1.3 Tropospheric Model	68
5.1.4 Satellite Ephemeris Model	69
5.1.5 Satellite Clock Model	76
5.1.6 WADGPS Network Clock Model	76
5.1.7 Multipath and Other Non-Common Mode Models	78
5.1.8 Selective Availability Effects	79
5.2 EVALUATION METHODOLOGY	80
5.3 WADGPS ERROR MODEL ASSESSMENT	80
5.3.1 WADGPS Network Models	80
5.3.2 Ionospheric Model	89
5.3.3 Tropospheric Model	91
5.3.4 Satellite Ephemeris Model	91
5.3.5 Satellite Clock Model	97
5.3.6 WADGPS Network Clock Model	97
5.3.7 Multipath and Other Non-Common Mode Error Models	98
6. REMAINING WORK	101
6.1 WADGPS ARCHITECTURE	101
6.1.1 Establish WADGPS Network Time Transfer and Synchronization Requirements	101
6.1.2 WADGPS Network Performance Simulation	101
6.1.3 Obtain Availability of Accuracy Estimates	102
6.1.4 Perform Cost-Benefit Analysis	102
6.1.5 Develop a WADGPS Integrity Network	102
6.1.6 Investigate Alternate WADGPS Network Communications Systems	102
6.2 WADGPS MODEL DEVELOPMENT AND ASSESSMENT	103
6.2.1 Evaluate High Frequency (Spatial and Temporal) Ionospheric Effects	103
6.2.2 Refine the Minimum Variance Algorithm for the EC/WCA-DGPS Network	104
6.2.3 Evaluate Minimum Variance Algorithm with Field Data	104
6.2.4 Evaluate RAIM Integrity Software Performance	104
7. CONCLUSIONS AND RECOMMENDATIONS	107
7.1 WADGPS ARCHITECTURES	107
7.2 WADGPS MAJOR ISSUES	108
7.3 MODEL ASSESSMENT	112
7.4 RECOMMENDATIONS	112
REFERENCES	115
APPENDIX A - ERROR BUDGET ASSUMPTIONS	A-1
APPENDIX B - NETWORK DGPS ACCURACY TEST CASES	B-1

LIST OF FIGURES

<u>Figure</u>	<u>Page</u>
1. DGPS SERVICE SYSTEM CONCEPT	11
2. PROPOSED CONUS, ALASKA & HAWAII DGPS COVERAGE.....	13
3. DGPS SERVICE ARCHITECTURE	15
4. DGPS SERVICE FUNCTIONAL DATA FLOW.....	19
5. FLA-DGPS NETWORK ARCHITECTURE.....	25
6. FLA-DGPS NETWORK FUNCTIONAL DATA FLOW	27
7. EC/WCA-DGPS NETWORK ARCHITECTURE.....	29
8. EC/WCA-DGPS NETWORK FUNCTIONAL DATA FLOW	30
9. CONUS-DGPS NETWORK ARCHITECTURE.....	32
10. CONUS DGPS NETWORK FUNCTIONAL DATA FLOW.....	33
11. AFSFC TRANS-IONIC SENSING SYSTEM (TISS) NETWORK.....	36
12. WIDE AREA DIFFERENTIAL GPS (WADGPS) CONCEPT.....	39
13. WADGPS NAVIGATION ACCURACY (2 drms).....	45
14. AVAILABILITY OF ACCURACY (L = 8 m (2 drms)).....	49
15. MAJOR GEOGRAPHIC REGIONS OF THE IONOSPHERE	62
16. IONOSPHERIC VERTICAL TOTAL ELECTRON CONTENT (VTEC).....	63
17. MONTHLY OVERPLOTS OF TEC DIURNAL CURVES VS. UNIVERSAL TIME (HAMILTON, MA. 1979)	66
18. DUAL-FREQUENCY MEASUREMENT DRIVEN IONOSPHERIC DELAY MODEL	67
19. WADGPS (REGIONAL) NETWORK SYSTEM MODEL	81
20. WADGPS (CONUS) NETWORK SYSTEM MODEL.....	82
21. GENERIC DGPS NETWORK.....	84
22. 340 KM NETWORK DGPS ACCURACY VS BASELINE.....	86
23. 680 KM NETWORK DGPS ACCURACY VS BASELINE.....	87
24. 1000 KM NETWORK DGPS ACCURACY VS BASELINE.....	87
25. THREE-SITE NETWORK PARTIAL DERIVATIVE ALGORITHM DGPS ACCURACY VS SITE SEPARATION	88
26. THREE-SITE NETWORK MINIMUM VARIANCE ALGORITHM DGPS ACCURACY VS SITE SEPARATION	88
27. IONOSPHERIC DELAY COSINE MODEL COEFFICIENTS (BENT MODEL VS. GEOMAGNETIC LATITUDE).....	92
28. LINEARITY OF PSEUDORANGE ERROR DUE TO RADIAL ERROR	94
29. LINEARITY OF PSEUDORANGE ERROR DUE TO CROSS-TRACK ERROR	95
30. EXTREME MULTIPATH CONDITIONS.....	99
31. REDUCED MULTIPATH.....	100

LIST OF TABLES

<u>Table</u>	<u>Page</u>
1. WADGPS NETWORK SUMMARY	5
2. WADGPS NETWORK PERFORMANCE SUMMARY	7
3. DGPS SERVICE TIME LINE	12
4. DGPS BROADCAST SITES	14
5. DGPS SERVICE ARCHITECTURE SELECTION CRITERIA [4]	21
6. DGPS SERVICE ARCHITECTURE SELECTION [3]	22
7. NETWORK DIFFERENTIAL GPS APPROACHES	23
8. AIR FORCE SPACE FORECAST CENTER (AFSFC) NEAR-REAL-TIME IONOSPHERIC EFFECTS DATA	35
9. WADGPS NETWORK COST ESTIMATES	41
10. WADGPS NETWORK ERROR BUDGET (m)	44
11. WADGPS NETWORK GROUND SYSTEM AVAILABILITY	46
12. AVAILABILITY OF ACCURACY ESTIMATES FOR FAULT-TOLERANT WADGPS NETWORKS	48
13. WADGPS NETWORK INTEGRITY GROUND SYSTEM AVAILABILITY	50
14. WADGPS NETWORK GROUND SYSTEM RELIABILITY	51
15. DGPS ERROR SPATIAL AND TEMPORAL DECORRELATION	54
16. DIFFERENTIAL GPS NETWORK ALGORITHM SUMMARY	55
17. NETWORK DGPS PARTIAL DERIVATIVE ALGORITHM	57
18. MINIMUM VARIANCE ALGORITHM DERIVATION	59
19. NETWORK DGPS MINIMUM VARIANCE ALGORITHM	60
20. KLOBUCHAR IONOSPHERE MODEL	65
21. GPS TROPOSPHERIC DELAY MODELS SUMMARY	68
22. DAVIS TROPOSPHERIC DELAY MODEL	70
23. SATELLITE ORBITAL FILTER OPTIONS	73
24. BROADCAST EPHEMERIS ALGORITHM	74
25. HILL'S DIFFERENTIAL EQUATIONS	75
26. GPS ERROR BUDGET METHODOLOGY	83
27. NETWORK DGPS ERROR COVARIANCE METHODOLOGY	83
28. SPATIAL DECORRELATION FUNCTIONS	86
29. IONOSPHERIC STATISTICS	90
30. COMPARISON OF BENT AND IRI-86 IONOSPHERIC DELAY MODELS [35]	90
31. DAVIS TROPOSPHERIC DELAY MODEL ERROR BUDGET	93
32. GPS ORBIT DETERMINATION ACCURACY	96
33. WADGPS NETWORK PHYSICAL ASSETS	109
34. WADGPS NETWORK HARDWARE AND SOFTWARE	110

GLOSSARY OF ACRONYMS

AFSFC	-	Air Force Space Forecast Center
BE	-	Broadcast Ephemeris
CONUS	-	Continental United States
CPU	-	Central Processing Unit
DBSM	-	Differential Broadcast Service Monitor
DGPS	-	Differential Global Positioning System
DOT	-	Department of Transportation
EC/WCA DGPS	-	East Coast/West Coast Area DGPS
FAA	-	Federal Aviation Administration
FLA DGPS	-	Federated Local Area DGPS
FRP	-	Federal Radionavigation Plan
GPS	-	Global Positioning System
HDOP	-	Horizontal Dilution of Precision
HE	-	Hill's Equations
HHA	-	Harbor and Harbor Approach
IFM	-	Ionospheric Forecast Model
IFR	-	Instrument Flight Rule
IRI	-	International Reference Ionosphere
LPE	-	Lagrange Planetary Equations
LPF	-	Low Pass Filter
MF	-	Mapping Function
MSK	-	Minimum Shift Keying
MVA	-	Minimum Variance Algorithm
NASA/JSC	-	National Aeronautics and Space Administration/Lyndon B. Johnson Space Center
NEM	-	Newton's Equations of Motion
NGS	-	National Geodetic Survey
PAD	-	Packet Assembler/Disassembler
PDA	-	Partial Derivative Algorithm
PL	-	Protection Limit
P(MD)	-	Probability of Missed Detection
PR' & ADR'	-	Expected Pseudorange & Accumulated Delta Range
PR _m & ADR _m	-	Measured Pseudorange & Accumulated Deltarange

GLOSSARY OF ACRONYMS (continued)

PRC & RRC	-	Pseudorange & Range Rate Corrections
PRE & ADRE	-	Pseudorange & Accumulated Delta Range Errors
PRISM	-	Parameterized Real-Time Ionospheric Specification Model
PSS	-	Packet Switching Service
RAIM	-	Receiver Autonomous Integrity Monitoring
RNP	-	Required Navigation Performance
RTCM	-	Radio Technical Commission for Maritime Services
SA	-	Selective Availability
SPS	-	Standard Positioning Service
TAR	-	Threshold Accuracy Requirement
TASC	-	The Analytic Sciences Corporation
TEC	-	Total Electron Content
TID	-	Traveling Ionospheric Disturbances
TISS	-	Trans-Ionospheric Sensing System
TTA	-	Time To Alarm
UERE	-	User Equivalent Range Error
USCG	-	United States Coast Guard
VNTSC (Volpe Ctr.)	-	John A. Volpe National Transportation Systems Center
WADGPS	-	Wide Area Differential Global Positioning System
WWDGPS	-	Worldwide Differential GPS

1. INTRODUCTION

The objective of this report, Wide Area Differential GPS Design Study Issues, is to investigate the potential advantages and disadvantages of the implementation of a Wide Area Differential Global Positioning System (WADGPS) network by the United States Coast Guard (USCG) for marine applications. This study will address the specific needs of the USCG in terms of coverage, accuracy, update rate, and other parameters, as well as determine what additional steps should be taken to fully assess these requirements and interests.

1.1 FAA INTERESTS

The Federal Aviation Administration (FAA), Research and Development Service has a comprehensive Differential Global Positioning System (DGPS) program of which WADGPS has become an active and significant area of research. In addition, other organizations are assessing the benefits of WADGPS networks. Due to the aeronautical applications of most of this research, full Continental U.S. (CONUS) coverage is required and hence, not all of the results of this research are directly applicable to the satisfaction of the USCG marine requirements.

The John A. Volpe National Transportation Systems Center (Volpe Center) is therefore currently providing support to the USCG in the application of WADGPS technology to USCG operations. The specific role of the Volpe Center is to evaluate the applicability of WADGPS networks to the satisfaction of the USCG marine DGPS operations requirements and to make recommendations.

1.2 COAST GUARD INTERESTS

The Coast Guard is charged with establishing, maintaining, and operating electronic aids to navigation to serve the needs of the U.S. armed forces, maritime commerce, and air commerce. The first electronic aids to navigation introduced by the USCG were radiobeacons in 1921. These were followed by Loran A and C as well as Omega.

While these radio aids provide an all-weather service whose accuracy satisfies the requirements for ocean crossing (Omega) and coastal navigation (Loran C), they do not meet the navigational accuracy requirements for harbor approach and harbor navigation. The Federal Radionavigation Plan (FRP) [1] has specified the harbor and harbor approach (HHA) navigation accuracy requirements as: 8-20m (2 drms), with 99.7% availability. The FRP also defines the integrity of a navigation aid as the ability of the system incorporating this aid to provide timely warnings to users when the aid should not be used for navigation.

In 1983, the Coast Guard R&D Center and the Department of Transportation (DOT) Transportation Systems Center (TSC) cosponsored research into the use of Differential GPS (DGPS). This research focused on

determining the achievable accuracies and candidate system designs. Based on this research, it was concluded that DGPS using C/A-code receivers could achieve accuracies of 14m (2 drms) [2].

During 1983, the Radio Technical Commission for Maritime Services (RTCM) established Special Committee: SC-104 to develop standards for a message format for the DGPS corrections that would accommodate various communication systems and be robust enough to provide high accuracy and reliable service for air, marine, and land users. With Coast Guard participation, this committee established a minimum differential correction transmission rate of 50 bps, based on the requirements imposed by Selective Availability (SA).

It was also determined that the radiobeacon band of 285-325 KHz was the only band that met the needs of DGPS for Coast Guard radionavigation use without requiring changes in the international frequency allocations. It was further established by the Coast Guard in 1984 that the existing radiobeacon network would be a convenient approach to transmission of the DGPS corrections. This was based on the fact that the beacons were located where marine navigators needed coverage, multipath was minimal compared to the higher frequencies, and the range of the beacons roughly corresponded to the operational range of the DGPS corrections.

1.3 REPORT OVERVIEW

This report presents results in two broad areas of WADGPS network technology: network architectures and network software. Hence, following a summary in Section 2, Section 3 presents an overview of WADGPS networks. Section 3 starts with a discussion and summary of the proposed DGPS service which the Coast Guard plans to implement. Using this as a baseline, the remainder of this section presents three candidate WADGPS network architectures. It also explores how these may be augmented by other resources or programs, such as the Air Force Space Forecast Center (AFSFC) Near-Real-Time Ionospheric Effects Data and the FAA WADGPS Program for Civilian Aircraft Users.

In Section 4, major WADGPS issues are explored which may limit (or enhance) the implementation or effectiveness of each of the three candidate WADGPS network architectures. Specifically, issues of cost, accuracy, availability, reliability, and integrity are examined, both for these WADGPS network architectures as well as for the DGPS service architecture. One of the new concepts introduced is that of a fault-tolerant network. This concept incorporates a flexible architecture which can reconfigure itself in the event of a failure of any of its components—such as the loss of some of the reference stations in the network.

The Model Assessment section, Section 5, examines the error mechanisms which contribute to Differential GPS errors, both for the DGPS (single reference station) service and each of the three WADGPS (multiple reference station) networks. This leads into a presentation of various candidate network algorithms for these three WADGPS networks. In particular, a new algorithm, developed under this contract, is presented which offers improved performance for two of the three WADGPS network architectures over existing algorithms in the literature. The discussion in Section 5 is supported by additional material presented in Appendices A and B.

Additional work that is required to fully assess the merits of each of the three WADGPS network architectures is summarized in Section 6. This summary includes the requirement for a cost-benefit analysis. Finally, Section 7 presents the recommendations and conclusions.

2. GENERAL

Under the base period of this contract, three candidate WADGPS network architectures are postulated and evaluated. These are the Federated Local Area DGPS (FLA-DGPS) network, the East Coast/West Coast Area DGPS (EC/WCA-DGPS) network, and the Continental US DGPS (CONUS-DGPS) network.

2.1 WADGPS NETWORK ARCHITECTURES

The three candidate WADGPS network architectures are summarized in Table 1.

TABLE 1. WADGPS NETWORK SUMMARY

Architecture	No. of Reference Stations/ Network	Reference Receiver Type	No. of Master Control Stations	Network Software Filter	Comments
DGPS Service	1	C/A Code		Implicit	50 broadcast beacons
FLA-DGPS Network	3	C/A Code	50	Implicit	Each reference station is own master
EC/WCA-DGPS Network	33 (East) 17 (West)	C/A Code C/A Code	1 (East) 1 (West)	Implicit Implicit	
CONUS DGPS Network	16	Dual-Frequency	1 (East/ West)	Explicit	Corrections transmitted to and broadcast from all 50 broadcast beacons

The FLA-DGPS network is formed by designating each DGPS reference station as its own master station and using the neighbor reference station on either side to form a three-station Local Area DGPS network. At the master station, the DGPS spatial decorrelation function and an inverse network spatial decorrelation matrix would be computed and broadcast to the user, together with the DGPS corrections from the three stations of the network. The user would compute the Minimum Variance Algorithm weighting coefficients for combining the individual reference station DGPS corrections to obtain a network DGPS correction valid for his location.

The EC/WCA-DGPS network nets all of the East Coast (including Great Lakes, Gulf Coast, and Puerto Rico) DGPS stations into a 33-station East Coast network. It also nets all the West Coast (including Alaska and Hawaii) DGPS stations into a 17-station West Coast network. The DGPS corrections from each site of the respective coast networks would be sent to the respective control centers for that coast. The control centers would use Minimum Variance Algorithms to compute DGPS correction "surfaces" for the beacon coverage area of that coast by calculating the corrections for a matrix of user locations. The control center would reformulate these

corrections for the local beacon site so as to provide the maximum accuracy for the user with a minimum of communication burden and minimum user complexity.

The CONUS DGPS network would place dual-frequency DGPS reference receivers at 16 of the 50 DGPS beacon sites. These receivers would compute the ionospherically adjusted DGPS corrections and send them, together with the iono corrections, to the redundant control centers. The control centers would use an explicit filter model to estimate the ionospheric delays, the satellite clock and ephemeris errors, and the network clock errors. These corrections would be reformulated into a practical user algorithm and sent back to each of the 50 beacon sites for transmission to the user.

All three architectures would be implemented with fault-tolerant network software. Hence, the architectures would be able to provide network DGPS corrections to the user even if some of the individual reference site DGPS corrections became unavailable to the network DGPS algorithm. Also, a capability is incorporated to always broadcast, as a minimum, the basic DGPS service corrections in case the network DGPS corrections are not available due to network communication outages or other reasons.

2.2 WADGPS MAJOR ISSUES

A summary of the WADGPS network performance is summarized in Table 2 and discussed in this section.

Estimates of the performance for these three WADGPS network architectures are presented in Section 4.2. It is shown that for a baseline of 300 kilometers, the FLA-DGPS network navigation accuracy is 20% better than for the DGPS service. For the EC/WCA-DGPS network, the navigation accuracy is 29% better than for the DGPS service. For both of these network cases, the results are computed for a near-worst case location of the user relative to the network. Hence, the results are conservative.

The estimated navigation accuracy under the CONUS DGPS network, which is baseline independent, is approximately 5% worse than the accuracy with the DGPS service at a baseline of 300 kilometers. The results for the CONUS DGPS network are very preliminary and should be verified with a performance simulation or field data.

Using a fault-tolerant approach, it is determined that the availability of accuracy for an HHA navigation accuracy requirement of 8 meters (2 drms) with an availability of 0.997 cannot be satisfied by the DGPS service out to a baseline of 300 kilometers, assuming no broadcast signal loss. Both the FLA-DGPS network and the EC/WCA-DGPS network also have an availability of accuracy out to 300 kilometers which cannot satisfy the stringent HHA 8 meter protection limit requirement. However, the FLA-DGPS network has the best availability of accuracy for the shorter baselines. The EC/WCA-DGPS network, in turn, has a higher availability of accuracy at the longer baselines. These results do not include the effects of broadcast errors. Also, the WADGPS network results are for a generic three and five station network for the FLA-DGPS and EC/WCA-DGPS network, respectively.

TABLE 2. WADGPS NETWORK PERFORMANCE SUMMARY

Performance Parameter	DGPS Service	FLA-DGPS Network	EC/WCA Network	CONUS Network
<u>Navigation Accuracy</u> (2 drms, m)				
• 0 km Baseline	3.5	3.5	3.4	6.9
• 100 km Baseline	4.5	4.0	4.0	6.9
• 300 km Baseline	6.6	5.3	4.7	6.9
<u>Fault-Tolerant Availability of Accuracy</u> (8 m protect limit; no transmit errors)				
• 0 km Baseline	0.994005	0.994287	0.989187	
• 100 km Baseline	0.962432	0.978746	0.975482	
• 300 km Baseline	0.771229	0.894151	0.938193	
<u>Ground System Availability</u>				
• Full Network	0.999068	0.988507	0.967915	
• Fault-Tolerant Network		0.999041	0.993899	
<u>Ground System Reliability</u> (outages/Mhr)	121.1	2917.8	8190.9	
<u>Integrity Ground System Availability</u>	0.998468	0.992482	0.992482	0.992482
<u>Basic Costs</u>				
• Acquisition (\$M)	\$ 5.38			
• Operations (\$M/Y)	\$ 1.00			
• Maintenance (\$M/Y)	<u>\$ 0.36</u>			
• Life-Cycle (\$M/Y)	\$15.42			
<u>Incremental Costs</u>				
• Acquisition (\$M)		\$2.30	\$2.29	\$3.43
• Operations (\$M/Y)		\$0.47	\$0.61	\$0.61
• Maintenance (\$M/Y)		<u>\$0.04</u>	<u>\$0.04</u>	<u>\$0.04</u>
• Life-Cycle (\$M/Y)		\$6.10	\$7.12	\$8.27

Evaluation of the network integrity will focus primarily on changes to the basic DGPS service integrity architecture and present a summary of the probability that the integrity ground system is available. The specific hardware changes involve adding a permanent dual-redundant integrity coverage monitor at the outer coverage limit of each beacon site in addition to the existing beacon co-located dual-redundant integrity monitors. Since these coverage monitors will provide a check of the network DGPS corrections at non-zero baselines, they are considered to be an essential part of the network integrity architecture. For the DGPS service, which does not factor in the non-permanent coverage monitors currently included under the DGPS service, the probability of integrity ground system

availability is estimated by TASC [3] to be 0.9985. For the three network architectures, which all use the same integrity architecture, the probability of integrity ground system availability is 0.9925.

Evaluation of the reliability of the architectures is also performed for the DGPS service and the first two network DGPS architectures. For the DGPS service, TASC estimates that 121.1 outages per million hours of operation will occur. Using the same component reliabilities and factoring in the fault-tolerant approach for the FLA-DGPS and EC/WCA-DGPS network architectures, reliabilities of 2918 and 8191 outages per million hours of operation are obtained, respectively. These low reliabilities arise from the use of the X.25 communications network in the critical data path for these WADGPS network architectures. While the use of the X.25 communications network minimizes the communications cost, the resulting reliability is not high enough. Hence, possible redundant communication networks, or a more reliable one, need to be considered for these architectures.

Finally, estimates are made of the incremental costs required to upgrade from the DGPS service architecture to any of the three WADGPS architectures. As summarized in Table 2, it was determined that while the DGPS service acquisition costs, as estimated by TASC, are \$5.4 million, the incremental acquisition costs for the FLA-DGPS, EC/WCA-DGPS, and CONUS DGPS networks are respectively: \$2.3 million, \$2.3 million, and \$3.4 million. The annual operations costs for the DGPS service are estimated to be \$1.0 million by TASC, while the incremental operations costs for the FLA-DGPS, EC/WCA-DGPS, and CONUS DGPS networks are respectively: \$0.5 million, \$0.6 million, and \$0.6 million. While the annual maintenance costs for the DGPS service are estimated by TASC to be \$0.4 million, the incremental maintenance costs for the FLA-DGPS, EC/WCA-DGPS, and CONUS DGPS networks are \$0.04 million each. Finally, TASC has estimated the total life cycle costs to be \$15.4 million for the DGPS service, the incremental life cycle costs for the FLA-DGPS, EC/WCA-DGPS, and CONUS DGPS networks are respectively: \$6.1 million, \$7.1 million, and \$8.3 million.

2.3 MODEL ASSESSMENT

The highlight of the model assessment was the derivation of a new network DGPS algorithm—the Minimum Variance Algorithm. It was motivated by the poor performance of the well-known Partial Derivative Algorithm under the difficult local area and regional network geometries of the FLA-DGPS and EC/WCA-DGPS networks. The Minimum Variance Algorithm differs from the Partial Derivative Algorithm in that it determines the weighting coefficients for the reference station DGPS corrections using a minimum variance approach which incorporates the spatial decorrelation functions of the DGPS corrections. It is also versatile in that it can be used with any number of reference stations. One drawback is that the calculation of the coefficients, which must be done with the users position, rapidly becomes complex for networks with more than three reference stations.

2.4 RECOMMENDATIONS

Based on the work completed to date, both the FLA-DGPS and ECWCA-DGPS network architectures look very promising as candidate architectures for a WADGPS service. These could be formulated and implemented as a two-phase WADGPS upgrade of the basic DGPS service. The principal drawback to all three WADGPS architectures, as currently postulated, is the use of the AT&T X.25 landline communications network in the critical data flow path. While the CONUS DGPS network results are very preliminary, they do suggest that the benefits of this architecture would be realized only at the outer regions of the coverage area.

Additional work should be performed to resolve issues raised under the base period of this contract. These issues are presented in Section 6.0. The specific additional tasks are summarized below.

WADGPS Architecture:

- Establish WADGPS Network Time Transfer and Synchronization Requirements
- Perform WADGPS Network Performance Simulation
- Obtain Availability of Accuracy Estimates
- Perform Cost-Benefit Analysis
- Develop a WADGPS Integrity Network
- Investigate Alternate WADGPS Network Communication Systems

WADGPS Model Development and Assessment:

- Evaluate High Frequency (Spatial and Temporal) Ionospheric Effects
- Refine the Minimum Variance Algorithm for the EC/WCA-DGPS Network
- Evaluate Minimum Variance Algorithm with Field Data

3. OVERVIEW OF WADGPS

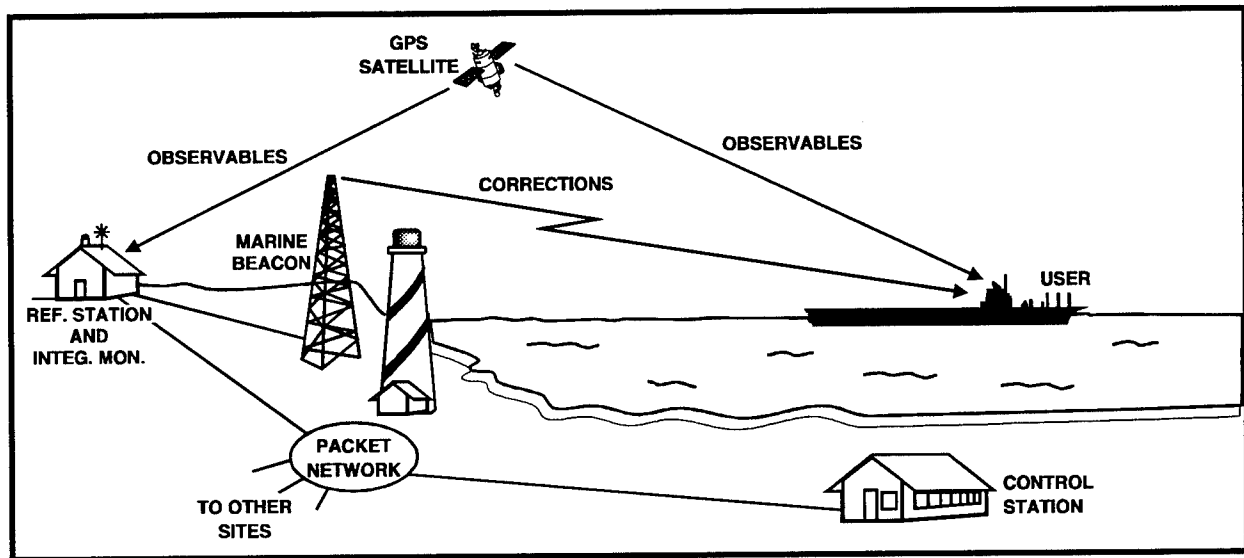
Presented in this section is a description of the architecture of the baseline DGPS service and the three candidate WADGPS networks.

3.1 BASELINE DGPS ARCHITECTURE

This section presents the physical location and interconnection of the equipment, the types of equipment, and a description of the system operating procedures.

In 1989, the Coast Guard performed a test involving transmissions of DGPS signals using a marine radiobeacon located at Montauk Point, Long Island. Based on the success of this test, Montauk Point began transmitting prototype DGPS data for public use in 1990. These tests demonstrated that marine beacons could be used effectively for a USCG DGPS service. This service would also be suitable for radio positioning and navigation.

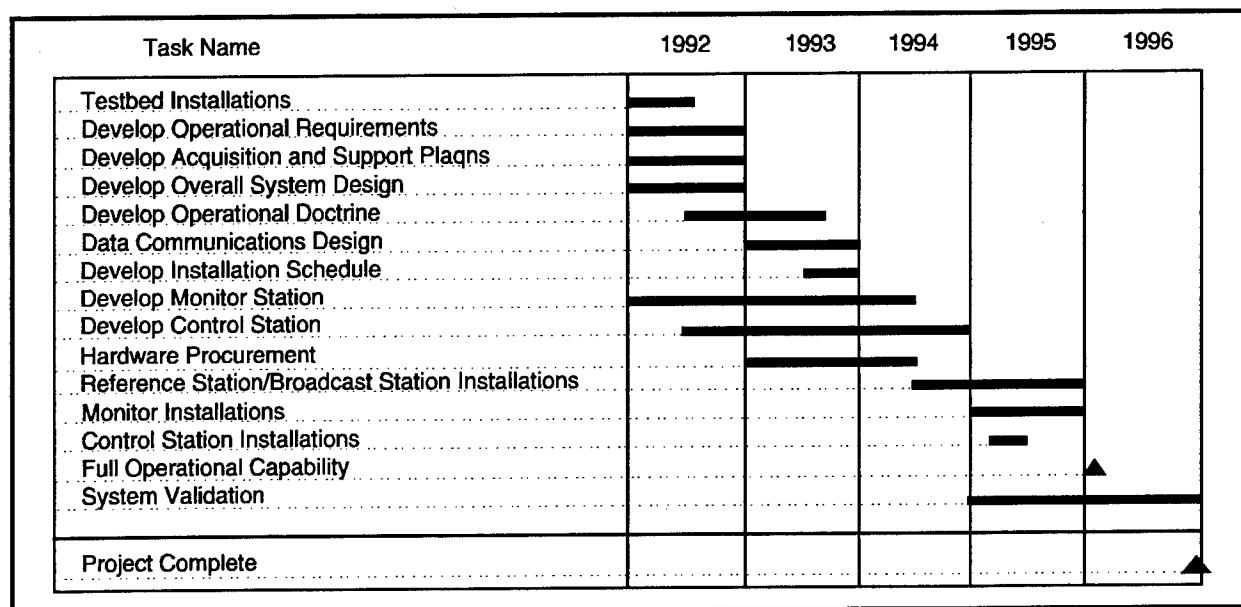
This DGPS service system concept is presented in Figure 1 [2], while the timeline for bringing this service up to full operational capability in 1996 is summarized in Table 3 [2].



1707-007(WP2)9/93

FIGURE 1. DGPS SERVICE SYSTEM CONCEPT

TABLE 3. DGPS SERVICE TIME LINE



As illustrated in Figure 1, DGPS reference stations will compute corrections which will be transmitted by existing marine beacons to the marine user. The user can then correct his own GPS measurements and obtain precise navigation information. The DGPS service insures the integrity of the transmitted corrections using integrity monitors, and uses control stations to provide overall control.

The DGPS service will provide coverage to the marine user for the coastal regions of the Continental U.S. (CONUS), the Great Lakes, Alaska, Hawaii, and Puerto Rico. The proposed location of the radiobeacons, which will transmit the DGPS corrections, and the beacon coverage is illustrated in Figure 2 [2]. A list of the radiobeacon locations used in Figure 2 is presented in Table 4 [2]. This listing shows that a proposed total of 50 radiobeacons will be used. They will transmit the DGPS corrections from approximately 50 dual-redundant DGPS reference stations, collocated with the radiobeacons.

The concept of DGPS involves placing a GPS receiver at a known (pre-surveyed) location. Since the satellite position and velocity as well as the receiver position are known, differences between the computed and measured pseudoranges and pseudorange rates from the receiver to each of the observed satellites can be computed. These pseudorange and pseudorange rate errors are used to derive the DGPS corrections. The corrections are then broadcast to GPS users in the vicinity who correct their measured pseudorange before computing their orthogonal position. This is the basic concept behind the local area DGPS service. The assumptions and limitations related to DGPS will be discussed in greater detail below.

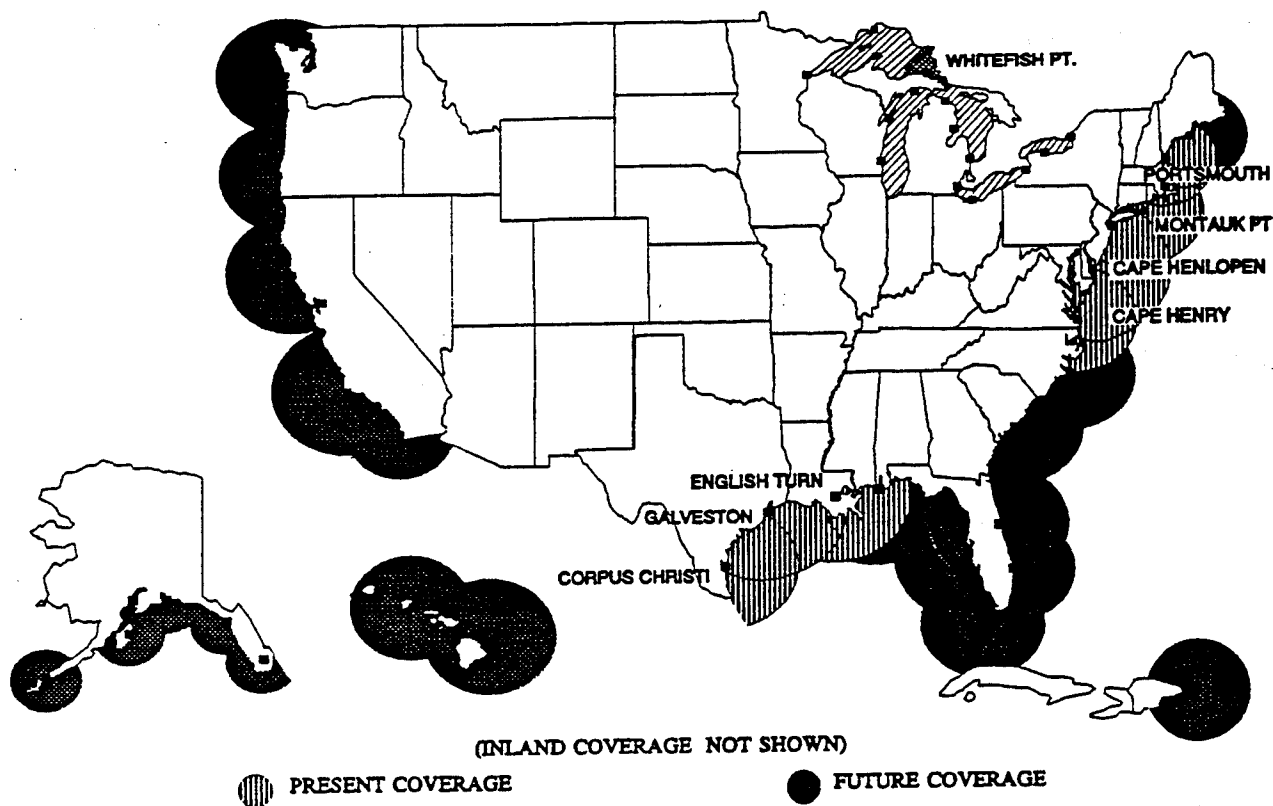


FIGURE 2. PROPOSED CONUS, ALASKA & HAWAII DGPS COVERAGE

3.1.1 System Architecture

The baseline architecture addresses the locations of the reference, monitor, and broadcast stations. It also addresses the communications requirements, equipment requirements, and system operating procedures.

The Coast Guard baseline Local Area DGPS service deployment illustrated in Figure 2 shows the service area that will be able to receive the DGPS corrections which are broadcast. Not shown in this figure are the locations of the 50 dual-redundant DGPS reference stations.

Figure 3 presents the DGPS system that will provide this local area DGPS service. It is based on [2] and shows the elements of the system: reference stations, broadcast transmitter, control station, integrity monitoring stations, and the marine user. It also displays the DGPS beacon sites currently available on the Great Lakes, the East Coast, and the Gulf Coast.

3.1.1.1 Reference, Monitor, and Broadcast Station Locations - DGPS, by its general nature, can only service a small area. Depending on the accuracy requirements and the state of the system, this can be from 40 to 300 miles in radius. At separation distances of more than 300 miles between reference station and user, joint visibility of the

TABLE 4. DGPS BROADCAST SITES

EAST COAST SITES				WEST COAST SITES			
NAME	LAT. (deg, min, N)	LONG. (deg, min, W)	RANGE* (mi)	NAME	LAT. (deg, min, N)	LONG. (deg, min, W)	RANGE* (mi)
GREAT LAKES REGION				PACIFIC COAST, ALASKA, & HAWAII			
DULUTH, MN	46 46.8	92 05.3	40	BARBERS PT., HI	21 18.0	156 06.5	170
EAGLE HARBOR, MI	50 27.7	88 09.5	160	UPOLO PT. HI	20 14.8	155 53.2	170
WHITEFISH PT., MI	46 46.3	84 57.5	80	PT. LOMA, CA	32 40.0	117 14.6	150
LOOKOUT 4, MI	46 17.1	84 12.7	40	PT. ARGUELLO, CA	34 34.7	120 38.6	190
SEUL CHOIX PT., MI	45 55.3	85 54.7	120	SF BAY, PT. BLUNT	37 51.2	122 25.2	60
STURGEON BAY, WI	50 47.7	87 18.8	60	PT. ARENA, CA	38 57.3	123 48.6	130
MILWAUKEE, WI	43 01.6	87 52.9	140	CAPE BLANCO, OR	42 50.3	124 33.8	130
PRESQUE IS. LT., MI	45 21.4	83 29.5	80	GRAYS HBR., WA	46 54.2	124 07.8	150
GRAVELY SHOAL, MI	44 01.2	83 32.3	40	EDIZ HOOK, WA	48 08.4	123 24.1	70
FORT GRATIOT, MI	43 00.3	82 52.4	140	ROBINSON PT., WA	50 23.3	122 22.4	60
DETROIT (BELLE IS.), MI	42 20.4	82 57.6	70	GUARD IS., AK	55 26.8	131 52.8	200
SANDUSKY, OH	41 30.0	82 40.5	130	CAPE SPENCER, AK	58 12.0	136 38.3	260
BUFFALO, NY	42 52.2	78 54.2	120	C. HINCHENBROOK, AK	60 14.3	146 38.8	120
ROCHESTER, NY	43 15.4	77 36.2	100	POTATO PT., AK	61 03.0	146 42.0	100
TIBBETS PT., NY	44 06.1	76 22.2	70	COOK INLET, AK	TBD	TBD	200
				KODIAK, AK	59 00.0	156 30.0	200
				COLD BAY, AK	TBD	TBD	200
ATLANTIC & GULF COASTS				CONTROL CENTERS			
ARANSAS PASS, TX	27 50.0	97 03.5	180	ALEXANDRIA, VA			
GALVESTON, TX	29 19.7	94 44.3	180	PETALUMA, CA			
MOBILE PT., AL	30 13.6	88 01.4	170				
ENGLISH TURN, LA	29 52.7	89 56.6	190				
EGMONT KEY, FL	27 36.0	82 45.7	210				
KEY WEST, FL	TBD	TBD	150				
TBD—PUERTO RICO	TBD	TBD	200				
MIAMI, FL	25 44.0	80 09.7	120				
CAPE CANAVERAL, FL	28 27.6	80 32.6	250				
CHARLESTON, SC	32 45.5	79 50.6	150				
FORT MACON, NC	34 41.5	76 41.0	130				
CAPE HENRY, VA	36 55.6	76 00.5	130				
CAPE HENLOPEN, DE	38 46.6	75 05.3	180				
SANDY HOOK, NJ	TBD	TBD	100				
MONTAUK PT., NY	41 04.0	71 51.8	130				
BOSTON, MA	42 02.4	70 03.7	60				
PORTSMOUTH, NH	43 04.3	70 42.5	100				
BASS HARBOR, ME	TBD	TBD	140				

*Coverage range of Marine
Beacons over water

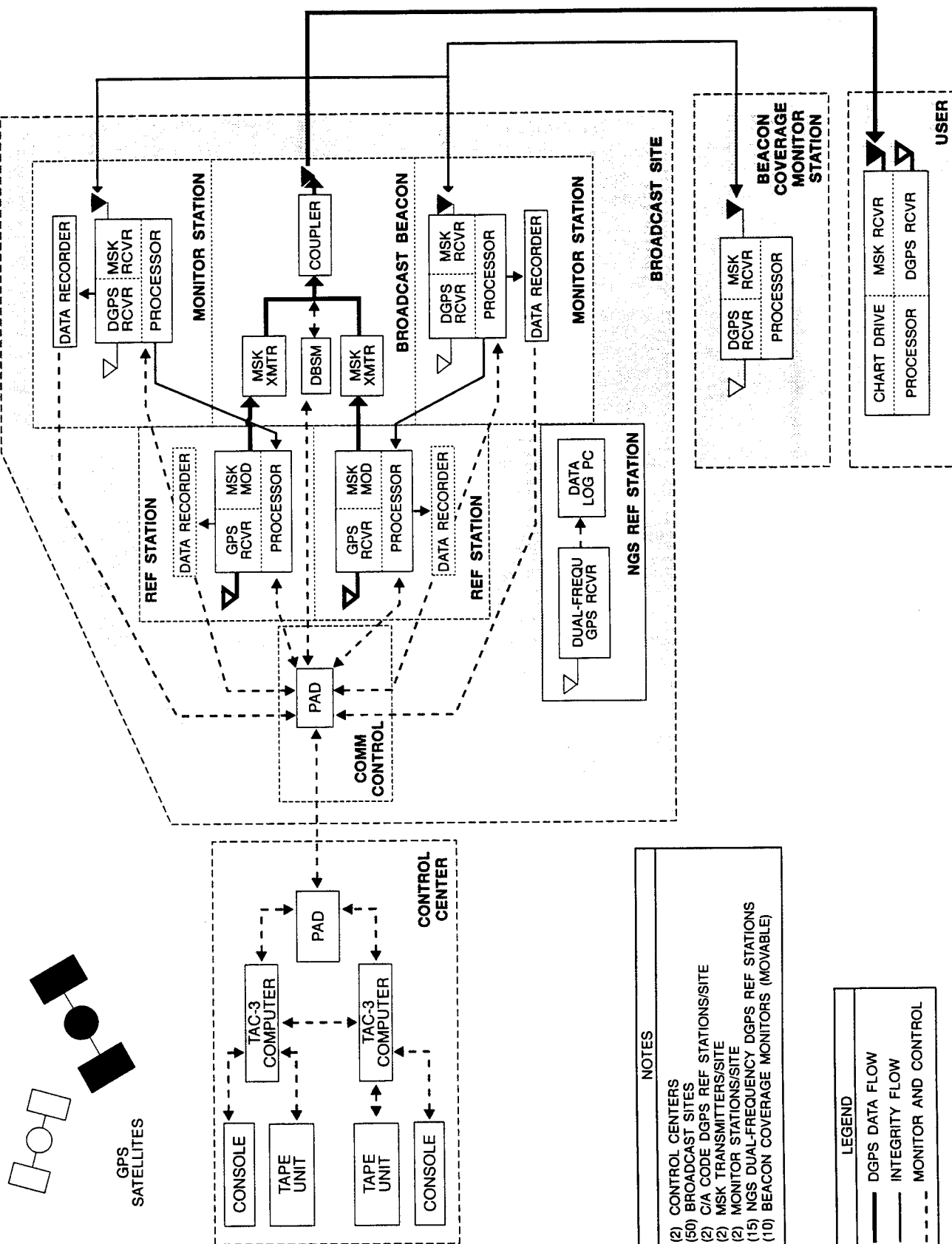


FIGURE 3. DGPS SERVICE ARCHITECTURE

1707-001(WP2)8/93

same satellites becomes a concern. For example, roughly 1% of the sky is lost for every 100 miles of separation. Thus, based on accuracy considerations, the reference stations should be as close as possible to the user and to each other to provide uniform coastal accuracy. The cost of the reference stations and supporting infrastructure will lead to a compromise solution of cost versus minimum required accuracy.

Location of the broadcast stations should be dictated by the transmission coverage requirements of the coastal regions and Great Lakes and the capabilities of the MSK transmitters. Since the original radiobeacon network is in place and was sited to be a marine navigation aid in its own right, there are more than enough sites to support the minimum transmission requirements of the USCG DGPS service. Therefore, the issue is what is the minimum set of broadcast stations required to provide continuous coastal coverage for the DGPS transmissions. This formed the basis for the proposed list of sites in Table 4.

Location of the monitor stations should be, as currently planned, one set per reference/broadcast site. The location of the monitor station relative to the broadcast site should probably be at a distance representative of that of a user. For reliability purposes, the monitors will be collocated with the broadcast beacons.

3.1.1.2 Communications Requirements - Status monitoring and control of the beacon site hardware will be accomplished by the control center using the AT&T FTS-2000, X.25 Packet Switching Service (PSS) communications network. This is a telephone line-based system configured for data transmission. Due to its low reliability, relative to the high-reliability requirements for the DGPS service, it is not used in the critical data flow path. All the hardware that is collocated at the beacon site is either hardwired together or connected via the beacon broadcasts.

The DGPS corrections will be transmitted in the RTCM SC-104, Version 2.1 [2] format which is typically sent at 100 bps. This format consists of "fixed" and "tentative" messages. For instance, the fixed messages include: Type 1 (DGPS corrections), Type 2 (delta DGPS corrections to accommodate ephemeris updates), Type 3 (reference station parameters including location), Type 6 (null frame), Type 7 (radiobeacon almanac), Type 9 (high-rate DGPS corrections to accommodate "SA" conditions), and Type 16 (special ASCII message to broadcast warnings of scheduled outages).

Since SA has been observed on Block II satellites since November 1991, there is an increased need for the Type 9 message. The Type 9 message will serve as the exclusive message for the broadcast of pseudorange corrections [2]. Hence, the Type 1 message will not be utilized. Also, due to the advent of continuous tracking receivers, the Type 2 message is no longer required and its use would only serve to increase the latency of the broadcast.

The "tentative" messages which will be used by the Coast Guard include: Type 5 (constellation health - unhealthy satellites which may be used for DGPS), Type 15 (atmospheric parameters), and Type 22 (integrity message providing information on both the current and future status of the broadcast). The Type 22 message will

replace the Type 16 message, if accepted by the RTCM committee. In addition, a new message will be required to send out the WADGPS unique corrections, such as partial spatial derivatives.

3.1.1.3 Equipment Requirements - Since the marine user will be using C/A-code receivers and the current Coast Guard DGPS service will only provide local area DGPS, C/A-code receivers appear justified for the reference stations. These receivers should, of course, provide an all-in-view satellite tracking capability with a 7.5 degree mask angle and survey quality measurement accuracy, as well as be able to transmit RTCM SC-104, Version 2.1 corrections.

The DGPS reference receiver will be a 12 channel C/A-code receiver. It will, most likely, incorporate the MSK (Minimum Shift Keying) modulator within its architecture. Candidate receivers include the Ashtech RANGER, the Magnavox 9012, and the Trimble DGPS/MSK Reference Station.

3.1.1.4 System Operating Procedures - Figure 3 shows the preferred DGPS service architecture. The primary data flow is indicated by the heavy solid lines. The light solid lines indicate the integrity monitoring at the beacon site, while the dotted lines show the status and control functions between the beacon site and the control site.

Each of the two DGPS reference receivers independently computes the DGPS corrections, formulates them into a MSK message, and sends them to separate transmitters. The choice of which message gets broadcast can either be controlled by the control center via the DBSM (Differential Broadcast Service Monitor) or automatically, based on the stronger of the two signals. The DGPS message is then broadcast by the beacon antenna. It is received by the user as well as by the dual-redundant monitor stations which are collocated with the beacon.

The user equipment demodulates the DGPS corrections, corrects the GPS measured pseudoranges, and computes a corrected position. This position can then be displayed on his chart drive, showing where he is relative to landmarks and the beacons.

The dual-redundant monitor stations repeat the same steps as the user to compute the corrected position of the monitor. By comparing this measured position to the surveyed position, it can be determined if the broadcast corrections are within acceptable limits. This information, together with any alarms, status messages and a message stating that the beacon is being monitored, is sent back to the corresponding DGPS reference receiver. This receiver then broadcasts these messages to the user.

Communication between the beacon site and the control center is via the AT&T FTS-2000 Packet Switched Service (PSS), the communication interface at either end is through the PAD (Packet Assembler/Dissassembler).

The beacon coverage monitors are located at 10 of the 50 beacon sites, near the outer limits of the beacon coverage area. They will be used to audit the coverage available and compare it to requirements. Their outputs are not transmitted in real time, either to the beacon site or the control center. The monitors will be moved periodically to the other sites.

The National Geodetic Survey (NGS) will also locate 15 dual-frequency DGPS reference receivers at 15 beacon sites. Their data will be archived and used primarily to support NGS efforts.

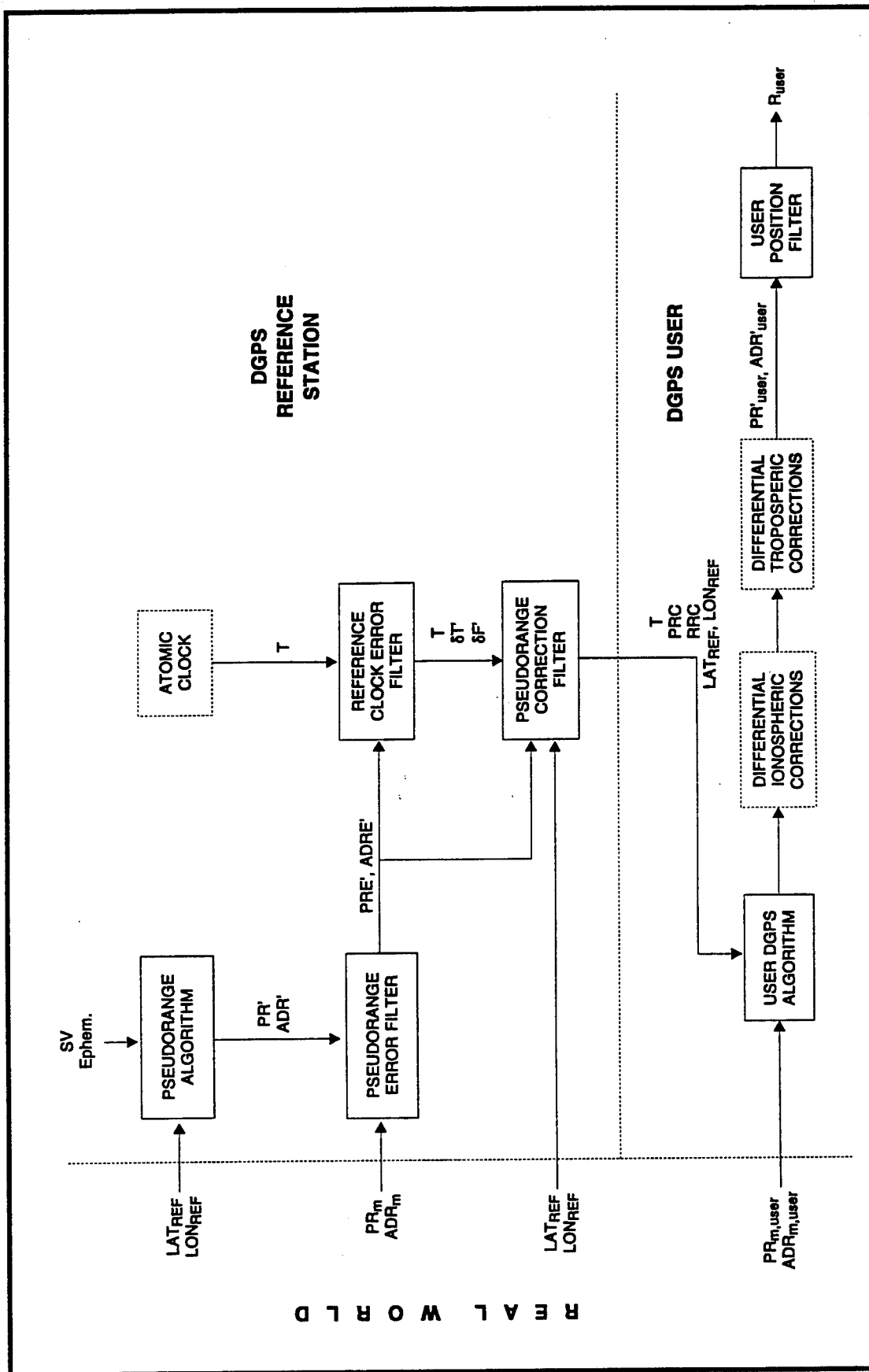
The functional data flow for the DGPS corrections is shown in Figure 4. Specifically, this figure shows the calculations that are performed at the reference station and those performed by the user. The monitor station, which is not shown, repeats the same calculations as the user except that additional calculations are performed in comparing the computed position with the known (surveyed) position of the monitor, in addition to the integrity message generation.

The reference station takes the surveyed location of the receiver together with the broadcast satellite ephemeris to compute the expected pseudorange and accumulated deltarange (PR' and ADR'). These values are differenced with the measured pseudorange and accumulated deltarange (PR_m and ADR_m) to compute the pseudorange and accumulated deltarange errors (PRE and ADRE). These errors are fed to both the Reference Clock Filter and the Pseudorange Correction Filter. The clock filter will estimate the receiver clock errors based on averaging the PREs and ADREs to isolate the clock bias and frequency offset errors (dT' & dF'). An option exists to use atomic clocks as the time reference. The clock error estimates are used to correct the PREs and ADREs in the Pseudorange Correction Filter in order to obtain the pseudorange and range rate corrections (PRC & RRC).

The user receives the RTCM SC-104 coded corrections, the time of the corrections, and the location of the reference station. He can directly apply the pseudorange correction, adjusted for transmission time delays, to the measured pseudoranges at his location and compute his position. Or, alternately, he can use his tropospheric model and the broadcast ionospheric model to differentially correct the pseudorange errors after they have been adjusted for transmission time delays, and before computing his position. This is accomplished by computing the tropospheric and ionospheric errors, using tropospheric and ionospheric (broadcast) delay models, at both his location and the reference station, and adjusting the pseudorange errors using the difference in tropospheric and ionospheric error estimates.

3.1.2 Component Architecture

This section discusses the component architectures of the reference station, the broadcast transmitter, the integrity monitor, the control station, and the maritime user.



1707-002(wp2)8/93

FIGURE 4. DGPS SERVICE FUNCTIONAL DATA FLOW

3.1.2.1 Reference Station - The reference station consists of a high quality all-in-view GPS receiver augmented with additional computational capability to generate the DGPS corrections in the RTCM SC-104 (Version 2.1) format. It also accepts inputs from the integrity monitor and can broadcast integrity warnings to the user. While co-location with the broadcast transmitter is not required, the reference stations will be co-located.

3.1.2.2 Broadcast Transmitter - The broadcast transmitter uses the medium frequency marine radiobeacons that are currently deployed. These beacons will have been modified to accept the RTCM SC-104 corrections by means of minimum shift keying (MSK) modulation of the carrier. The effective range of the beacons typically varies between 100 nm over land to 200 nm over water. The predicted coverage ranges for each of the transmitters of the local area DGPS service are shown in Table 4.

3.1.2.3 Integrity Monitor - The integrity monitor consists of a DGPS receiver, a computer, and a MSK radio receiver. Its function is to check the GPS broadcast, the DGPS correction data, and the MSK broadcast signal. There will be at least two monitors for each reference station/broadcast transmitter site. They will inform the collocated reference station, via cable, of the status and quality of the broadcast corrections.

3.1.2.4 Control Station - The control station will be connected to all the monitor stations and reference/broadcast sites in its area via a dedicated data communications network. Two computerized control stations operated by manned personnel will be established - one on the East Coast and one on the West Coast. The purpose of these stations is to perform system level monitoring and configuration control of the data communications network and equipment at the individual sites. Each control station will be capable of handling the entire network in an emergency.

3.1.2.5 Marine User - The marine user will typically have a MSK Radiobeacon Receiver, a GPS receiver capable of receiving DGPS corrections, and a chart display [2].

3.1.3 System Performance

In selecting the DGPS architecture described above, the Coast Guard considered two alternative architectures [3]. To determine which of these three architectures best met their needs for Harbor and Harbor Approach (HHA) navigation, as well as other precise navigation requirements, they established four selection criteria [4] which are summarized in Table 5. These requirements were developed for a vessel maneuvering in a harbor channel of different widths.

TABLE 5. DGPS SERVICE ARCHITECTURE SELECTION CRITERIA [4]

SELECTION CRITERIA	DEFINITION	DETERMINED BY
Availability of Accuracy	Required accuracy at the required level of availability throughout the coverage area	<ul style="list-style-type: none"> • DGPS ground system availability • Signal and noise environment
Reliability	Performing the specified function without failure under the given conditions for the specified period of time	<ul style="list-style-type: none"> • DGPS ground system failure rate • GPS satellite failure rate
Integrity	Threshold accuracy requirement (TAR) and probability of missed detection (P(MD)) are met for the required protection limit (PL) and time to alarm (TTA)	<ul style="list-style-type: none"> • Integrity ground system failure rate • DGPS signal unavailability at monitor sites • DGPS error spatial variability
Cost <ul style="list-style-type: none"> • Acquisition cost • Operations cost • Maintenance cost • Total life cycle cost 		

Table 6, which is based on *DGPS Architectures Analysis* [3], presents both the numerical requirements for these selection criteria and the resulting score for the preferred architecture as determined by TASC. As seen in this table, the Availability of Accuracy requirements for HHA were marginal, partly due to broadcast signal errors. Estimates of the accuracy of the DGPS corrections for this service will be presented in Section 4.

The reliability requirements were easily satisfied for all three categories of vessel maneuvers in a narrow harbor channel. While no integrity requirements have been specified by the Coast Guard, the loss of integrity was 10-20% for protection limits of 13m, corresponding to a narrow channel, and ranges to the beacon site of half of and maximum coverage range. The loss of integrity was 0.04-0.1% for the same ranges with a protection limit of 32 m, corresponding to a larger channel.

While there were no specific cost requirements specified, the total life cycle cost was estimated by TASC to be \$15.417 million. These costs would be considerably higher if the existing Marine radiobeacons and their facilities could not be used.

TABLE 6. DGPS SERVICE ARCHITECTURE SELECTION [3]

CRITERIA	REQUIREMENT	RESULTS
AVAILABILITY OF ACCURACY <ul style="list-style-type: none"> • Availability of Ground System • Availability of Signal 	8-20 m (2 drms) 99.7% (HHA)	Marginal (6 sites evaluated) 99.906% <99.79% (Required)
RELIABILITY <ul style="list-style-type: none"> • Ground System • Satellite Service 	2000 Fails/Mhr (CAT I) 1000 Fails/Mhr (CAT II) 500 Fails/Mhr (CAT III)	Exceeds requirements (121 Fails/Mhr) 121.1 Fails/Mhr 0.06 - 0.17 Fails/Mhr
INTEGRITY <ul style="list-style-type: none"> • 13 m Protection Limit • 32 m Protection Limit 	None	10% @ 0.5 of Coverage Limit 20% @ Coverage Limit 0.04% @ 0.5 of Coverage Limit 0.1% @ Coverage Limit
COST <ul style="list-style-type: none"> • Acquisition • Operations • Maintenance • Total life cycle (25 yr; 10% Discount Rate) 	None	\$ 5.381 M \$ 1.004 M/Yr <u>\$ 0.357 M/Yr</u> \$15.417 M

3.2 SYSTEM UPGRADE TO WADGPS ARCHITECTURE

Starting with the baseline DGPS architecture, three candidate system upgrades to obtain a WADGPS network architecture are presented in this section. These architectures are the federated local area DGPS (FLA-DGPS) network, the East-Coast/West-Coast Area DGPS (EC/WCA-DGPS) network, and the Continental U.S. (CONUS) DGPS Network.

When multiple independent receivers are used, with each receiver servicing its own area, two undesirable features occur. First, the accuracy degrades along the boundaries of the service area. Second, when passing from one service area to another, and from one reference station to another, significant step changes in the position can occur. Also, changing constellations in the outer regions of the service area can cause significant step changes in position. In contrast, it is possible in a network DGPS solution to have better accuracy when between stations rather than when close to a single reference station. This is due to the averaging process of reference receiver noise errors in the network solution.

If the network of reference receivers is large enough, in terms of area covered and number of sufficient receivers, the individual GPS error sources may be estimated separately. In this case, the corrections become, theoretically, reference station location independent. This concept was explored by TAU on the National

Aeronautics and Space Administration/Lyndon B. Johnson Space Center (NASA/JSC) Worldwide Differential GPS system design study [5,6,7].

The benefits of using a WADGPS network architecture include better accuracy coverage of an area, higher reliability to reference station failures, potentially fewer reference stations than required with a local area DGPS service, and better integrity information. This study assumes that the Coast Guard will implement a local area DGPS service that may be modified in the future to a WADGPS network, if the benefits warrant it.

The following paragraphs summarize some of the major issues in upgrading the local area DGPS service to a WADGPS network service. Principal issues are overall cost, accuracy improvement, correction and transmission integrity, and redundancy and reliability.

In defining a WADGPS network, a number of different architectures can be selected, as discussed in [8] and summarized in Table 7. Ideally, one selects the area over which one wishes to provide DGPS coverage, selects the WADGPS network software, then specifies the type, number, and location of the GPS reference receivers, and finally, selects the communications network.

TABLE 7. NETWORK DIFFERENTIAL GPS APPROACHES

NETWORK	APPROACHES
EXTENDED DGPS	<ul style="list-style-type: none"> • User selects closest reference receiver DGPS corrections, <u>or</u> • User interpolates between closest reference receiver DGPS corrections
LOCAL AREA DGPS NETWORK	<ul style="list-style-type: none"> • User computes average of reference receiver DGPS corrections, <u>or</u> • User computes weighted sum of reference receiver DGPS corrections
REGIONAL/WIDE AREA DGPS NETWORK	<ul style="list-style-type: none"> • Network consists of a quiltwork of local networks (dense network), <u>or</u> • Network estimates coefficients to partially functionalized DGPS errors (sparse networks)
WORLD-WIDE DGPS NETWORK	<ul style="list-style-type: none"> • Network measures/estimates tropo and iono errors, <u>and</u> • Network estimates satellite clock and ephemeris errors (sparse networks)

In Table 7, if one wishes to provide DGPS coverage over a larger area than can be covered by one reference receiver, multiple reference receivers can be used in an Extended DGPS approach. A more accurate and efficient use of these local reference stations is to net them together into a local area DGPS Network and provide DGPS corrections to the user in the form of spatial partial derivatives. This approach, described in [8], was developed by the authors for the U.S. Army Corps of Engineers [9].

If the coverage area increases to the size of CONUS or a fraction thereof, a regional or wide area DGPS approach is warranted. As discussed in *Differential DGPS Network Design* [8], this can be achieved with a quiltwork of local area DGPS networks or with an optimized regional DGPS network. The disadvantage of the former is that it requires a denser reference station network than the latter. The latter approach requires a sparser reference station network but with the disadvantage of increased communication network costs. It can also estimate

some of the separate DGPS error sources. The advantage of estimating separate DGPS error sources is that it minimizes spatial decorrelation in the corrections.

Finally, if one needs to provide continental or global coverage, a worldwide network DGPS approach can be selected, such as the TAU Worldwide DGPS network prototype system which was developed for NASA/JSC [6,7]. Based on the design philosophy used by TAU for the DGPS network software, this software is also suitable for a regional application.

Since the Coast Guard DGPS coastal coverage requirements encompass the CONUS, either the quiltwork of local DGPS networks or the partially functionalized DGPS error networks are potential candidates for a Coast Guard WADGPS network. However, the DGPS network software will differ considerably between these two approaches.

3.2.1 Federated Local Area DGPS Network

As discussed above, there are at least three approaches the Coast Guard can use to obtain a WADGPS network. The first is the quiltwork of local area DGPS networks, which was described in [8] as the simpler WADGPS approach. This will be called the Federated Local Area DGPS (FLA-DGPS) network. It represents a conservative approach that may be the best given the fact that the WADGPS network will evolve out of the local area DGPS service.

Figure 5 presents the proposed FLA-DGPS network architecture. Not shown in this figure are the redundant components. The basic concept is to designate each beacon site as its own DGPS master station and use the neighboring beacon sites, on either side, as the DGPS reference stations to form a three-station local area DGPS network. Using its own estimated DGPS corrections and those from the two neighboring sites, the master station computes the network corrections using a network algorithm. These algorithms are transmitted to the user, the collocated integrity monitor, and a coverage monitor. The coverage monitor is permanently assigned to each beacon site and located near the outer limits of the coverage area.

The user and the monitor stations compute their corrected positions using the broadcast network corrections. The monitor stations are now able to establish the null baseline integrity of the corrections as well as the integrity of the corrections near the coverage limits. As before, the monitor stations notify the master station that it is being monitored, whether the corrections are within the specified integrity limits, and of any alarm status messages. This information will then be broadcast to the user.

The control stations perform the same operations as they do for the DGPS service, which is to monitor the beacon site and control the individual components as required. As before, the critical navigation data flow does not go through the control center.

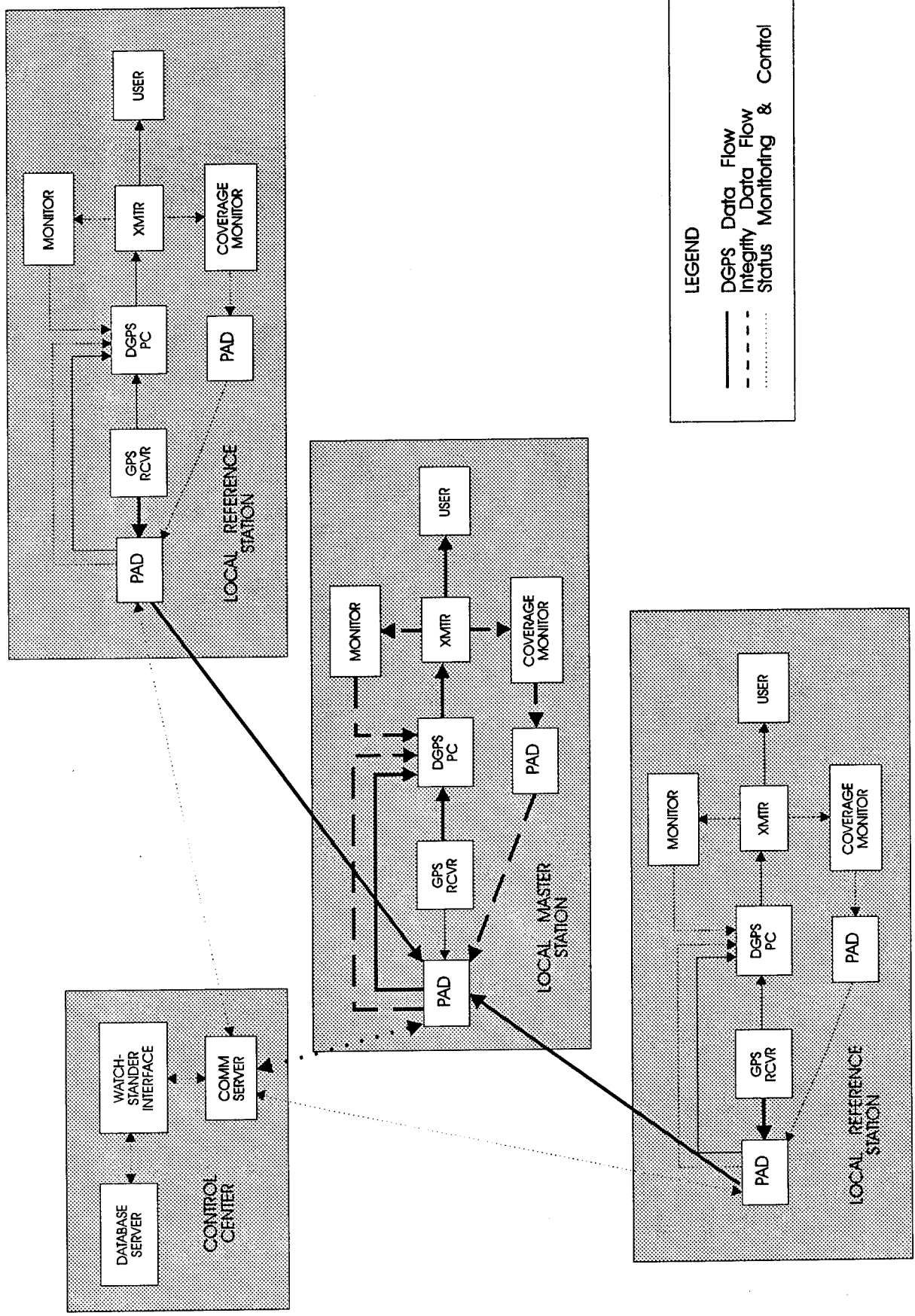


FIGURE 5. FLA-DGPS NETWORK ARCHITECTURE

Not shown in Figure 5 are the redundant components of the FLA-DGPS network. Basically, the same redundant DGPS reference receivers, transmitters, and monitor stations will be used here as were used for the DGPS service. Now, however, redundant PCs have been added to perform the Network Correction Algorithm calculations. Alternately, the DGPS receiver processors would have been upgraded. Also, a dual-redundant coverage monitor has been assigned to each beacon site. These coverage monitors and the neighboring beacon sites are connected to the master site using the AT&T X.25 communication network. This places the X.25 communication network in the critical navigation data path. However, by incorporating a fault-tolerant (flexible) software architecture at the master site, the network corrections will gracefully degrade to the DGPS service corrections with the loss of the corrections from the neighboring beacon sites.

Figure 6 shows the functional data flow for the network corrections to the user. Each of the beacon site DGPS reference receivers compute their own DGPS corrections, as they did under the DGPS service architecture. These corrections are sent to the network processor at the local master station (Station B in Figure 6). Then the processor formulates the network corrections for that site and broadcasts them to the user, as well as to the monitor stations which are not shown in this figure.

The specific network algorithm outlined in this figure is a new algorithm which was developed under this study and is designated the Minimum Variance Algorithm (MVA). As will be discussed in more detail in Section 5, it outperforms the Partial Derivative Algorithm (PDA), particularly for the difficult coastal geometries of the Coast Guard DGPS service.

The MVA algorithm establishes the DGPS spatial decorrelation function, $r(b)$, and sends it, together with the inverse network correlation matrix, $[G]$, to the user. The user evaluates his spatial decorrelations relative to each of the three sites in the network using the locations of the sites and the broadcast correlation function. Next, he uses these spatial decorrelation functions, together with the broadcast network inverse correlation matrix, to compute his weighting coefficients. He applies the weighting coefficients to each of the three site broadcast corrections, PRCs, to determine his network weighted correction. The user can then compute his position using the corrections.

3.2.2 East-Coast/West-Coast Area DGPS Network

A second approach is to form two networks. An East Coast network would include all East Coast, Great Lakes, Gulf Coast and Puerto Rican reference stations. A west Coast network would include all West Coast, Alaskan, and Hawaiian reference stations. This network, designated the East-Coast/West-Coast Area DGPS (EF/WCA-DGPS) network, might be a natural solution due to the fact that there will be separate East Coast and West Coast control centers under the proposed local area DGPS service as described in [2, 10, 11].

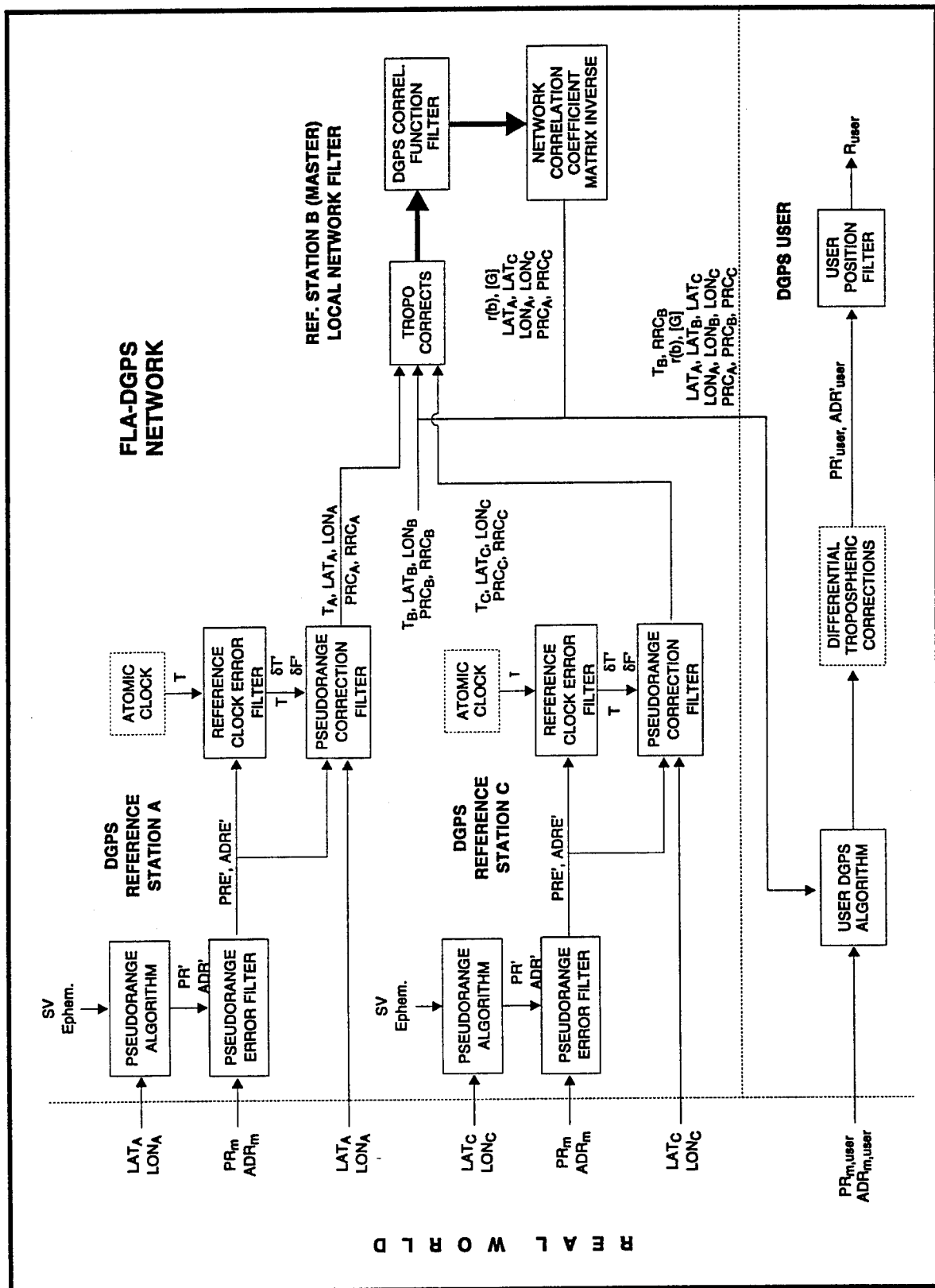


FIGURE 6. FLA-DGPS NETWORK FUNCTIONAL DATA FLOW

1707 OFEA-00-018-03

Figure 7 presents the EC/WCA-DGPS network architecture. This architecture takes the FLA-DGPS network architecture and eliminates the PCs at each beacon site and the necessity for direct communications between the beacon sites. It also places the Network Correction Algorithm at the regional (East Coast or West Coast) control center. This places the X.25 communications network, which is baselined to interconnect the sites with the control centers, in the critical data flow path. The impact of losing the connection with the control center could be minimized by allowing the local stations to always broadcast their DGPS corrections in the absence of a network correction.

The operational flow of the data proceeds as follows. Each of the reference stations sends its corrections to their regional control center. The control center computes the network correction valid for each beacon site and sends it back to them. The beacon sites then broadcast the network corrections to the user and the monitor as well as coverage monitors at that site. The monitors perform the same function in this system as they do for the FLA-DGPS network.

Figure 8 presents the functional data flow for the EC/WCA-DGPS network. The individual beacon sites compute their DGPS corrections and send them to their regional control center. The regional control center uses a network algorithm to determine the regional DGPS correction matrix based on a matrix of possible user locations. This matrix is then used at the control center to formulate the local network corrections for each beacon site.

Shown in Figure 8 is a network algorithm based on the Minimum Variance Algorithm used in the FLA-DGPS architecture. While the accuracy of this algorithm is high, the complexity of the user algorithm for a network of more than three beacon sites makes it impractical to broadcast the elements of this algorithm to the user. Instead, the control center will establish the corrections for a matrix of potential user positions in the regional network coverage area using the MVA algorithm and inputs from all the sites in that region. It will then perform a fit of a local network algorithm, such as the Partial Derivative Algorithm. This fit should be much better than the locally (directly) computed Partial Derivative Network corrections since it is based on not only the local beacon site but also "pseudo-sites" located at each of the user location matrix points. The specific local Network Correction Algorithm shown includes two first-order and three second-order partial derivative coefficients for completeness. This will be examined further in Section 5. The user and monitor calculations proceed as before.

3.2.3 CONUS DGPS Network

The third DGPS network approach is a more regional, or wide area, DGPS approach. It nets all of the CONUS, Hawaiian, and Puerto Rican reference stations into a single network. For simplicity, it will be designated the CONUS DGPS network. This network might achieve a separation of the individual DGPS error sources due to the more favorable geometry of the distributed reference receivers. It might also achieve a potentially better overall accuracy at a potentially higher communications cost.

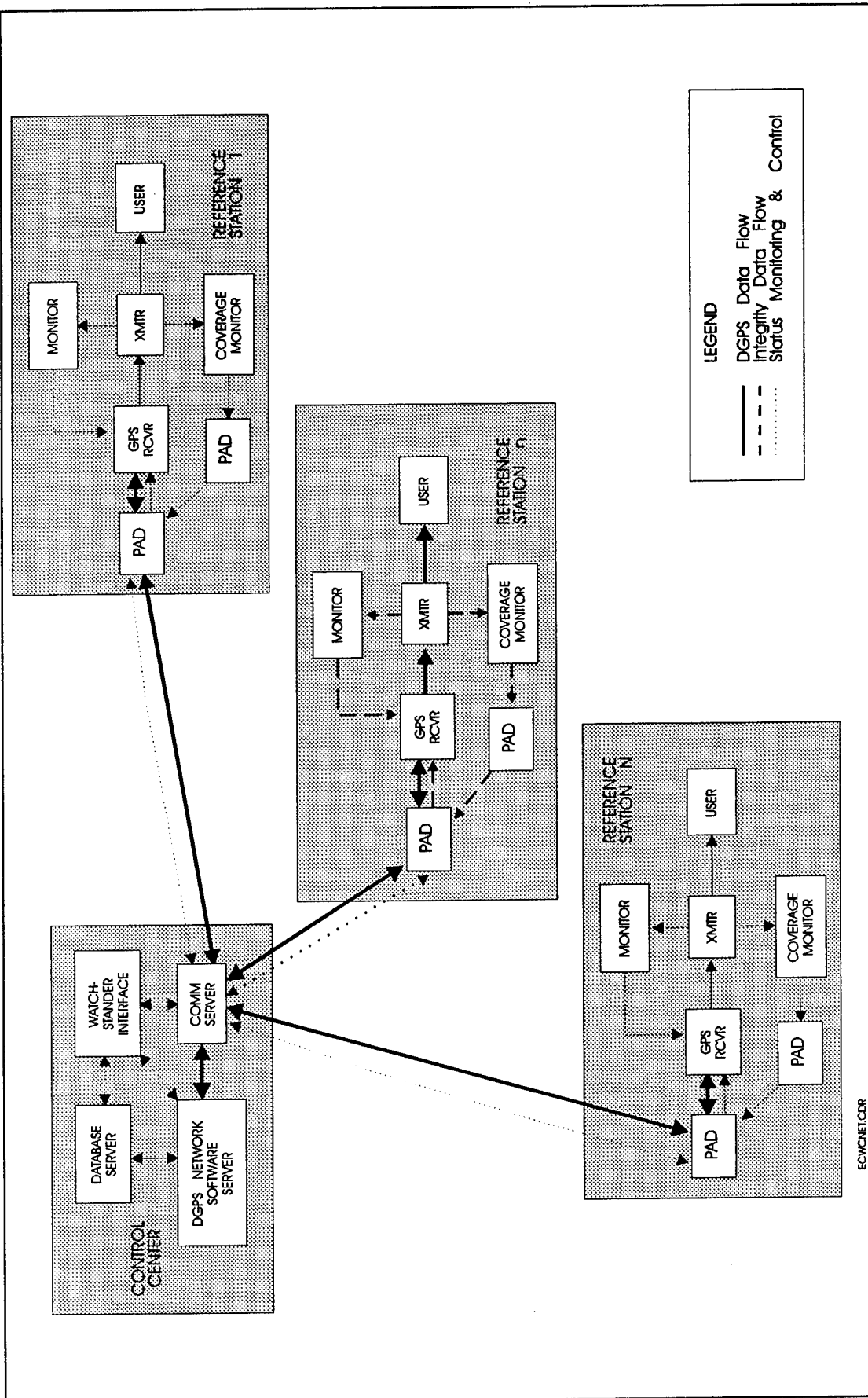
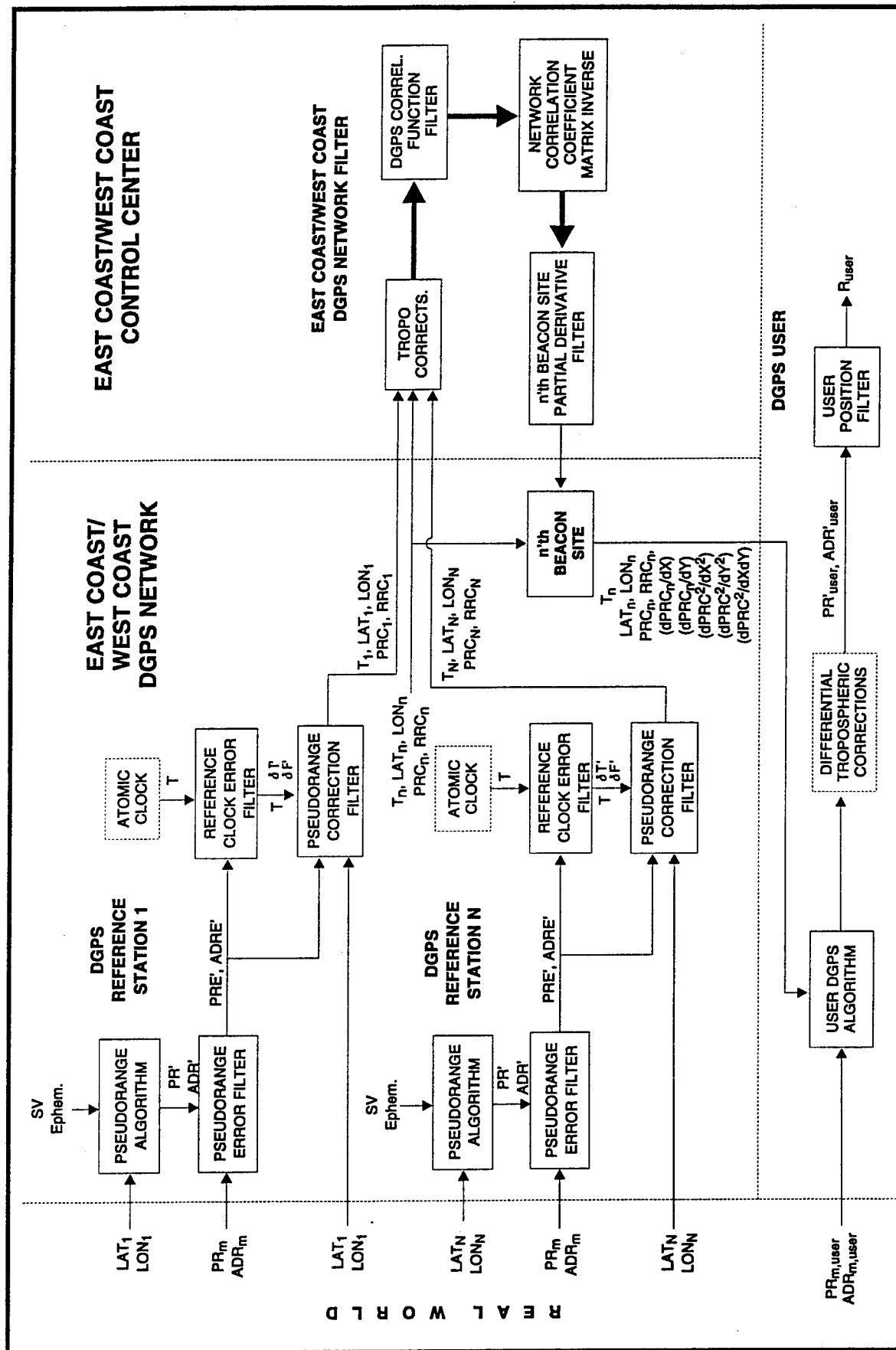


FIGURE 7. EC/WCA-DGPS NETWORK ARCHITECTURE



1707-004/wp2/893

FIGURE 8. EC/WCA-DGPS NETWORK FUNCTIONAL DATA FLOW

While the previous two network DGPS architectures have used the same assets as the DGPS service, with minor changes in the communications and the addition of permanent coverage monitors, the proposed architecture for the CONUS DGPS network introduces additional DGPS reference receivers. Specifically, at 16 of the 50 beacon sites dual-redundant, dual-frequency DGPS reference receivers would be introduced.

One option might be to use the 15 National Geodetic Survey (NGS) dual-frequency DGPS reference receivers and supplement them with an equal number of USCG receivers, thereby minimizing the cost of new receivers. This would have to take into consideration the possible different requirements of the USCG and the NGS, the type of NGS receivers, and their intended locations to determine if this is a feasible option. The choice of 15-16 receivers is based on the maximum number of satellites visible to the extended CONUS network.

Figure 9 presents the proposed CONUS DGPS network architecture. DGPS corrections and dual-frequency measured ionospheric delays will be sent from the 16 dual-frequency beacon sites to each of the control centers. The control centers will estimate, redundantly, the CONUS network corrections. These corrections will then be sent to all 50 beacon sites for broadcast to the users, as well as to the local beacon site monitors. The beacon site monitors will perform the same integrity monitoring as previously specified for the FLA-DGPS and EC/WCA-DGPS networks.

As was the case for the previous two networks, the X.25 communications network will be used to transmit navigation correction data between the beacon sites and the control centers. To make this architecture more immune to failure of this data link, the beacon sites would always be able to broadcast their basic DGPS (single frequency) corrections, even if the network DGPS corrections were not available.

Figure 10 presents the functional data flow for the CONUS DGPS network. The software at the 16 dual-frequency beacon sites has been enhanced to include a dual-frequency ionospheric delay filter that uses the dual-frequency measured pseudorange and accumulated delta-range measurements. In addition to estimating the ionospheric delay, the iono filter must estimate the inter-channel bias for the dual-frequency DGPS receiver. These estimated dual frequency delays are used to provide an iono-free estimate of the pseudorange and accumulated delta-range errors.

The iono-free pseudorange and range rate corrections as well as the iono delays are sent to the control center network filter. The ionospheric delays are sent to the network ionospheric delay model estimator which updates the CONUS network ionospheric model. The outputs of this model are then sent to the n'th Beacon Correction Formulation Algorithm.

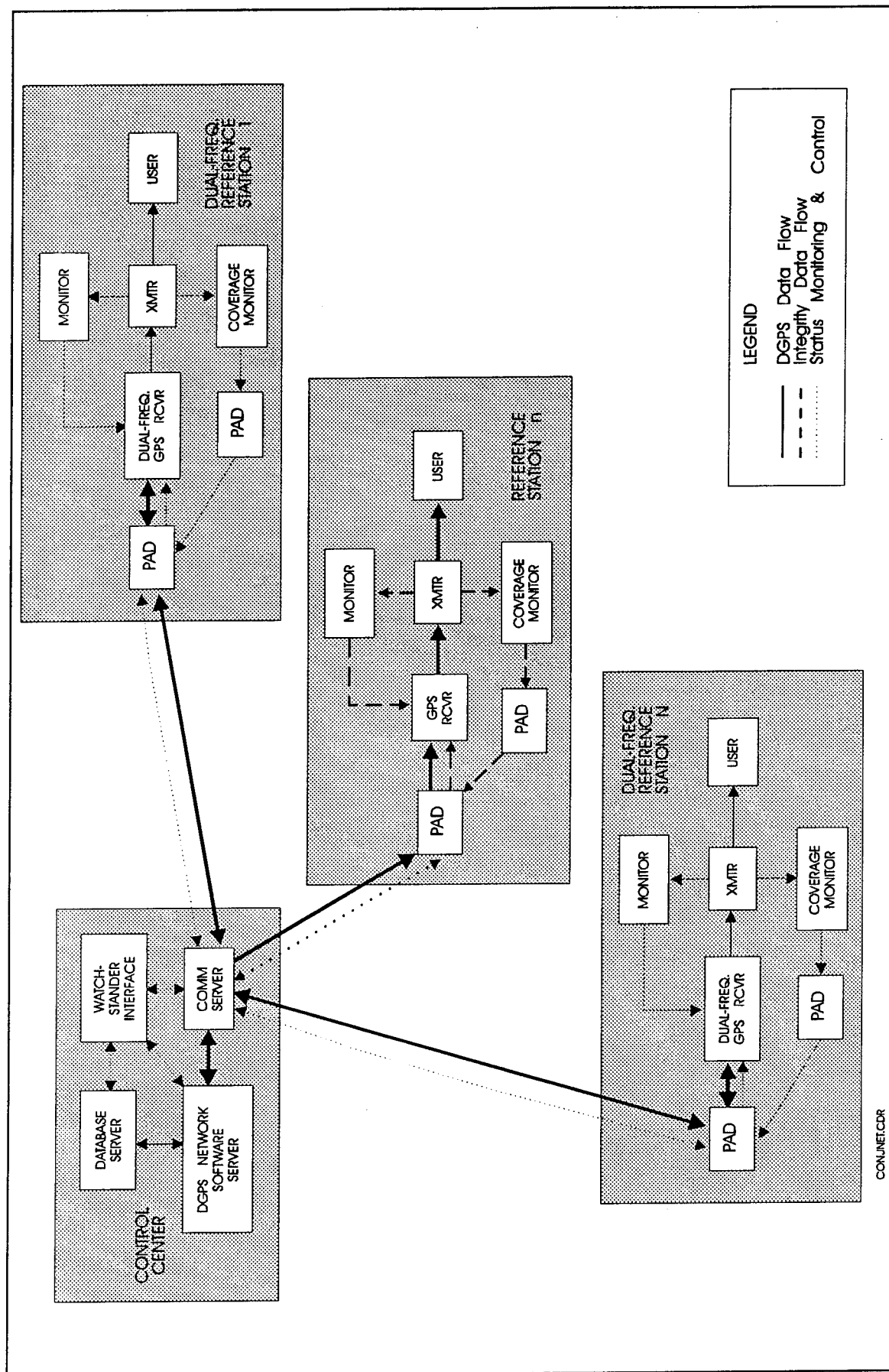
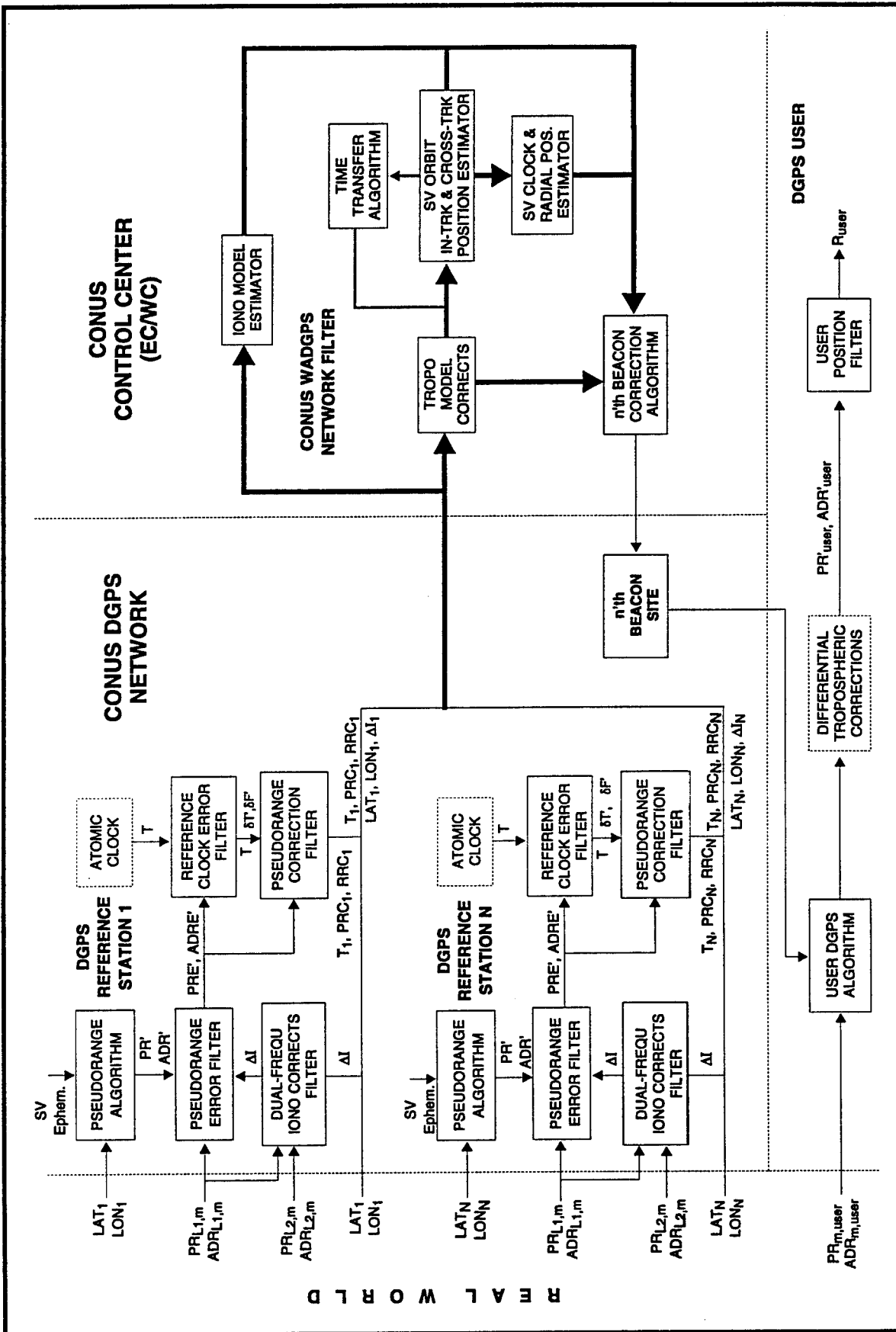


FIGURE 9. CONUS-DGPS NETWORK ARCHITECTURE



1707-003(w2)1993

FIGURE 10. CONUS DGPS NETWORK FUNCTIONAL DATA FLOW

The pseudorange and range rate corrections are passed to the tropospheric delay model which determines and applies tropospheric corrections to the data. These tropospheric corrections are also sent to the n'th Beacon Correction Formulation Algorithm.

The tropospheric and ionospheric delay corrected pseudorange and range rate corrections are then passed to the satellite lateral and normal orbit position estimator. This algorithm preprocesses the corrections and uses them to estimate the satellite lateral and normal orbit positions. The preprocessed corrections are also passed to the Time Transfer Algorithm which synchronizes the individual beacon reference receiver clocks.

The satellite lateral and normal orbit position errors are passed to the n'th Beacon Correction Algorithm as well as to the satellite clock and radial orbit position estimator. The satellite clock and radial position estimator also accepts the pseudorange and range rate errors and corrects individual error estimates relevant to that site. These estimates are calculated by the control center network filter software.

The n'th Beacon Correction Formulation Algorithm provides a means for the control center to formulate a custom practical network correction solution for each of the 50 beacon sites. This might again be a local Partial Derivative Algorithm Solution. It also could send the individual error estimates relevant to that site, which have been estimated by the control center network filter software.

The control center transmits to the local beacon sites their network corrections. They are broadcast to the user as well as the monitor stations. The monitor stations again perform the same data integrity calculations that were specified for the previous two candidate DGPS networks.

3.3 WADGPS ARCHITECTURE AUGMENTATION

To maximize the performance and minimize the cost of the proposed Coast Guard WADGPS network, at least two additional resources have been reviewed as candidates for augmenting this network. The first is the use of the ionospheric data which will be available from the Air Force Space Forecast Center (AFSFC). The second is the potential synergy between the Coast Guard and the proposed FAA WADGPS networks.

This section examines the potential synergies between these related programs and the WADGPS architecture. Specifically, the benefits of using the AFSFC Near-Real-Time Ionospheric Effects Data and the synergies with the FAA WADGPS network will be discussed. Potential benefits from this augmentation might include lower deployment and operational costs, higher or more extended DGPS accuracy, and higher reliability of the system.

3.3.1 AFSFC Near-Real-Time Ionospheric Effects Data

A number of efforts that are most directly applicable to the USCG WADGPS network are summarized in Table 8, based on [12]. The Air Force plans to deploy a global network of 17 ionospheric monitoring sites which

have been designated the Trans-Ionospheric Sensing System (TISS). The TISS network, which is illustrated in Figure 11 [12], will measure the Ionospheric Total Electron Content (TEC) and Ionospheric Scintillation for all GPS satellites with elevation angles greater than 15 degrees, in real time, at 15-minute intervals. Prototype dual-frequency GPS receivers will be deployed at: Shemya and Eileson, Alaska; Thule, Greenland; Goose Bay, Labrador; and Otis AFB, Massachusetts by June 1993. Full operational deployment of the TISS network is planned for September 1995.

The Phillips Laboratory, Geophysics Directorate, AFSC, and Computational Physics, Inc. are jointly developing an ionospheric delay model for AFSFC that is designated the Parameterized Real-Time Ionospheric Specification Model (PRISM). This model is based on parameterized physical models, rather than on statistical or climatological models. In addition to a wide variety of input parameters, it incorporates near-real-time measurement data, such as will be provided by the TISS network. This model was to be tested with TISS data in September 1992, and it is planned to be fully operational by September 1994. The outputs of this model will be available in near-real-time, on an hourly basis, from AFSFC to Air Force or other authorized governmental users. While the accuracy goal is to estimate the ionospheric TEC to < 1 TEC, an accuracy of 2-2.5 TEC (0.3 - 0.4 m) will probably be achieved, according to the Phillips Laboratory. Specific arrangements will have to be made with AFSFC to obtain this data and specify the required format, frequency, and the means of transmission.

TABLE 8. AIR FORCE SPACE FORECAST CENTER (AFSFC)
NEAR-REAL-TIME IONOSPHERIC EFFECTS DATA

AFSFC efforts that are most directly applicable to the Coast Guard WADGPS network are:

1. Trans-Ionospheric Sensing System (TISS)

- Consists of a global network of 17 sites monitoring ionospheric TEC and scintillation for all GPS satellites visible (>15° elevation) at sites in real time
- Install prototype monitors by June 1993 at Shemya & Eileson, Alaska; Thule, Greenland; Goose Bay, Labrador; and Otis AFB, Massachusetts — FOC: September 1995

2. Parameterized Real-Time Ionospheric Specification Model (PRISM)

- Developed by the Phillips Laboratory, Geophysics Directorate & Computational Physics, Inc.
- Based on parameterized physical models — not statistical or climatological models
- Incorporates near-real-time data and a wide variety of input parameters
- Currently under validation, it was scheduled to be tested with TISS data in September 1992 — FOC: September 1994

3. Ionospheric Forecast Model (IFM)

- Derives ionospheric 12-hour forecast based on the ionosphere derived by PRISM, using a highly accelerated "first-principles" physical calculation
- First version available for validation in FY94 — FOC: FY95

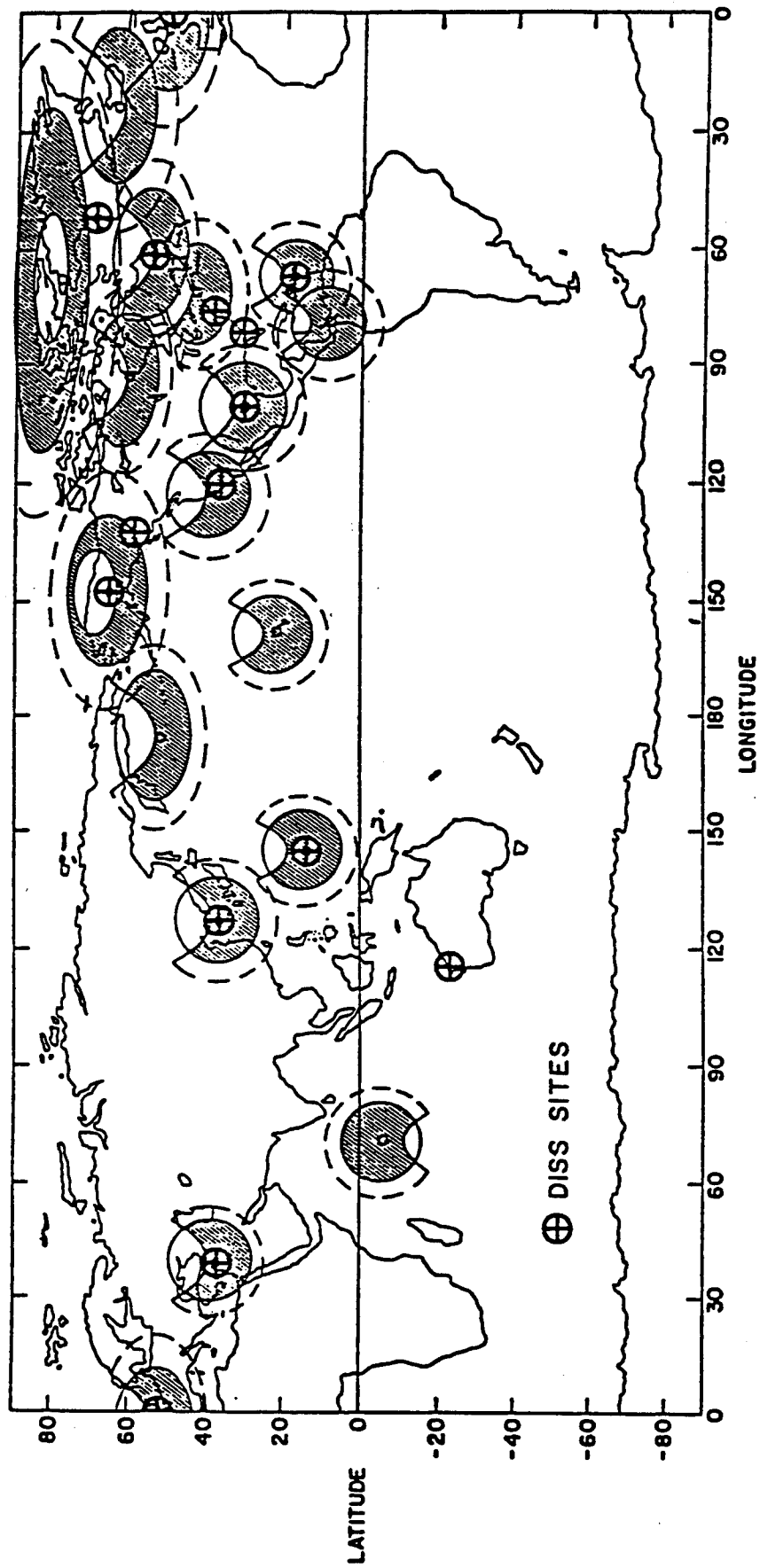


FIGURE 11. AFSFC TRANS-IONIC SENSING SYSTEM (TISS) NETWORK

In addition, an ionospheric prediction model is being developed that has been designated the Ionospheric Forecast Model (IFM). It will be able to derive a 12-hour ionospheric forecast based on the PRISM ionospheric data. It is based on a highly accelerated first-principles' set of physical calculations. Validation will be started in FY94, and it is planned to be fully operational in FY95.

Depending on the accuracy of the PRISM data, the format of the data, and the required user algorithms, the IFM could extend the C/A-code DGPS user accuracy significantly. This would be accomplished by providing parameters necessary for the computation of the local versions of the ionospheric delay model. Questions that will need to be addressed are: when will this data become available; how frequently is it updated; what is the area of coverage; how accurate is it; and, how can it be accessed. Separately, further work is required to determine the benefits of using this data. It will be based on any limitations of the data and consideration of its optimal usage in the WADGPS network software.

3.3.2 FAA Wide Area Differential Global Positioning System (WADGPS)

Based on information provided by contacts in the FAA, the following section summarizes the FAA Wide Area Differential Global Positioning System (WADGPS).

The FAA has an aggressive program to integrate satellites into the National Airspace System and civil aviation, worldwide. It has approved the use of GPS as an input to multisensor navigation systems and as a supplemental radionavigation system. The FAA Satellite Program Office is now involved in an extensive research and development effort to augment the basic DoD-provided GPS Standard Positioning Service (SPS) to meet civil aviation Required Navigation Performance (RNP) for all phases of flight.

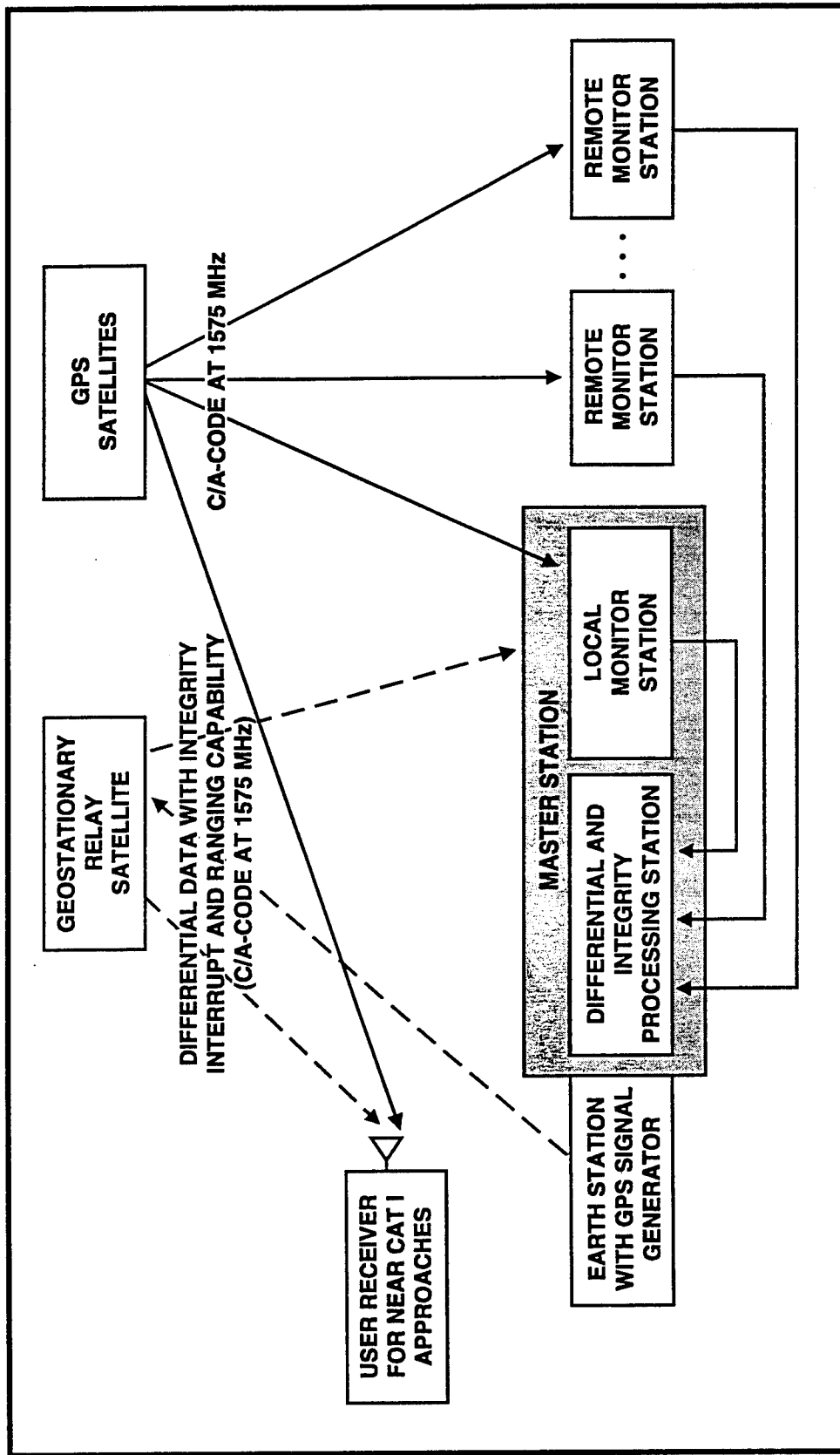
The current goal is to develop and implement a WADGPS system suitable for all phases of flight. It is expected to be operational by about the year 2000. However, this does not include Instrument Flight Rule (IFR) precision approach and landing Category II and III. It does include a local area carrier differential system for IFR precision approach and landing Category II and III. No operational date has been established for this capability since it is a feasibility study at this time.

The FAA's WADGPS system is to be composed of 20 to 30 wide area reference stations separated by about 500 miles. They will be located across the conterminous US and will not be as close in Alaska, Hawaii, Canada, Mexico (possibly), the Caribbean area, and Bermuda. These reference stations will be dual-frequency and collect information on GPS and GPS-like geostationary satellites. The information which will be collected includes integrity, clock errors, orbital position, and ionospheric information. The information from each reference station will be linked to at least two (maybe up to four) wide area master stations. At these master stations the wide area integrity broadcast and WADGPS messages will be calculated using the information from all of the reference stations.

This data will be sent from each master station to at least two satellite-earth stations for each geostationary satellite. Here the messages will be included in a GPS-like signal suitable for ranging. This GPS-like signal will be transmitted to geostationary satellites for broadcast on the GPS L₁ frequency with unique codes. The broadcast message will contain GPS and GPS-like satellite integrity, clock correction, ephemeris correction, ionospheric parameters, and other information required for the integrity and differential service.

Users suitably equipped to receive this broadcast are expected to obtain position fixing and navigation guidance to meet civil aviation requirements for all phases of flight except IFR precision approach and landing Categories II and III. This FAA WADGPS concept is summarized in Figure 12. The FAA requirements include integrity warning to the user within six seconds of when a satellite is first out of tolerance, with an undetected error of less than 1×10^{-8} . Additional requirements are for a vertical accuracy of about 4 meters (95%), a probability of loss of the navigation function during a precision approach of less than 1×10^{-4} , and an availability of 99.999%.

Since the requirements for the FAA WADGPS system are to provide coverage over the conterminous U.S., Alaska, Hawaii, Canada, Mexico, and adjacent oceanic areas, there appears to be a very strong potential synergy with the US Coast Guard WADGPS system. The FAA WADGPS system will also be expandable to a worldwide system.



1707-006(WP2)

FIGURE 12. WIDE AREA DIFFERENTIAL GPS (WADGPS) CONCEPT

4. WADGPS MAJOR ISSUES

This section identifies the major issues that must be addressed before upgrading the DGPS service to a WADGPS network architecture. Those which are not resolved during this phase of the contract will be identified. The steps required to resolve these issues will be discussed below. The key issues can be summarized under five headings: Cost, Performance, Integrity, Reliability, and Other.

4.1 COST

Based on Table 9 [3], the proposed Coast Guard DGPS Service Total Life Cycle Cost is estimated to be \$15.4 million, based on a 25-year life and incorporating a ten-percent discount rate. This figure is based on planning cost estimates of \$5.38 million for acquisition, \$1.00 million per year for operation, and \$0.357 million per year for maintenance. This cost incorporates the fact that the Marine beacons and their facilities are already in place and do not have to be purchased. Also, the communication network will be leased from AT&T, and hence, will not have to be purchased. As indicated in *Implementation of the U.S. Coast Guard's Differential GPS Navigation Service* [2], however, total program costs might be considerably higher for the proposed DGPS service.

TABLE 9. WADGPS NETWORK COST ESTIMATES

CATEGORY	COST	INCREMENTAL COST INCREASE ¹		
	DGPS [3]	FLA-DGPS	EC/WCA-DGPS	CONUS DGPS
Acquisition (\$M):	\$ 5.381	\$2.300 ²	\$2.290 ³	\$3.432 ⁴
Operations (\$M/Yr):	\$ 1.004	\$0.470	\$0.610	\$0.610
Maintenance (\$M/Yr):	\$ 0.357	\$0.045	\$0.045	\$0.045
Life-Cycle Cost ⁵ (\$M)	\$15.417	\$6.102	\$7.125	\$8.267

¹ Each WADGPS architecture is treated as if it is derived from the basic DGPS service architecture—not the previous WADGPS architecture.

² Includes purchase of 90 coverage monitor DGPS-MSK receivers, 100 master site central processing units (CPUs) or upgrades to DGPS reference receivers, and 100 coverage monitors (data recorders).

³ In addition to 90 coverage monitor DGPS-MSK receivers, it includes four workstations for the two control centers.

⁴ In addition to (3), it includes 32 P-code DGPS reference receivers.

⁵ Based on 25-year life cycle and 10% discount rate.

The basic guideline that has been used in formulating the three candidate WADGPS network architectures is to take maximum advantage of the assets of the DGPS service so as to minimize the additional cost required to upgrade to a WADGPS network. Thus, for all three network architectures the ten coverage monitors will be

increased to 50 dual-redundant coverage monitors. Each monitor will be permanently assigned to a beacon site which requires that they have appropriate facilities and communications with the beacon site. The communications will be the X.25 AT&T network, which is currently baselined for the DGPS service to provide communications both between the beacon sites and with the coverage monitors. The facilities might be existing Coast Guard facilities located near the outer limits of each beacon coverage area, thus requiring, at most, the leasing of a room for the equipment.

For the FLA-DGPS network, dual-redundant processors will be required to host the local master station network software. Depending on the complexity of this software, it might be ported in the DGPS reference receiver itself, which might need to be upgraded with additional processing capability. This might require only a firmware change in the existing receivers. For the EC/WCA-DGPS and CONUS DGPS networks, a dual-redundant network software workstation would have to be acquired for each of the two control stations. In addition, extra staff would be required at the control centers for these two WADGPS architectures to monitor and control the network software workstations.

Finally, for the CONUS DGPS network, 16 dual-redundant, dual-frequency P-code DGPS reference receivers would have to be acquired. The cost might be minimized by using the planned 15 NGS P-code DGPS reference receivers for redundancy. In Table 9, it was assumed that the NGS receivers would not be available to the CONUS DGPS network.

Examining the incremental acquisition costs involved in acquiring any of the three WADGPS network architectures, one of the major contributors (\$1.35 million) is the cost of additional coverage monitors. These may be acquired as part of the DGPS service architecture, whether or not a WADGPS architecture is pursued, based on discussions in the RTCM Monitor Sessions. Therefore, their cost should not be used to penalize the WADGPS architectures.

Overall, it can be seen that there is no significant cost difference between the FLA-DGPS and EC/WCA-DGPS network acquisition costs. If one looks at the incremental cost of moving from the FLA-DGPS architecture to the EC/WCA-DGPS architecture, the incremental acquisition costs are \$0.228 million and the incremental operations costs are \$0.140 million. This might suggest selecting the EC/WCA-DGPS network architecture and implementing it as a phased development from a modified FLA-DGPS network architecture to a full-blown EC/WCA-DGPS network architecture.

Finally, the incremental acquisition costs for the CONUS network are dominated by the coverage monitors and the P-Code DGPS reference receivers.

Life Cycle Costs were computed by TASC for the DGPS service as \$15.417 million for a 25-year life cycle and assuming a 10 percent annual discount rate. The corresponding incremental Life Cycle Costs to implement the three WADGPS network architectures are, respectively: \$6.102 million, \$7.125 million, and \$8.267 million.

It should be noted that the WADGPS network costs presented in Table 9 are very preliminary and reflect the best judgments of the authors. Their purpose is to identify the major cost elements as well as to provide a comparison of the costs between the three WADGPS architectures.

4.2 PERFORMANCE

One of the key benefits in upgrading to a WADGPS network is that the overall accuracy will be improved and more uniform over the coverage area. For local area networks, this is achieved by using weighted corrections and broadcasting the corrections, as well as the additional information required to determine the weighting coefficients, to the user [8]. For WADGPS networks, this is achieved by partially, or totally, isolating the separate error components of the DGPS error. This facilitates the broadcasting of correction algorithms to the user that are more accurate than the individual reference station corrections and are valid over a much larger area.

Table 10 presents GPS Error Budgets for GPS (stand-alone), DGPS, and the three WADGPS network architectures. The errors are separated into Satellite Errors, Selective Availability, Atmospheric Errors, and Reference Receiver Errors. These are combined to obtain the DGPS error. With the user receiver errors, the User Equivalent Range Error (UERE) is obtained in the measurement domain. Using an average Horizontal Dilution of Precision (HDOP) and specifying the Navigation Accuracy in terms of 2 drms, the horizontal navigation accuracy is obtained. While the average beacon coverage range is closer to 300 kilometers, the baseline accuracy is extended out to 500 kilometers in this table. The sources and assumptions used to derive these error estimates will be discussed both in Section 5 and Appendix A, and therefore, will not be repeated here.

In summary, the GPS and DGPS error estimates were obtained from various sources. The FLA-DGPS and EC/WCA-DGPS network DGPS error estimates were then derived from the DGPS error estimates of the second column. For the FLA-DGPS network case, a generic three-station network was assumed based on the average geometries found for the East, Gulf, and West Coast DGPS beacon sites. The Minimum Variance Algorithm was used to derive the weighting coefficients, and the error covariance was evaluated to obtain the FLA-DGPS network error estimate. This same process was used to obtain the EC/WCA-DGPS network error estimates, except that a generic five-station network was used. Finally, the CONUS WADGPS error estimates were obtained from various sources.

Focusing on the navigation accuracy, we see that DGPS navigation accuracy degrades almost linearly with distance. This can also be seen by comparing the DGPS error estimates shown in Figure 13. For the FLA-DGPS network, the navigation accuracy is improved by 20% at 300 kilometers over the corresponding DGPS navigation accuracy. In turn, the EC/WCA-DGPS network navigation accuracy is improved by 29% at 300 kilometers over the corresponding DGPS case. These estimates are conservative, as discussed in Section 5.3.1, since the user is located in nearly the worst case direction relative to the generic network.

TABLE 10. WADGPS NETWORK ERROR BUDGET (m)

ERROR	GPS	DGPS				FLA-DGPS				EC/WCA-DGPS				CONUS WADGPS
BASELINE (km)		0	100	300	500	0	100	300	500	0	100	300	500	
<u>Satellite Errors</u>														
Clock	3.0	0	0	0	0									0
Ephemeris	2.4	0	0.04	0.13	0.22									0.09
<u>Selective Availability</u>														
Dither	24	0.25	0.25	0.25	0.25									0.25
Epsilon	24	0	0.43	1.30	2.16									0.81
<u>Atmospheric Errors</u>														
Ionosphere	4.0	0	0.73	1.25	1.60									1.8
Troposphere	0.4	0	0.40	0.40	0.40									0.3
<u>Reference Receiver Errors</u>														
Noise & Multipath	n/a	0.5	0.5	0.5	0.5									0.5
Survey	n/a	0.2	0.2	0.2	0.2									0.2
DGPS ERROR (rss)														
User Receiver Errors	n/a	0.59	1.11	1.94	2.79	0.57	0.91	1.46	2.14	0.57	0.88	1.20	1.46	2.1
	1.0	1.0	1.0	1.0	1.0	1.0	1.0	1.0	1.0	1.0	1.0	1.0	1.0	1.0
UERE (rms)	34.4	1.16	1.49	2.19	2.96	1.15	1.35	1.77	2.36	1.15	1.33	1.56	1.77	2.3
NAV ACCURACY (2 drms; HDOP=1.5)	103.2	3.5	4.5	6.6	8.9	3.5	4.0	5.3	7.1	3.4	4.0	4.7	5.3	6.9

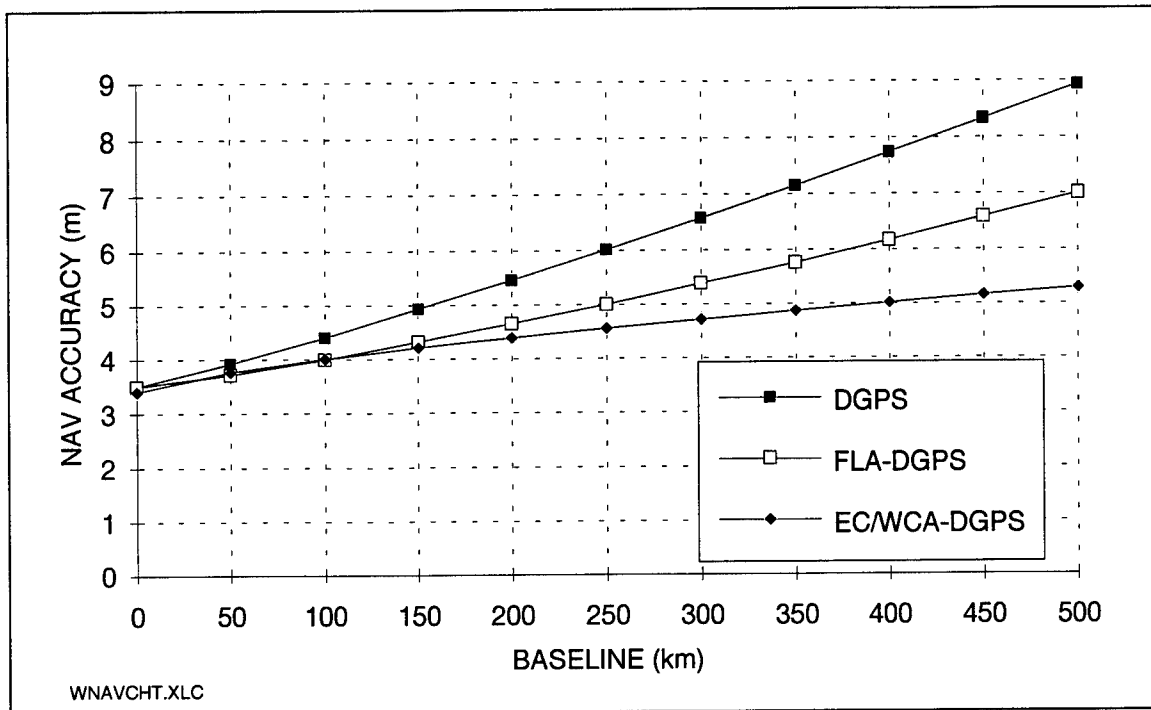


FIGURE 13. WADGPS NAVIGATION ACCURACY (2 drms)

CONUS WADGPS navigation accuracy is baseline independent—the accuracy will be the same at 100 kilometers as it is at 1000 kilometers, theoretically. As can be seen from Table 10, the CONUS accuracy is not as good at the shorter baselines to the previous two network DGPS cases as well as the DGPS case. Conceptually, one might use the DGPS error estimates until their accuracy becomes worse than the CONUS WADGPS estimates. Some caution should be used in discounting the CONUS WADGPS network software until a more thorough analysis can be performed. As will be discussed in Section 5, this analysis would take into consideration the error observability for the 16-site dual-frequency DGPS network.

To obtain estimates of the availability of accuracy for these three WADGPS networks, the statistics of Table 10 would have to be combined with the probabilities that the ground system is available to compute and transmit these corrections and the probabilities that the corrections broadcast by the beacon sites are received error-free by the user. The individual probabilities of availability for the components of the ground system are summarized in Table 11. A sophisticated tool was developed by TASC for the Coast Guard, designated the COAST Methodology [13], and was used by TASC to evaluate the availability of accuracy for three candidate DGPS service architectures (Table 6). Since it will be available to the Coast Guard, it should be used to evaluate these three candidate WADGPS architectures, as discussed in Section 6.

TABLE 11. WADGPS NETWORK GROUND SYSTEM AVAILABILITY

COMPONENTS	DGPS [3]	FLA-DGPS	EC/WCA-DGPS [4]	CONUS DGPS
GROUND SYSTEM AVAILABILITY:				
•Full Network	0.999068	0.988507	0.967915	
•Fault-Tolerant Network		0.999041	0.993899	
<u>Broadcast Station Communications:</u>		0.99980004	0.99480104	0.99480104
•PAD		(0.99980004)	<----->	(0.99980004)
•PSS Network			(0.995) [1]	(0.995) [1]
<u>Broadcast Station:</u>	0.99906751	<----->	<----->	0.99906751
•Power	(0.99999933)	<----->	<----->	(0.99999933)
•Two GPS Receivers	(0.99999984)	<----->	<----->	(0.99999984)
•Two Modulators & Transmitters	(0.99998073)	<----->	<----->	(0.99998073)
•Coupler & Antenna	(0.99908759)	<----->	<----->	(0.99908759)
<u>Reference Station Communications:</u>		0.99480104	<----->	0.99480104
•PAD		(0.99980004)	<----->	(0.99980004)
•PSS Network		(0.995) [2]	(0.995) [1]	(0.995) [1]
<u>Reference Station:</u>		0.99999917	<----->	0.99999917
•Power		(0.99999933)	<----->	(0.99999933)
•Two GPS Receivers		(0.99999984)	<----->	(0.99999984)
<u>Control Station Communications:</u>			0.99480104	0.99480104
•PAD			(0.99980004)	(0.99980004)
•PSS Network			(0.995) [3]	(0.995) [3]
<u>Control Station:</u>			0.99999929	0.99999929
•Power			(0.99999933)	(0.99999933)
•Two Workstations			(0.99999996)	(0.99999996)

Note: Probabilities shown in parentheses are component probabilities under the corresponding major headings.

¹ DGPS measurements sent to control station

² DGPS measurements sent to master reference (broadcast) station

³ WADGPS corrections sent to broadcast station

⁴ Assuming five-station network

While a simplified model for the Availability of Accuracy estimates for the three network architectures would not be as accurate as the COAST methodology, it can illustrate one of the hidden benefits of a WADGPS network—redundancy of sites. Taking the navigation accuracies of Table 10 and Figure 13, and using a simple Gaussian probability distribution function, it is possible to determine the probability that a specific navigation error will exceed the 8-meter (2 drms) HHA requirement, given that the network is operating and the corrections are received error-free by the user. These availabilities are illustrated in Table 12 for the FLA-DGPS (3-site) network for various baselines and network site failures. If the probability that the sites are available is combined with the probability that the navigation error is less than 8 meters, one can obtain an approximate availability of accuracy.

By comparing these approximate availability of accuracy estimates for the DGPS, FLA-DGPS, and EC/WCA-DGPS networks, the common probability of broadcast signal loss can be ignored.

These availability of accuracy estimates are shown in Table 12 and are also plotted in Figure 14. The HHA requirement that was selected was 8 meters (2 drms) with an availability of 0.997, which includes the probability of signal loss. One can see how the site redundancy not only increases the accuracy at the longer baselines (Table 10), but also leads to a higher availability of accuracy at the longer baselines. In deriving these WADGPS network estimates, it was assumed that the network will continue to broadcast WADGPS network corrections to the user based on the sites which are available, except when the broadcast (master) station fails. Hence, Cases 4-6 were not used. Also, it can be seen that for some of the failure modes, such as Case 2, the geometry is so bad that the accuracy is not very good.

Finally, it should be noted that for the specific scenario selected, the user is on a baseline which is near-worst case for the FLA-DGPS and the EC/WCA-DGPS networks. Therefore, the average performance for all possible baselines will be better for the WADGPS network cases while remaining the same for the DGPS case.

4.3 INTEGRITY

The use of monitor stations, which are currently part of the proposed USCG DGPS service, is the preferred way to check the correction and transmission integrity of the broadcast corrections. The monitor stations are placed at surveyed locations and use the broadcast corrections to compute their location. The difference between the known and computed location of the receiver can be used to identify and flag out-of-tolerance differential corrections.

When there are more than the minimum number of satellites available (three for a horizontal position fix), the additional satellite pseudorange measurements and their corrections can be used to identify and isolate out-of-tolerance pseudorange measurements and their corrections. This can be implemented mathematically with a methodology based on parity vectors. Parity vectors are computed using the measurement matrix and a priori estimates of the measurement statistics as well as the measurement residuals. This is the concept employed in Receiver Autonomous Integrity Monitoring (RAIM). To assist in identifying and isolating out-of-tolerance pseudorange measurements, Trimble has proposed adding the surveyed location of the monitor site as additional measurements to the parity vector methodology.

The basic difference in integrity monitoring between the DGPS service and the three WADGPS networks is the addition of the permanent coverage monitors to the existing monitors collocated with the beacons, as shown in Table 13. These additions will afford a more accurate assessment of the integrity of the broadcast corrections at the outer limits of the coverage area of the beacon sites, in addition to validating the WADGPS network corrections for the non-zero baseline case.

TABLE 12. AVAILABILITY OF ACCURACY ESTIMATES FOR FAULT-TOLERANT WADGPS NETWORKS

(Accuracy Limit, L=8m, 2 drms)

AVAILABILITY OF ACCURACY ESTIMATES, $P(L,B)_{AVAIL}$

BASELINE, B (km):	0	100	300	500
DGPS:	0.994005	0.962432	0.771229	0.555345
FLA-DGPS NETWORK:	0.994287	0.978746	0.894151	0.717220
EC/WCA-DGPS NETWORK:	0.989187	0.975482	0.938193	0.887470

FAULT-TOLERANT FLA-DGPS NETWORK AVAILABILITY OF ACCURACY CALCULATIONS

CASE	AVAIL. SITES			PROB. AVAIL.	NAV. ACCURACY (m) & PROB THAT NAV ACCURACY < L											
					0			100 km			300 km			500 km		
	B	C	M		σ_{NAV}	$P_1(\sigma_{NAV})$	σ_{NAV}	$P_1(\sigma_{NAV})$	σ_{NAV}	$P_1(\sigma_{NAV})$	σ_{NAV}	$P_1(\sigma_{NAV})$	σ_{NAV}	$P_1(\sigma_{NAV})$		
1	X	X	X	1.73	0.995244	2.02	0.979794	2.66	0.895815	3.55	0.718995					
2		X	X	1.74	0.995016	2.18	0.965180	3.24	0.781570	4.39	0.564583					
3		X	X	1.74	0.995016	2.09	0.974072	2.86	0.859149	3.80	0.669508					
4		X	X	2.44	(0.931946)	2.31	(0.950135)	2.66	(0.895784)	3.60	(0.709040)					
5		X		3.52	(0.725093)	3.25	(0.780146)	3.25	(0.780146)	3.90	(0.650740)					
6			X	3.52	(0.725093)	3.60	(0.709040)	4.17	(0.601532)	5.05	(0.466016)					
7			X	1.74	0.994883	2.21	0.962660	3.29	0.771839	4.44	0.556003					

- Notes:
- Probability of Broadcast Signal Loss, which is same for all three architectures, was not included.
 - Cases 4-6 were not included in FLA-DGPS Availability of Accuracy calculations since broadcast site (M) is lost.
 - When any site is lost, the network computes weighting coefficients for the remaining sites.

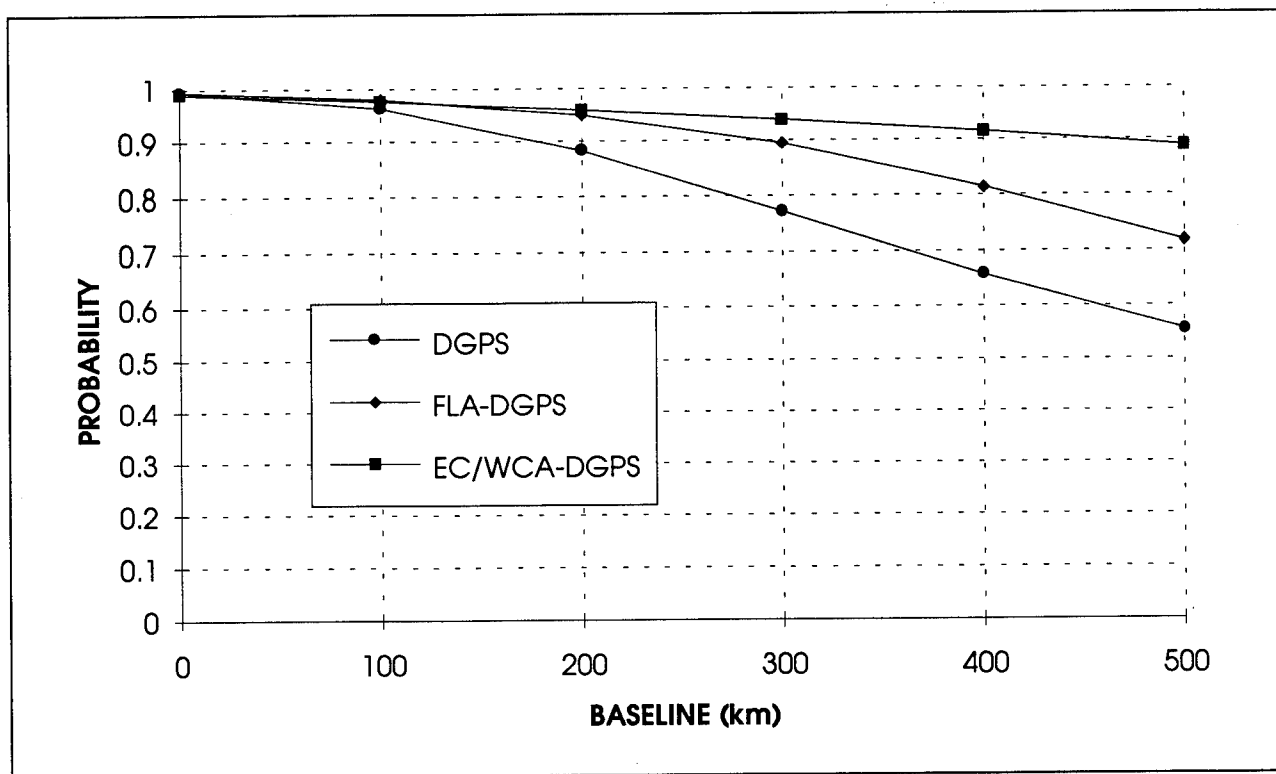


FIGURE 14. AVAILABILITY OF ACCURACY ($L = 8$ m (2 drms))

The proposed Integrity Monitoring Architecture, which has been described so far for the three network architectures, is an (coverage monitor) enhanced DGPS Integrity Monitoring Architecture. This suggests that there may be additional benefits available if the beacon site monitor stations are netted together into an integrity network, analogous to the DGPS accuracy networks which have been the primary focus of this study. This is briefly discussed in Section 6.1.5.

4.4 RELIABILITY

The related issues of reliability and redundancy have been addressed for the various elements of the WADGPS network. To be more tolerant to reference receiver failure, the WADGPS network architectures have assigned dual-redundant receivers to each of the beacon sites. Another approach to assure that a reference receiver is more tolerant to off-nominal oscillator performance is to use an external atomic clock as a reference. This has been included as an option in the three network architectures. Also, each of the beacon sites incorporates dual-redundant transmitters. The component reliabilities are summarized in Table 14 for the WADGPS network architectures.

TABLE 13. WADGPS NETWORK INTEGRITY GROUND SYSTEM AVAILABILITY

COMPONENTS	DGPS [3]	FLA-DGPS	EC/WCA-DGPS	CONUS DGPS
INTEGRITY GROUND SYSTEM AVAILABILITY:	0.99846831	0.99248242	<----->	0.99248242
<u>Monitor:</u> Two MSK GPS Receivers	0.99940024	<----->	<----->	0.99940024
<u>Broadcast Station Communications:</u>		0.99980004	<----->	0.99980004
PAD		(0.99980004)	<----->	(0.99980004)
<u>Broadcast Station:</u>	0.99906751	<----->	<----->	0.99906751
Power	(0.99999933)	<----->	<----->	(0.99999933)
Two GPS Receivers	(0.99999984)	<----->	<----->	(0.99999984)
Two Modulators & Transmitters	(0.99998073)	<----->	<----->	(0.99998073)
Coupler & Antenna	(0.99908759)	<----->	<----->	(0.99908759)
<u>Coverage Monitor Communications:</u>		0.99480104	<----->	0.99480104
PAD		(0.99980004)	<----->	(0.99980004)
PSS Network		(0.995)	<----->	(0.995)
<u>Coverage Monitor:</u>		0.99939957	<----->	0.99939957
Power		(0.99999933)	<----->	(0.99999933)
Two MSK GPS Receivers		(0.99940024)	<----->	(0.99940024)

Note: For the WADGPS architectures, both the collocated monitors and the coverage monitors are required to verify the integrity of the broadcast DGPS corrections at the null baseline and at the maximum coverage range.

Probabilities shown in parentheses are component probabilities under the corresponding major heading.

To minimize the impact from the lower reliability of the X.25 communications network, wherever possible, its use in the critical data path has been minimized for the DGPS service. Unfortunately, however, for the three network architectures, this communications network is in the critical path. To minimize the impact from a failure in this communication link, all three network architectures would revert back to the DGPS service capability.

The reliabilities for the two WADGPS networks of Table 14 were computed assuming a fault-tolerant architecture. These calculations are similar to those performed in Table 12. For the DGPS service, the ground system reliability of 121.10 outages/million hours corresponds to one outage/year. For the FLA-DGPS network, the ground system reliability of 2,917.81 outages/million hours corresponds to a little over two outages/month.

4.5 OTHER

A formal selection between the three WADGPS network architectures should be based on a cost-benefit analysis. Under consideration would be the four major issues of cost, performance (Availability of Accuracy), integrity, and reliability, as well as any other qualitative factors. These factors would then be assigned scores.

TABLE 14. WADGPS NETWORK GROUND SYSTEM RELIABILITY
(Outages/MHR)

COMPONENTS	DGPS [3]	FLA-DGPS	EC/WCA-DGPS*	CONUS DGPS
GROUND SYSTEM RELIABILITY:	121.10	2917.81	8190.90	
<u>Broadcast Station</u>		100.00	1356.28	1356.28
<u>Communications:</u>				
PAD		(100.00)	<----->	(100.00)
PSS Network			(1256.28)	(1256.28)
<u>Broadcast Station:</u>	121.10	<----->	<----->	121.10
Power	(1.00)	<----->	<----->	(1.00)
Two GPS Receivers with	(5.95)	<----->	<----->	(5.95)
Two Modulators &				
Transmitters				
Coupler & Antenna	(114.15)	<----->	<----->	(114.15)
<u>Reference Station</u>		1356.28	<----->	1356.28
<u>Communications:</u>				
PAD		(100.00)	<----->	(100.00)
PSS Network		(1256.28)	<----->	(1256.28)
<u>Reference Station:</u>		1.08	<----->	1.08
Power		(1.00)	<----->	(1.00)
Two GPS Receivers		(0.08)	<----->	(0.08)
<u>Control Station</u>			1356.28	1356.28
<u>Communications:</u>				
PAD			(100.00)	(100.00)
PSS Network			(1256.28)	(1256.28)
<u>Control Station:</u>			1.04	1.04
Power			(1.00)	(1.00)
Two Workstations			(0.04)	(0.04)

*Based on five-station network.

Note: Reliabilities in parentheses are component reliabilities under the corresponding major headings.

The individual scores would be weighted and summed, thus requiring a suitable set of weighting coefficients. Finally, the total score for each of the three network architectures would be compared, and the network architecture with the highest score would be recommended for deployment.

Another approach is to view the three WADGPS network architectures as evolutionary enhancements to the DGPS service architecture. Hence, one would implement the FLA-DGPS network first and determine how well it works in operation, retaining the capability to revert back to the DGPS service. Next, one would upgrade the FLA-DGPS network to the EC/WCA-DGPS network, retaining the basic capability to revert back to the FLA-DGPS network or the DGPS service. Finally, if it is justified, the EC/WCA-DGPS network would be upgraded to the CONUS DGPS network, retaining the capability to revert back the previous three DGPS architectures. The merits of this approach are that it is evolutionary and provides a very robust WADGPS architecture.

5. MODEL ASSESSMENT

In order to gain a full understanding of the benefits of WADGPS, the error mechanisms contributing to the DGPS error budget must be understood. In addition, practical error models for the more significant GPS error sources need to be obtained and used by the WADGPS network software. This is required in order to achieve maximum accuracy with reasonable burdens on the WADGPS data link. A practical error model is defined as one which is both reasonably accurate and has parameters that are reasonably well known, based on historical data, or are observable and can be estimated by the WADGPS filter.

5.1 WADGPS ERROR MODELS

In order to gain a proper understanding of the advantages of WADGPS, an assessment was made of the mathematical models for each of the error mechanisms whose effects can be reduced by DGPS. This assessment was based on the applicability of the model to WADGPS.

An examination of the major DGPS error sources, as presented in Table 15 [8], shows what factors determine both the spatial and the temporal decorrelation for each error source. While the main focus of this study is on the spatial decorrelation of these error sources, the temporal decorrelation determines how sensitive these error sources are to latency in applying the corrections. It is shown in this table that the satellite clock errors are totally correlated while the reference receiver clock, multipath, and location errors are totally uncorrelated spatially. The SA errors are included under both the satellite ephemeris errors (epsilon error) and the satellite clock errors (dither error).

The following sections first present a summary of WADGPS network algorithms which directly or indirectly model and correct for the various DGPS error sources. This is followed by a more detailed discussion of the separate error sources themselves.

5.1.1 WADGPS Network Models

There are two classes of network DGPS error filters: implicit (measurement domain) and explicit (state space domain). The implicit filters do not attempt to estimate the separate error contributors, but are only interested in an accurate total DGPS error estimate. This is the basis for the DGPS service software. The explicit filters attempt to estimate the DGPS error state vector. While the former is simpler to implement, the latter is able to isolate the rapidly time-varying error contributors from the quasi-stationary errors. Hence, the individual DGPS error models are of prime interest when developing and evaluating explicit filters.

The baseline WADGPS network filters for the FLA-DGPS and EC/WCA-DGPS networks are implicit DGPS error filters. Only the CONUS WADGPS network will use explicit DGPS error filters. Hence, the evaluation of both sets of filters needs to be considered.

TABLE 15. DGPS ERROR SPATIAL AND TEMPORAL DECORRELATION

ERROR	SPATIAL DECORRELATION*	TEMPORAL DECORRELATION ⁺
Ephemeris	Elevation & Azimuth Angle Dependent	Position, Velocity, & Acceleration Error Dependent
Satellite Clock	None (Totally Correlated)	Clock Drift & SA Dither Rate & Acceleration Dependent
Iono	Elevation Angle, Local (Sub-350 Km Alt) Time & Geomagnetic Latitude Dependent (Klobuchar Model)	Local Time & Geomagnetic Latitude Dependent
Tropo	Elevation & Azimuth Angle Dependent (Locally) - Temperature, Pressure, & Humidity Spatially Dependent	Satellite & User Motion Dependent - Temperature, Pressure, & Humidity Temporally Dependent
Ref Clock	Total (No Correlation)	Clock Drift & Acceleration Dependent
Multipath	Total (No Correlation)	Satellite & User Motion Dependent
Ref Location	Total (No Correlation)	Total (No Correlation)

*Determines Achievable Accuracy Of DGPS Correction

⁺Determines Required Frequency Of DGPS Correction

Table 16 presents a partial summary of some of the network algorithms which have been developed. The first four algorithms are implicit error estimators, while the last four are explicit estimators. All eight are applicable as real-time DGPS network algorithms. Tang's Multi-Reference Station Algorithm allows the user to incorporate DGPS corrections from multiple reference stations. It does this by weighting these corrections with coefficients determined by a Kalman filter which considers the DGPS spatial decorrelation function between the reference stations and the user. In his paper [14], Tang assumed that the DGPS spatial decorrelation function is an exponential function which can be described by a Gauss-Markov process.

The U.S. Army Corp of Engineers' network filter [9], developed by Loomis, et al., assumes that the network DGPS error can be represented as a Taylor-series expansion of the DGPS error with respect to the location of the user relative to the master reference station. A generalized version of this Network Partial Derivative Algorithm is presented in Table 17. This table shows the derivation of the network weighting coefficients for a first and second-order Partial Derivative Algorithm for a 6-reference station network. While only six stations are considered in this table, more than six stations would permit a least squares filter solution for the weighting coefficients. The basic premise for this algorithm is that there exists a two-dimensional DGPS correction "surface" over the network and the user, which can be approximated with a truncated first or second order Taylor Series expansion.

TABLE 16. DIFFERENTIAL GPS NETWORK ALGORITHM SUMMARY

NAME	REFERENCE RECEIVER	DIFFERENTIAL GPS ERROR PROCESSING				COMMENTS
		Ref Clock	Tropo	Iono	Satellite Clock	Satellite Pos
1. Multi Ref Station DGPS - Tang (89) [14]	C/A Code	DGPS corrections from each reference station statistically weighted with Kalman Filter using 1-dimensional (Gauss-Markhov) spatial decorrelation functions from user to reference stations				<ul style="list-style-type: none"> Local application Application as user filter
2. USCE Network Filter - Loomis (90) [9]	Dual Frequency Kinematic	DGPS corrections from 3 reference stations fit to 1st-order Taylor Series expansion of 2-dimensional (horizontal) spatially correlated error model (1 bias & 2 pos. partials) using Least Squares Filter				<ul style="list-style-type: none"> Local application Applicable to C/A Code ref receivers
3. Minimum Variance Estimator - Mueller (93) [15]	C/A Code	DGPS corrections from each reference station weighted with Minimum Variance estimated weighting coefficients based on spatial decorrelation function between reference stations and between reference station and user				<ul style="list-style-type: none"> Local or regional applications Can be used with any number of reference stations Spatial decorrelation function determined by error budget, field data, or real-time estimation
4. DNETSIM Network Filter - McBurney (90) [16]	C/A Code or Dual Frequency	Residual DGPS errors from reference stations fit to 1st-order Taylor Series expansion of 3-dimensional spatially correlated error model (2 biases, 3 pos partials & 2 bias rates) using Kalman Filter (LSF)				<ul style="list-style-type: none"> Regional application Two filter options: network-centered & satellite-centered
5. Extended DGPS Concept - Brown (89) [17]	Dual Frequency	Not considered	Refract. meas. & (3-term) Altschuler Model	Meas & (8-Term) Model fit to Bent Model	Least Squares Filter	<ul style="list-style-type: none"> Regional application Three filters: tropo, iono, & satellite errors - output to user

TABLE 16. DIFFERENTIAL GPS NETWORK ALGORITHM SUMMARY
(continued)

NAME	REFERENCE RECEIVER	DIFFERENTIAL GPS ERROR PROCESSING				COMMENTS
		Ref Clock	Tropo	Iono	Satellite Clock	Satellite Pos
6. WWDGPS Network Filter - Loomis (90) [7]	Dual Frequency	Eliminated by pre-processor	Measured and removed using collocated weather station and Davis Model	Measured and removed (separate iono filter based on scaling IRI-90 model)	Housholder Transformed, ephemeris corrected meas. used to obtain clock errors with LSF	Housholder Transformed meas. used to obtain orthog. pos. errors which are used to estimate 15 ephemeris correct. using 2-step LSF
7. WADGPS - Kee (90) [18]	Dual Frequency	Atomic	Not considered	Measured and fit to 8-term Klobuchar Model	Least Squares Filter	Least Squares Filter
8. WADGPS - Ashkenazi (92) [19,20]	C/A Code	Ref. to master clock & est. with satellite clock error	Combined with Iono and modeled as (1-term) inverse cosine function. SF est. with orbit errors. SFs fit to 8-term Klobuchar model using non-linear LSF.	Combined with Tropo and modeled as (1-term) inverse cosine function. SF est. with orbit errors. SFs fit to 8-term Klobuchar model using non-linear LSF.	Est. with net. clock after atmospheric & orbit error est. LSF	8x8 gravity sun, moon, & Pt. mass gravity, earth tides, solar press. force models & double diff. GPS data LSF
						<ul style="list-style-type: none"> Worldwide application Worldwide ref. station network - requires each satellite to be seen by 5 ref stations Network of 33 ref stations
						<ul style="list-style-type: none"> Regional application Two iono filters: Kalman & nonlinear state est.
						<ul style="list-style-type: none"> Regional application Sparse network Orbit estimated over 48 hr arcs

TABLE 17. NETWORK DGPS PARTIAL DERIVATIVE ALGORITHM

(6-Node Network)

IF THE NETWORK DGPS ERROR, Z, IS:

$$Z = X - X'$$

WHERE

$$\begin{aligned} X' &= Y_M + A(x-x_M) + B(y-y_M) + C(x-x_M)^2 + D(y-y_M)^2 + E(x-x_M)(y-y_M) \\ &= aY_A + bY_B + cY_C + dY_D + eY_E + mY_M \\ &= Y_M + a(Y_A-Y_M) + b(Y_B-Y_M) + c(Y_C-Y_M) + d(Y_D-Y_M) + e(Y_E-Y_M) \end{aligned}$$

AND X, X'

$Y_A, Y_B, Y_C, Y_D, Y_E, Y_M$
 $(x, y), (x_M, y_M)$

A, B, C, D, E

a, b, c, d, e, m

= USER GPS ERROR & ESTIMATED USER GPS ERROR

= REFERENCE STATION A-E & MASTER STATION GPS ERRORS

= USER & MASTER STATION LOCATIONS

= NETWORK DGPS FIRST & SECOND ORDER PARTIAL DERIVATIVES

= NETWORK DGPS WEIGHTING COEFFICIENTS

THE PARTIAL DERIVATIVE NETWORK COEFFICIENTS ARE:

$$\begin{aligned} \begin{pmatrix} A \\ B \\ C \\ D \\ E \end{pmatrix} &= \begin{pmatrix} (x_A - x_M) & (y_A - y_M) & (x_A - x_M)^2 & (y_A - y_M)^2 & (x_A - x_M)(y_A - y_M) \\ (x_B - x_M) & (y_B - y_M) & (x_B - x_M)^2 & (y_B - y_M)^2 & (x_B - x_M)(y_B - y_M) \\ (x_C - x_M) & (y_C - y_M) & (x_C - x_M)^2 & (y_C - y_M)^2 & (x_C - x_M)(y_C - y_M) \\ (x_D - x_M) & (y_D - y_M) & (x_D - x_M)^2 & (y_D - y_M)^2 & (x_D - x_M)(y_D - y_M) \\ (x_E - x_M) & (y_E - y_M) & (x_E - x_M)^2 & (y_E - y_M)^2 & (x_E - x_M)(y_E - y_M) \end{pmatrix}^{-1} \begin{pmatrix} Y_A - Y_M \\ Y_B - Y_M \\ Y_C - Y_M \\ Y_D - Y_M \\ Y_E - Y_M \end{pmatrix} = [G] \begin{pmatrix} Y_A - Y_M \\ Y_B - Y_M \\ Y_C - Y_M \\ Y_D - Y_M \\ Y_E - Y_M \end{pmatrix}, \text{ PARTIAL DERIVATIVES} \end{aligned}$$

$$\begin{pmatrix} a \\ b \\ c \\ d \\ e \end{pmatrix} = [G]^T \begin{pmatrix} (x - x_M) \\ (y - y_M) \\ (x - x_M)^2 \\ (y - y_M)^2 \\ (x - x_M)(y - y_M) \end{pmatrix}$$

$$, m = 1 - a - b - c - d - e, \text{ WEIGHTING COEFFICIENTS}$$

When the performance was evaluated for the first-order Partial Derivative Algorithm for a generic Coast Guard 3-reference station network (FLA-DGPS), the performance of this algorithm was disappointing, as will be discussed in Section 5.3.1. This prompted the author to explore alternative algorithms and resulted in the development of the Minimum Variance Algorithm [15].

The derivation of the Minimum Variance Algorithm can best be understood by considering the general DGPS correction approach as presented in Table 18. Basically, one would like to take the GPS error estimates measured at a reference station (Y) to correct the unknown GPS error (X) of a user. If it is assumed that the error X is the same as Y, one sets the weighting coefficient a to 1 and differences the two, leading to the DGPS error Z. If however, one asks the question, "What is the weighting coefficient such that the DGPS error is minimized?", one obtains the result of this table that: $a = \rho (\sigma_X / \sigma_Y)$ or for $\sigma_X = \sigma_Y$, that $a = \rho$, where ρ is the spatial decorrelation function of the GPS errors between the user and the reference station.

Table 19 summarizes the derivation of the Minimum Variance Algorithm, which extends the single reference station case of Table 18 to a 5-reference station network. Clearly, this derivation can be extended to any number of reference stations and, by definition, provides the optimum solution. Taking a closer look at the derivation of the weighting coefficients, the inverse correlation matrix describes the spatial decorrelations among the reference stations of the network. Only the spatial correlation vector, to the right of the matrix inverse, considers the spatial correlations between the user location and the network reference stations. While the matrix inverse can be computed by the network, the spatial correlation vector must be computed by the user using his approximate location relative to the reference stations. Thus, for the application of this algorithm to a three-reference station FLA-DGPS network, the matrix inverse and the functional form of the spatial decorrelation function together with the location and DGPS corrections of the reference stations must be sent to the user.

When this algorithm is extended to a 33-reference station East-Coast network, the direct use of this algorithm by the user becomes prohibitive. Hence, combining the Minimum Variance Algorithm with a more practical user algorithm, like the Partial Derivative Algorithm, is warranted for the EC/WCA-DGPS network. This might take the form of using the Minimum Variance Algorithm to map out the correction 'surface' for a matrix of potential user locations. Then a local beacon site fit to this "surface" could be made and sent to the user based on a first (or second) order Partial Derivative Algorithm.

A comparison of the Minimum Variance Algorithm to the Multi-Reference Station Algorithm of Tang indicates full agreement when the same spatial decorrelation function is used. This is to be expected since the Kalman filter used by Tang is a minimum variance estimator.

Continuing with a review of the network algorithms of Table 16, the network filter by McBurney [16] combines a 3-dimensional first-order Taylor series expansion of the DGPS pseudorange error with two bias terms

TABLE 18. MINIMUM VARIANCE ALGORITHM DERIVATION

IF THE DGPS ERROR, Z, IS:	$Z = X - X'$
WHERE	$X' = aY$, ESTIMATE OF X AND
	Z = DGPS ERROR
	X = USER GPS ERROR (UNKNOWN)
	Y = REFERENCE STATION GPS ERROR
	a = WEIGHTING COEFFICIENT
THE MINIMUM VARIANCE WEIGHTING COEFFICIENT, a, IS:	
	$\begin{aligned} \text{MIN}[E\{(X - aY)^2\}] &= d/da \ E\{(X - aY)^2\} = 0 \\ &= E\{-2Y(X - aY)\} = 0 \\ &= E\{XY\} - aE\{Y^2\} = 0 \end{aligned}$
OR	$a = \frac{\rho(\sigma_X/\sigma_Y)}{\quad} \quad \text{IF} \quad \begin{aligned} E\{X\} &= E\{Y\} = 0 \\ E\{XY\} &= \rho\sigma_X\sigma_Y \\ E\{Y^2\} &= \sigma_Y^2 \end{aligned}$
THE DGPS ERROR STATISTICS ARE:	
OR	$\begin{aligned} E\{Z^2\} &= E\{(X - aY)^2\} \\ \sigma_Z^2 &= \sigma_X^2 - 2a\rho\sigma_X\sigma_Y + a^2\sigma_Y^2 \\ &= \sigma_X^2 - 2\rho^2\sigma_X^2 + \rho^2\sigma_X^2 \end{aligned}$
OR	$\sigma_Z = \sigma_X \sqrt{1 - \rho^2}^{0.5}$
MINIMUM VARIANCE ALGORITHM ACCURACY	

TABLE 19. NETWORK DGPS MINIMUM VARIANCE ALGORITHM
(5-Node Network)

IF THE NETWORK DGPS ERROR, Z, IS: $Z = X - X'$

WHERE $X' = aY_A + bY_B + cY_C + dY_D + mY_M$

AND $X, X' =$ USER GPS ERROR AND ESTIMATED USER GPS ERROR
 $Y =$ REFERENCE AND MASTER STATION GPS ERRORS

THE MINIMUM VARIANCE NETWORK COEFFICIENTS ARE:

$$\begin{pmatrix} a \\ b \\ c \\ d \\ m \end{pmatrix} = (\sigma_x / \sigma_y) \begin{pmatrix} 1 & \rho_{AB} & \rho_{AC} & \rho_{AD} & \rho_{AM} \\ \rho_{AB} & 1 & \rho_{BC} & \rho_{BD} & \rho_{BM} \\ \rho_{AC} & \rho_{BC} & 1 & \rho_{CD} & \rho_{CM} \\ \rho_{AD} & \rho_{BD} & \rho_{CD} & 1 & \rho_{DM} \\ \rho_{AM} & \rho_{BM} & \rho_{CM} & \rho_{DM} & 1 \end{pmatrix}^{-1} \begin{pmatrix} \rho_{AX} \\ \rho_{BX} \\ \rho_{CX} \\ \rho_{DX} \\ \rho_{MX} \end{pmatrix}$$

FOR $\sigma_{yA} = \sigma_{yB} = \sigma_{yC} = \sigma_{yD} = \sigma_{yM} = \sigma_y$

WHERE $a-m =$ WEIGHTING COEFFICIENTS

$\sigma_x, \sigma_y =$ USER & REFERENCE STATION ERROR STANDARD DEVIATIONS

$\rho_{ij} =$ DGPS SPATIAL DECORRELATION FUNCTION BETWEEN LOCATIONS i & j

(receiver clock bias as well as satellite orbit and clock bias combined with iono and tropo biases). It also includes two bias terms (rate terms for the pseudorange bias errors) for the accumulated delta-range error. This model is starting to bridge the gap between the fully implicit models and the explicit models by combining both partial derivative formulations with partially functionalized forms of some of the separate DGPS errors.

The next four filters of Table 16 are explicit. These will be briefly discussed in this section, while the DGPS component error models which they employ will be discussed more thoroughly in the remaining paragraphs of Section 5.1. The Extended DGPS Concept by Allison Brown [17] was the original paper that took the idea of DGPS networks from the realm of the surveyor and moved it to the realm of the navigator. While her network filter was presented in conceptual terms, it offered a strawman approach which helped to inspire the Worldwide Differential GPS (WWDGPS) Network Filter by Peter Loomis [5,6,7] and others. The WWDGPS network filter was motivated as an emergency NASA shuttle navigation aid which assumed P-code receivers, both for the network and the user. In addition, it postulated a sparse (33 reference station) network and satellite communications within and outside the network.

The WADGPS Filter of Changdon Kee [18] was motivated as a terminal landing aid for commercial aircraft in the Continental United States. It envisioned a network of 15 P-code receivers located within the 50 states, which would estimate DGPS corrections for C/A-code users. Finally, the WADGPS Filter by Vidal Ashkenazi [19,20] was motivated by the desire of INMARSAT to provide DGPS error corrections to its marine users in an Ocean Region of its satellite coverage with a sparse network of C/A-code reference stations for C/A-code receiver users. All four explicit filters use least squares filters to perform the satellite orbit estimation.

5.1.2 Ionospheric Model

The ionosphere is a shell of electrons and ions surrounding the earth stretching from a height of 50 kilometers to more than 1000 kilometers. Its existence is primarily derived from the ultraviolet radiation of the sun, resulting in diurnal ion density variations or changes in the Total Electron Content (TEC). The TEC is the number of electrons in a vertical column with a cross-sectional area of one square meter. The TEC can also vary on a much shorter time scale, on the order of 10 minutes or so, due to Traveling Ionospheric Disturbances (TIDs). These are believed to be caused by severe weather fronts or volcanic eruptions. Variability of the ionosphere occurs on a monthly, seasonal, and 11-year sun-spot cycle basis.

The typical geographic regions of the ionosphere are shown in Figure 15 [12], while the contours of constant TEC are illustrated in Figure 16 [21], based on the Bent Model. While the mid-latitude ionosphere is relatively uniform and well-behaved, the other regions are much less predictable. The trough region, for instance, is a density valley which can vary daily in its location, extent, and ionization profile. The polar cap region variability can more than double the ionospheric range error in a few minutes. Finally, the equatorial region range errors can be significantly greater than in the adjacent mid-latitude. All of these regions are of interest to users of GPS, since

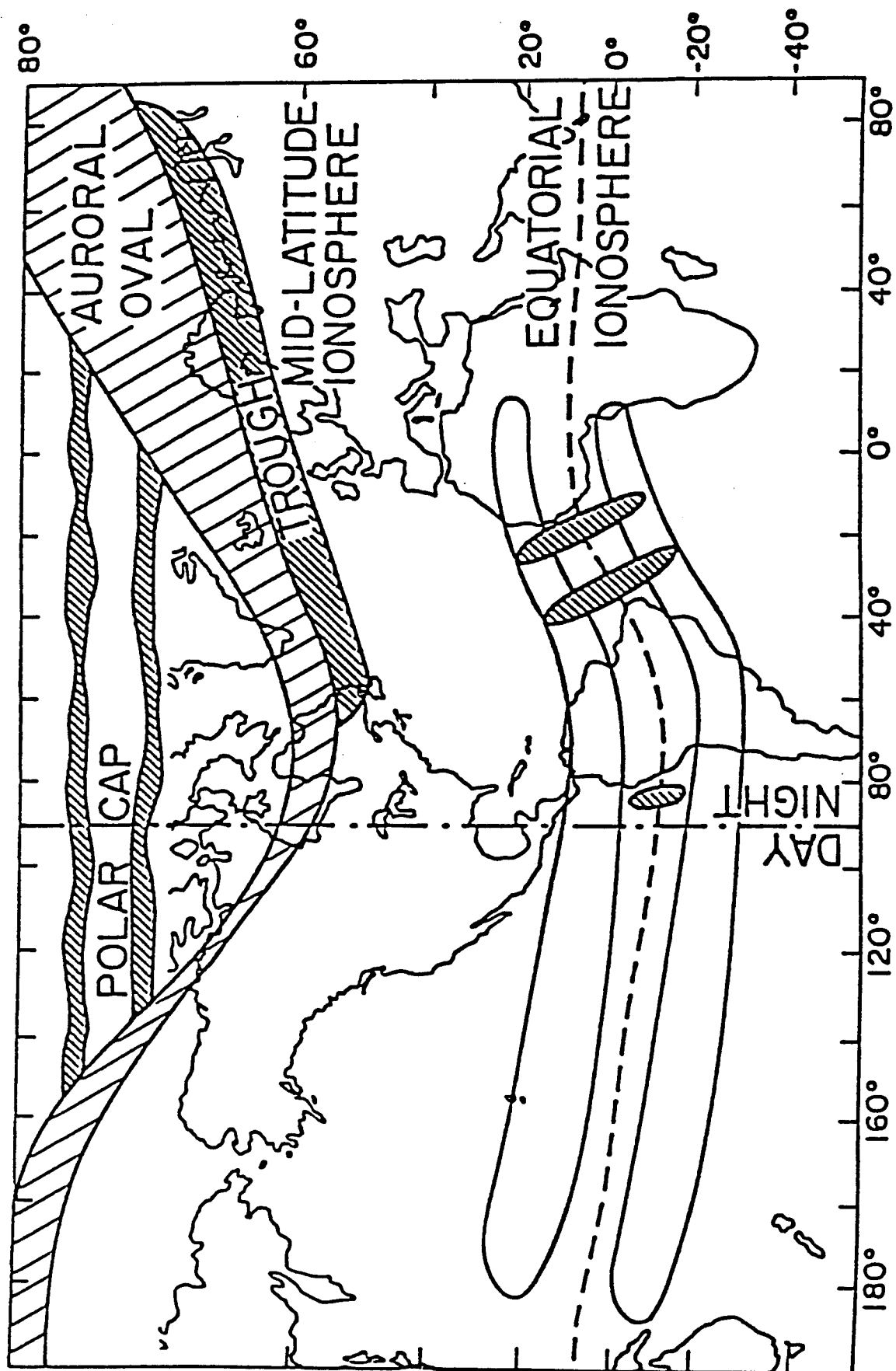
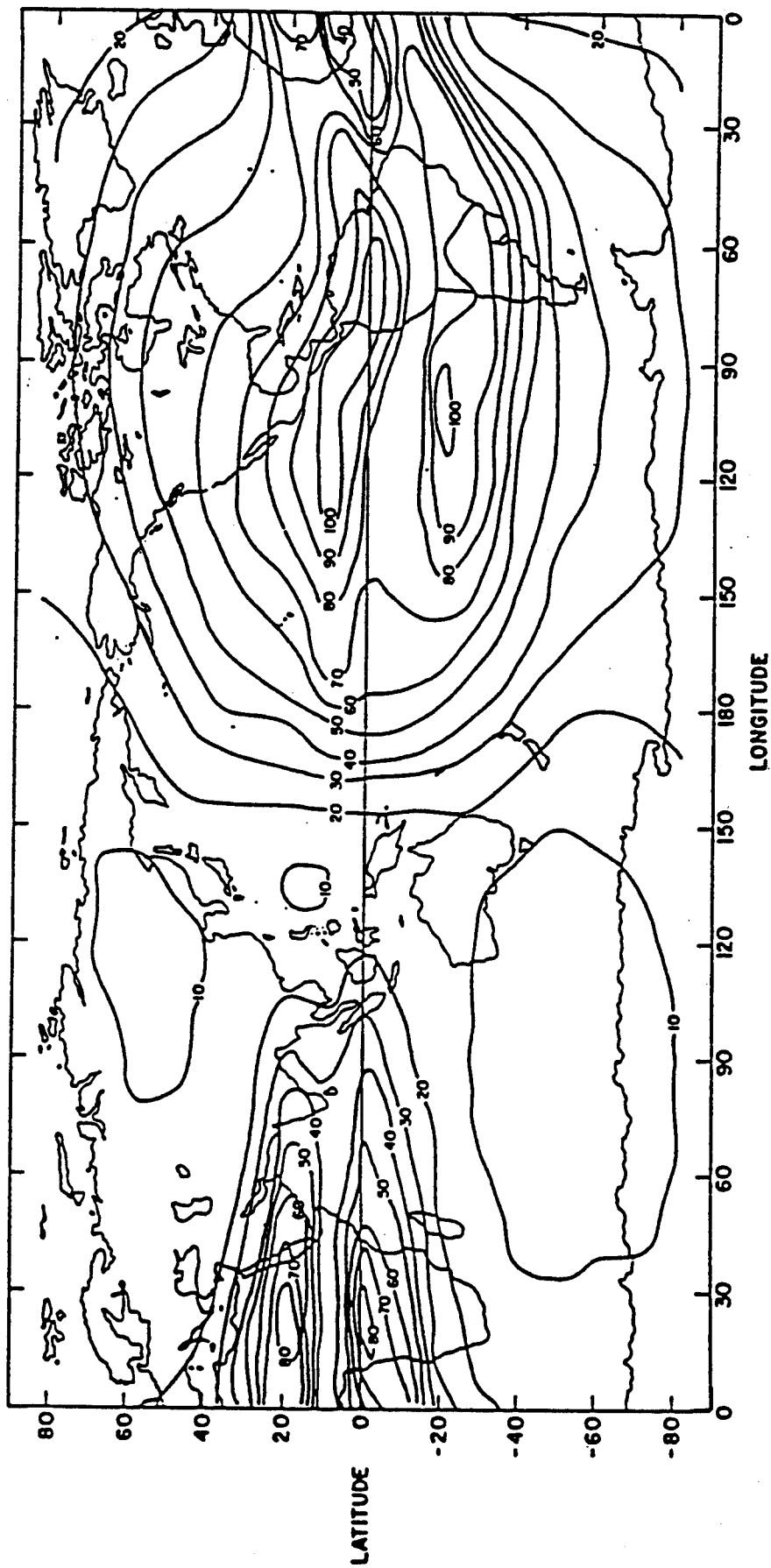


FIGURE 15. MAJOR GEOGRAPHIC REGIONS OF THE IONOSPHERE



TEC in units of 10^{16} electrons/m²

FIGURE 16. IONOSPHERIC VERTICAL TOTAL ELECTRON CONTENT (VTEC)

for low elevation satellites the line-of-sight may penetrate through these regions of the ionosphere. The delay in the GPS signal, τ_{IONO} , can be related to the TEC along the line of sight to the satellite, as follows:

$$\tau_{\text{IONO}} = (40.28/f^2) \text{ TEC}$$

where τ_{IONO} = Ionospheric delay (m)
 TEC = Total Electron Content (electrons/m²)
 f = GPS broadcast frequency (hertz)

As the GPS signal travels through the ionosphere, the code experiences a delay while the carrier experiences an equal and opposite delay. This delay can either be measured with a GPS receiver that is capable of dual-frequency code measurement, since this delay is RF frequency dependent, or it can be modeled. We shall be primarily concerned with modeling this error. Dual frequency code receivers have negligible ionospheric measurement errors, if the interchannel bias can be estimated accurately and removed.

The Satellite Navigation Message includes an Ionospheric Delay Model for C/A-code receivers which is based on the Ionospheric Delay Model developed by Klobuchar [22,23,24]. This broadcast model, which is presented in Table 20, predicts the GPS ionospheric delay (D_1) along the line-of-sight from the product of a zenith delay (D_{IZ}) and mapping function (MF). It was derived primarily for the North American mid-latitude region and assumes that the ionosphere can be treated as a thin shell located at an altitude of 350 kilometers. The daytime zenith delay is assumed to have the characteristics of a cosine function, while the nighttime amplitude is assumed to be a constant. This assumption is based on the observed behavior of the mid-latitude ionospheric zenith delay which is illustrated in Figure 17 [21]. This model is characterized by a nighttime bias, a four-coefficient daytime polynomial, a constant daytime phase (1400 hours), and a four-coefficient daytime polynomial for the period. These eight coefficients, which are broadcast in the Navigation Message, are updated every 10 days, or more frequently if required.

In addition to the PRISM and IFM ionospheric delay models discussed in Section 3.3.1, there are a number of other sophisticated models which have been used by the GPS community. These include the Bent Model [25] and the International Reference Ionosphere, of which the most recent update was in 1990 (IRI-90) [26]. These models provide detailed descriptions of the global ionosphere and have been, or are being, considered for use by WADGPS networks such as the NASA Worldwide DGPS and the Coast Guard CONUS networks. Their accuracy will be highest if they are updated with real-time dual-frequency GPS ionospheric delay measurements.

When the WADGPS network has available direct ionospheric measurements, either from outside sources such as the Air Force Space Forecast Center, from the FAA WADGPS network, or from its own network of dual-frequency GPS reference receivers, a number of approaches can be used. One of the key approaches will be to explore the use of the measurement driven iono models for this WADGPS application.

TABLE 20. KLOBUCHAR IONOSPHERE MODEL

$D_I = D_{IZ} \text{ MF}$	LINE-OF-SIGHT IONO DELAY MODEL
<p>WHERE,</p> $\text{MF} = \frac{1}{\cos\{\sin^{-1}([R_E / (R_E + h_I)] \cos(\epsilon))\}}$ $= 1 + 2[(96 - \epsilon) / 90]^3$ $h_I = 350 \text{ km}$	<p><u>MAPPING FUNCTION</u></p> <p>IONO ALTITUDE</p>
<p>AND, $D_{IZ} = A_0 + A_1 \cos(x)$</p> $A_0 = 5 \text{ nsec}$ $A_1 = \sum_{n=0}^3 a_n \lambda^n$ $\cos(x) = \sum_{k=0}^3 \frac{(-1)^k x^{2k}}{(2k)!}$ $x = 2\pi(\tau - \tau_0) / P$ $\tau_0 = 1400 \text{ hrs}$ $P = \sum_{l=0}^3 b^l \lambda^l$	<p><u>ZENITH DELAY</u></p> <p>AMPLITUDE (NIGHTTIME)</p> <p>AMPLITUDE (DAYTIME)</p> <p>LOCAL TIME OF MAX IONO DELAY</p> <p>LOCAL TIME PERIOD (>24 hrs)</p>

The authors have developed a global ionospheric delay model [27], for which a patent has been applied (March 1992), under the TAU Worldwide Differential GPS (WWDGPS) Network contract with NASA/JSC. This model, which is described in [6,27] and illustrated in Figure 18, is a real-time global ionospheric delay model. It relies on dual-frequency GPS receiver ionospheric measurements to derive the coefficients for the model. The model can then be used to provide estimates to a user who only has a C/A-code receiver. The filter is a 2-step estimator which estimates both the zenith delay and the ionospheric (thin-shell) altitude as a function of geomagnetic latitude and local time.

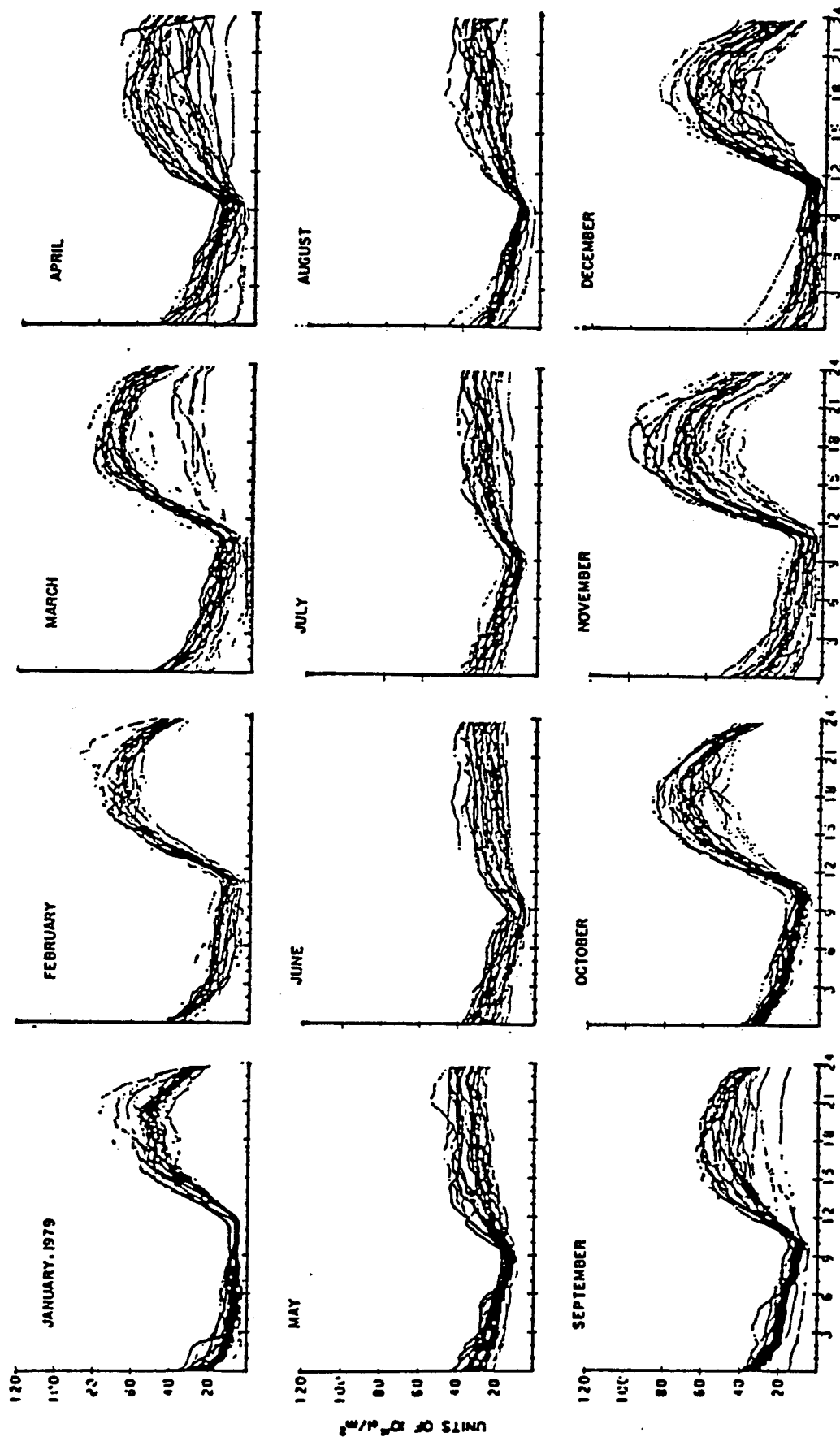


FIGURE 17. MONTHLY OVERPLOTS OF TEC DIURNAL CURVES VS. UNIVERSAL TIME (HAMILTON, MA, 1979)

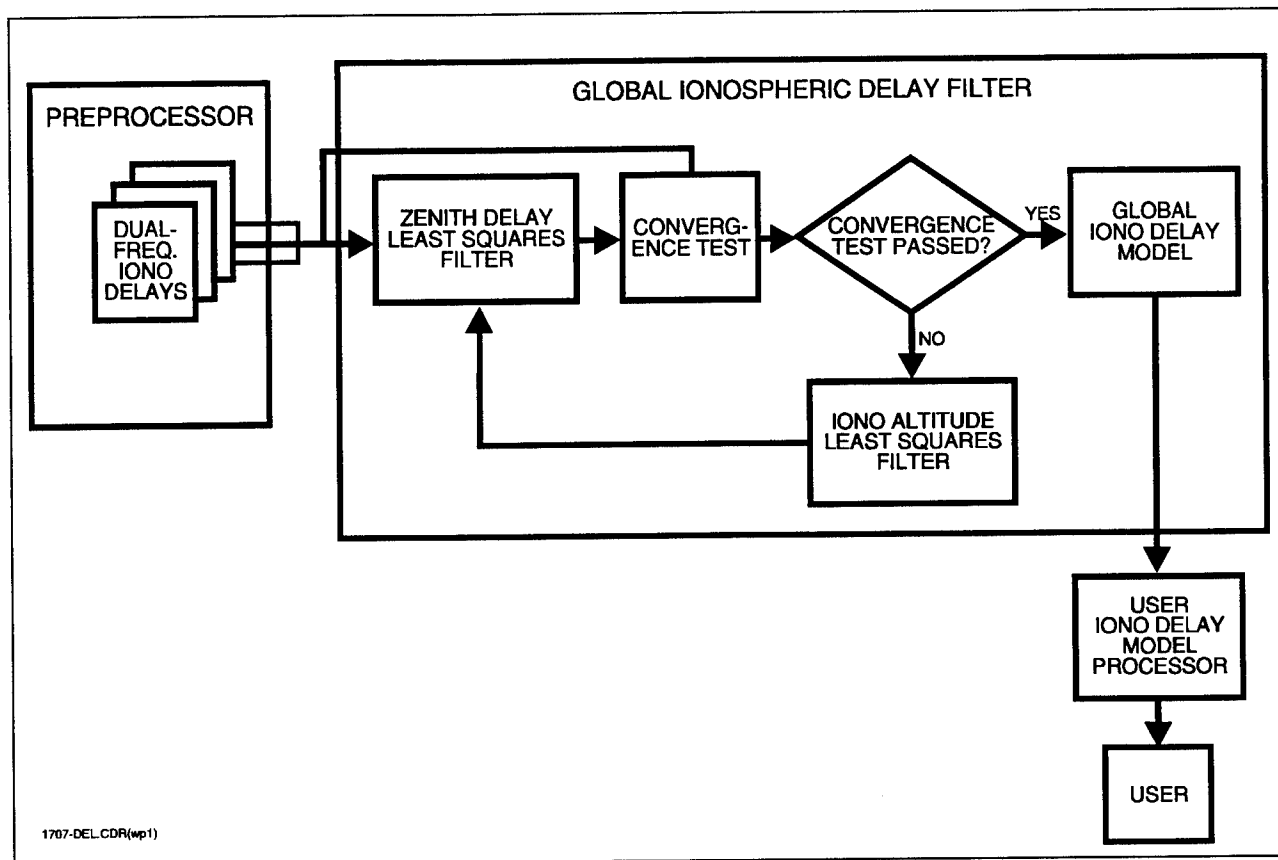


FIGURE 18. DUAL-FREQUENCY MEASUREMENT DRIVEN IONOSPHERIC DELAY MODEL

An alternate Ionospheric Delay Model Estimator was also developed under the WWDGPS network contract [7]. It consists of the IRI-90 Ionospheric Delay Model which is updated using dual-frequency GPS measured ionospheric delay, real-time data. The model is adjusted by estimating and correcting the mean solar sunspot number, since this provides a measure of the intensity of the solar radiation which determines the level of ionospheric activity. This was found to be a more practical approach than using the first WWDGPS Ionospheric Delay Model.

A review of the explicit filters in Table 16 indicates that the WADGPS filters by Kee and by Ashkenazi estimate corrections to the eight variables of the broadcast (Klobuchar) model. The WWDGPS filter by Loomis estimates the solar radiation constant for the IRI-90 model and adjusts it based on the real-time dual-frequency ionospheric delay measurements of the WWDGPS network. Finally, The Extended DGPS Concept by Brown uses dual-frequency ionospheric delay measurements to update the Bent Model and then performs an 8-term fit to this model for broadcast to the user.

5.1.3 Tropospheric Model

The tropospheric delay in the GPS measurement is an unwanted delay in the code and carrier data introduced by the troposphere (actually the neutral atmosphere which extends from sea level to approximately 50 km altitude). Since the tropospheric delay is RF-frequency independent, it cannot be measured independently by a dual-frequency GPS receiver. Hence, it must be modeled or measured with other instrumentation, such as refractometers. Use of refractometers is generally not justified for the WADGPS network architecture since the accuracy of existing Tropospheric Delay Models is quite good.

The total tropospheric signal delay consists of a dry and a wet component. The dry component, which accounts for about 90% of the total delay, can be reasonably well modeled without any meteorological data. The wet component, on the other hand, requires measurements of the local weather conditions along the line-of-sight for maximum accuracy. The best models extrapolate surface pressure measurements to the higher altitudes using standard atmospheric profiles. When surface temperature and relative humidity measurements are extrapolated to the higher altitudes, worse accuracies can be obtained than if the default values had been used in the tropospheric delay model. This arises from the fact that the temperature and relative humidity measurements taken near the ground are only weakly related to the values for these measurements at higher altitudes.

All tropospheric models are good above 15-degree mask angles. Table 21 [6] provides a summary of the major tropospheric delay models.

TABLE 21. GPS TROPOSPHERIC DELAY MODELS SUMMARY

MODEL	COMPONENTS		VARIABLES						ACCURACY (cm)	COMMENTS
	Dry	Wet	Elev	Alt	Lat	Temp	Press	Vap P		
Bean & Dutton Altschuler (74)	• •		• •	• •	•				6% of Total (Elev > 5°)	Isotropic Atmos. Seasonal (Month) Dependence
Chao (72)	•	•	•	•	•	•	•	•	1-2% of Total (Elev > 5°)	
Hopfield Zenith (72)	•	•				•			0.7-2 (Dry) 3- 5 (Wet)	Polytropic Atmosphere Hopfield Zenith
Goad & Goodman (74)	•	•	•			•	•	•		
Saastamoinen Zenith (73)	•	•		•	•	•	•	•	0.2-0.3 (Dry) 3-5 (Wet)	Polytropic & Isotropic Atmos.
Saastamoinen Standard (73)	•	•	•	•	•	•	•	•	1-2 (Dry) 10- 20 (Wet) (Elev>10°)	
Davis (86)	•	•	•	•	•	•	•	•	1-2% of Total (Elev > 5°)	Saastamoinen Zenith, Marini & Murray Map Function

Note:

- Tropo delays vary from 2 m (zenith) to 25 m (5° elev), typically
- 90% of delay due to "dry" component and 10% due to "wet" component

The Davis model [28], which was selected for use by TAU on the WWDGPS contract for NASA/JSC, is summarized in Table 22. This model predicts the line-of-sight tropospheric delay (D_T) from the product of a zenith component (D_{TZ}) and a mapping function (MF). It allows real-time inputs for the local atmospheric pressure, temperature, and relative humidity. These data could be provided by a meteorological sensor package (local weather station), as was used on the WWDGPS contract. Alternately, this information could be provided from other sources (local airports) or be based on atmospheric models.

For DGPS navigation networks, with hundreds of kilometers between reference stations, tropospheric errors become rapidly uncorrelated, and are considered to be reference station unique. For small networks, especially mini-fiducials, tropospheric model error between the reference stations and the users may be correlated and the network solution can help improve user accuracy by including this correction. Following the guidelines of RTCM SC-104, the WADGPS reference station tropospheric errors will not be removed, allowing the user to accept these as valid for his GPS receiver or giving him the option of differentially removing them, given the location of the reference sites.

An examination of the explicit filter algorithms of Table 16 indicates a number of different approaches to modeling the tropospheric errors. Brown's Extended DGPS Concept uses refractometer measurements of the tropospheric delay to perform a 3-term adjustment of the Altschuler model. Loomis's WWDGPS filter uses local weather station measurements of temperature, pressure, and relative humidity as inputs to the Davis Model. Ashkenazi, in turn, combines the tropo and iono errors in a simple inverse cosine model. As a first step, he estimates the reference station scale factors to all the inverse cosine models. He then takes these scaled models and uses them to estimate the 8-term corrections to the Klobuchar model for that network.

5.1.4 Satellite Ephemeris Model

The satellite position is required to solve for the position of the user utilizing the navigation equations. The GPS system is designed to communicate the satellite position through a set of orbit parameters which is a 15-parameter expansion of the six Keplerian elements. The GPS Control Segment generates a set of predicted orbit parameters using satellite tracking data from authorized dual-frequency GPS receivers at five monitor stations. The orbit parameters are derived from processing the pseudorange data with an extensive predictive satellite orbit and atomic clock dynamic model. Using the Control Segment parameters sets, user range accuracy has been demonstrated to be on the order of 1 to 3 meters.

For real-time DGPS networks, extensive predictive models are not required. The system of satellites is observed in near-real time, tracking any dynamics processes that cannot be predicted. Prediction intervals for the purposes of local (single-station) real-time differential GPS are very short because of error build-up in Selective Availability over only a few seconds. With a typical range error magnitude of 30 meters and a period of more than 4 hours (the minimum period for broadcast orbit parameters), orbit errors are nearly stationary and can be modeled as a first-order process (constant velocity bias) over intervals on the order of a few minutes. Type 2 (ephemeris

TABLE 22. DAVIS TROPOSPHERIC DELAY MODEL

TOTAL TROPOSPHERIC DELAY (m)	
$D_T = D_{TZ} \text{ MF}$	
WHERE, $D_{TZ} = \frac{0.002277}{g'} P_o + \frac{1255}{T_o} + 0.05 e_o$	<u>SAASTAMONINEN STANDARD ZENITH DELAY MODEL</u> (Accuracy: 2-3 mm rms - Dry Component 3-5 cm rms - Wet Component)
$MF = \frac{1 + \chi}{\sin(E) + \frac{\chi / (1 + \chi)}{[\sin(E) + 0.015]}}$	<u>MARINI & MURRAY MAPPING FUNCTION</u> (Accuracy: 1-2% of D_T for $E > 5^\circ$)
$e_o = 6.108 RH_e \frac{[17.15 T_o - 4684]}{[T_o - 38.45]}$	<u>GOAD & GOODMAN WATER VAPOR PRESSURE ALG.</u>
$g' = 1 + 0.0026 \cos 2\phi + 0.00028 h_o$ $\chi = \frac{0.002644}{D_{TZ} g'} e^{-(0.14372 h_o)}$ $P_o = \text{Atmospheric Pressure (millibars)}$ $T_o = \text{Temperature } (^\circ K)$ $e_o = \text{Water Vapor Pressure (millibars)}$	<u>STANDARD GRAVITY CORRECTION (m/s²)</u> <u>SURFACE METEOROLOGY MAPPING FUNCTION</u> RH = Relative Humidity (fraction of 1) E = Elevation Angle (deg) ϕ = Station Latitude (deg) h_o = Station Orthometric Height (km)

adjustment) messages use this model successfully to correct for orbit parameter differences between successive ephemerides.

Orbit error is potentially the most limiting factor in the pseudorange of local differential GPS and consequently, the most important to be addressed in differential GPS networks. The formula for the effect of orbit error with increasing distance from the reference station is well-known. Denoting the reference receiver position as \underline{r} , that of a nearby user receiver as \underline{u} , and the satellite position as \underline{S} with a position error $\delta\underline{S}$, the differential range error is:

$$\delta\rho = (|\underline{S} + \delta\underline{S} - \underline{u}| - |\underline{S} + \delta\underline{S} - \underline{r}|) - (|\underline{S} - \underline{u}| - |\underline{S} - \underline{r}|).$$

Using the notation $\underline{R} = (\underline{S} - (\underline{r} + \underline{u})/2)$ for the vector from baseline midpoint to satellite, the above can be rewritten (to second order approximation) as:

$$\delta\rho = (\underline{u} - \underline{r}) \cdot [\underline{R} \times (\delta\underline{S} \times \underline{R}) / |\underline{R}|^3]$$

Maximum differential range error occurs for a given satellite error when the baseline $(\underline{u} - \underline{r})$ is parallel to the satellite position error $\delta\underline{S}$ and perpendicular to the line-of-sight \underline{R} . Under these circumstances, the range error is $(|\underline{u} - \underline{r}| |\delta\underline{S}| / |\underline{R}|)$. Over short ranges, this is roughly proportional to the distance between reference and user, and is often expressed as parts per million (ppm): 3 ppm, for instance, is 3 mm of range error per kilometer of baseline separation. As reported by Loomis, et al. [8], under normal Selective Availability conditions the differential range error effect due to orbit error can be much larger than differential ionospheric model error, at perhaps 13 ppm (2 drms) horizontal error and 30 ppm vertical error at the 95th percentile level.

Given the linear nature of the orbit error effect on differential accuracy, there are three general approaches to modeling the orbit error. Over local and small-network DGPS applications, an error that is a linear function of the baseline is adequate. As the baselines approach a world-wide scale, an approach that resolves the satellite error, $\delta\underline{S}$, is required. The less ambitious approach resolves only the along-track and cross-track directions, recognizing that radial error is not easily observable in the presence of clock error; any radial error is included in the pseudorange correction (PRC). The more ambitious approach attempts to estimate all three satellite position coordinates and perhaps set up a long-term prediction model.

In any of these three types of models, it is expected that the measurements driving the estimator will be double-difference pseudoranges from a network of receivers that have not been synchronized. Alternately, single differences among receivers with synchronized atomic clocks can be used. Consequently, satellite clock errors, which under Selective Availability have essentially no model, are removed from the estimation process.

The first approach is a simple linear function of the baseline, which is probably adequate for small-network application. The relationship between baseline and differential orbit error is nearly linear, especially over small areas where the line-of-sight is almost the same for all users in the area. Each satellite would have a two-dimensional gradient, \underline{g} , associated with it, and the pseudorange correction at a user location, \underline{u} , would be $\underline{g}^T \underline{u}$.

The gradient would be derived directly for measurements from as few as three stations; although satellite position error would not be specifically derived, the gradient would equal the expression:

$$g = \left[\frac{\underline{R} \times (\underline{\delta S} \times \underline{R})}{|\underline{R}|^3} \right]$$

in the absence of other spatially decorrelated errors.

The second approach models the cross-track and along-track errors of the satellites as time functions, ranging from a constant model for short intervals (position offsets only), through first order (position and velocity offsets), to a second-order model (position, velocity, and acceleration) for longer update intervals.

The last approach is a simplified orbit model, as described in the paragraphs below. Studies in the TAU WWDGPS Network study found six-element Keplerian elements to be insufficient for more than a few hundred seconds of propagation, so a more complicated orbit model of nine or more parameters, reflecting the ellipticity of the gravity field, is required.

Under the WWDGPS Network contract, TAU performed a survey of GPS Orbit Filter Models which is summarized in Table 23 [6]. The classical approach determines the orbit in an inertial coordinate frame and thus requires complex force models. Due to the nearly circular GPS orbits, there are two classes of orbital filters called Orbit Relaxation Filters, which are very attractive candidates for a WADGPS network. These orbit relaxation approaches are based on linearizing the orbit errors around the broadcast or nominal orbit.

The first class of Orbit Relaxation Filters are the Keplerian Element Filters. These focus on and estimate the corrections to the GPS orbit Keplerian elements which are slowly varying for nearly circular orbits. The broadcast ephemeris, which is summarized in Table 24 [29], is expressed in terms of these Keplerian elements.

The second class of Orbit Relaxation Filters are the Orbit Plane Coordinate Filters. For the nearly circular GPS orbits, one can use Hills Differential Equations (summarized in Table 25 [30]), which describe the orbit plane orthogonal position error dynamics. It was shown by Colombo, that the solution to these equations could be expressed in terms of two variables: time (t) and the mean motion (n_0) of the satellite, as well as a maximum of 18 unknown coefficients. Since Colombo's solution eliminates the need for integration and can be conveniently truncated, this will be a second candidate model for the WADGPS satellite orbit filter.

The approach used on the WWDGPS network contract [6,7] was to estimate corrections to the broadcast ephemeris Keplerian elements. This was accomplished in three steps. The first step was to take the ionospheric and tropospheric corrected and carrier-smoothed pseudorange errors and remove the network and satellite clock errors using a Householder transformation. Next, the orthogonal orbit position errors were estimated using a Least Squares Filter. Finally, using a set of these position error estimates collected over the period of 20 minutes to an hour, the perturbations to the broadcast ephemeris were estimated using a second Least Squares Filter.

TABLE 23. SATELLITE ORBITAL FILTER OPTIONS

FILTER OPTIONS	STATE EQUATIONS	STATES ESTIMATED	COMMENTS
Keplerian Element Filters*	<ul style="list-style-type: none"> • <u>Lagrange Planetary Equations (LPE)</u> - No Perturbs 	<ul style="list-style-type: none"> • Six ICs 	<ul style="list-style-type: none"> • Slowly Varying States • Short - Arc Approach
	<ul style="list-style-type: none"> • LPE - C_{20} & Resonant C_{nm} Perturbations 	<ul style="list-style-type: none"> • Six ICs, C_{20}, & Resonant C_{nm}'s 	
	<ul style="list-style-type: none"> • <u>Broadcast Ephemeris (BE)</u> - LPE with 6 Perturbations 	<ul style="list-style-type: none"> • 15 Coeffs. 	
Orbit Plane Coordinate Filters*	<ul style="list-style-type: none"> • <u>Hill's Equations (HE)</u> - No Perturbations 	<ul style="list-style-type: none"> • Six ICs 	<ul style="list-style-type: none"> • Short - Arc Approach
	<ul style="list-style-type: none"> • HE - Perturbations (Colombo's Solution) 	<ul style="list-style-type: none"> • (18) Coeffs 	<ul style="list-style-type: none"> • No Integrations Required
Inertial Coordinate Filters	<ul style="list-style-type: none"> • <u>Newton's Equations of Motion (NEM)</u> - 4x4 Gravity, No Polar Motion 	<ul style="list-style-type: none"> • Six ICs & (k) C_{nm}'s 	<ul style="list-style-type: none"> • Long Arc Solutions • Sophisticated Models Required
	<ul style="list-style-type: none"> • NEM - 4x4 Gravity, Sun & Moon Point Mass Gravity 	<ul style="list-style-type: none"> • Six ICs & (k) C_{nm}'s 	

*Orbit Relaxation Filters - estimation of orbit errors relative to a nominal orbit.

TABLE 24. BROADCAST EPHEMERIS ALGORITHM

EPHEMERIS CALCULATIONS	DEFINITIONS OF VARIABLES
$n_0 = \sqrt{\frac{\mu}{A^3}}$	$\mu = 3.986005 \times 10^{14} \text{ m}^3 / \text{sec}^2$ GS 84 value of the earth's universal gravitational parameter
$t_k = t - t_{oe}^*$	$\dot{\Omega}_e = 7.292115167 \times 10^{-5} \text{ rad/sec}$ WGS 84 value of the earth's rotation rate
$n = n_0 + \Delta n$	$A = (\sqrt{A})^2$ Semi-major axis
$M_k = M_0 + nt_k$	M_0 Mean anomaly at reference time
$M_k = E_k - e \sin E_k$	Δn Mean motion difference from computed value
$\cos f_k = (\cos E_k - e) / (1 - e \cos E_k)$	e Eccentricity
$\sin f_k = \sqrt{1 - e^2} \sin E_k / (1 - e \cos E_k)$	\sqrt{A} Square root of the semi-major axis
$E_k = \cos^{-1} \left[\frac{e + \cos f_k}{1 + e \cos f_k} \right]$	Ω_0 Longitude or ascending node of orbit plane at weekly epoch
$\phi_k = f_k + \omega$	i_0 Inclination angle at reference time
$\delta u_k = C_{us} \sin 2\phi_k + C_{uc} \cos 2\phi_k$ Argument of Lat. correction	ω Argument of perigee
$\delta r_k = C_{rs} \cos 2\phi_k + C_{rc} \sin 2\phi_k$ Radius correction	$\dot{\Omega}$ Rate of right ascension
$\delta i_k = C_{is} \cos 2\phi_k + C_{ic} \sin 2\phi_k$ Correction to inclination	IDOT Rate of inclination angle
$u_k = \phi_k + \delta u_k$	C_{uc} Amplitude of the cosine harmonic correction term to the argument of latitude
$r_k = A(1 - e \cos E_k) + \delta r_k$	C_{us} Amplitude of the sine harmonic correction term to the argument of latitude
$i_k = i_0 + \delta i_k + (\text{IDOT})t_k$	C_{rc} Amplitude of the cosine harmonic correction term to the orbit radius
$x_k = r_k \cos u_k$	C_{rs} Amplitude of the sine harmonic correction term to the orbit radius
$y_k = r_k \sin u_k$	C_{ic} Amplitude of the cosine harmonic correction term to the angle of inclination
$\Omega_k = \Omega_0 + (\dot{\Omega} - \dot{\Omega}_e)t_k - \Omega_e t_{oe}$	C_{is} Amplitude of the sine harmonic correction term to the angle of inclination
$x_k = x'_k \cos \Omega_k - y'_k \cos i_k \sin \Omega_k$	t_{oc} Ephemeris reference time
$y_k = x'_k \sin \Omega_k + y'_k \cos i_k \cos \Omega_k$	IODE Issue of Data (Ephemeris)
$z_k = y'_k \sin i_k$	

*1 is GPS system time at time of transmission, i.e., GPS time corrected for transit time (range/speed of light). Furthermore, t_k shall be the actual total time difference between the time t and the epoch time t_{oe} and must account for beginning or end of week crossovers. That is, if t_k is greater than 302,400, subtract 604,800 from t_k . If t_k is less than -302,400 seconds, add 604,800 seconds to t_k .

TABLE 25. HILL'S DIFFERENTIAL EQUATIONS

<p>HILL'S EQUATIONS:</p> $\delta\ddot{R} - 3n_0^2\delta R - 2n_0^2\delta\dot{T} = \delta A_R$ $\delta\ddot{T} + 2n_0^2\delta R = \delta A_T$ $\delta\ddot{N} + n_0^2\delta N = \delta A_N$	
<p>COLOMBO'S SOLUTION:</p> $\delta R(t) = a_R \cos(n_0 t) + b_R \sin(n_0 t) + c_R t \cos(n_0 t) + d_R t \sin(n_0 t) + e_R$ $\delta T(t) = a_T \cos(n_0 t) + b_T \sin(n_0 t) + c_T t \cos(n_0 t) + d_T t \sin(n_0 t) + e_T + f_T t + g_T t^2$ $\delta N(t) = a_N \cos(n_0 t) + b_N \sin(n_0 t) + c_N t \cos(n_0 t) + d_N t \sin(n_0 t) + e_N + f_N t$	
<p>WHERE</p> <p>$\delta R, \delta T, \delta N$</p> <p>$\delta A_R, \delta A_T, \delta A_N$</p> <p>$n_0$</p> <p>$t$</p> <p>$a_i, b_i, c_i, d_i, e_i, f_i, g_i$</p>	<p>= RANGE, TRACK, AND NORMAL ORBITAL POSITION ERRORS</p> <p>= RANGE, TRACK, AND NORMAL ORBITAL ACCELERATION PERTURBS</p> <p>= MEAN ORBITAL MOTION</p> <p>= TIME</p> <p>= UNKNOWN COEFFICIENTS - TO BE ESTIMATED (i = R, T, N)</p>

5.1.5 Satellite Clock Model

GPS navigation is basically a ranging navigation system and relies on measuring pseudoranges from four or more transmitters (satellites) with known positions and synchronized signal transmission. Small errors in the signal synchronizations occur, they are calibrated, and the corrections are broadcast by the DoD.

In recent years, satellite clock error has been the greatest source of stand-alone GPS navigation error. This is due almost completely to Selective Availability, which has a general wandering effect on the range error called clock dither. This can be described as having an amplitude of 30 meters, and a period of 300 seconds, maximum rates of about 0.2 m/s and maximum accelerations of .004 m/s/s. Although satellite clock error can be measured quite accurately at any instant, it changes quickly enough so that error due to message latency is one of the principal design criteria of any DGPS system.

All receivers experience the same clock error for each satellite, no matter how widely separated. Since there is no dependence on distance from the reference station, satellite clock error is not a direct contributing factor to networked DGPS performance. It does contribute to system performance in the sense that the greater baseline separation between reference and user, the more likely that the differential data link signal is not received by the user. A missed message causes longer latency and degrades accuracy, perhaps to the point of not achieving accuracy requirements.

Typical estimator models use a rate (frequency offset) term, although measurements from modern receivers are precise enough to justify acceleration (frequency drift) terms as well. Current RTCM messages use only the rate term, although a suggested alternative is to estimate the acceleration projected over the term of applicability and issued at an average rate to the user. One interesting innovation came in a study by Chou [31]. A filter with a variable number of states (as many as six derivatives) accurately predicted clock dither over many seconds.

On the WWDGPS system study of [6,7], the procedure used was to correct the pseudorange errors for tropospheric, ionospheric, ephemeris, and noise errors. These corrected pseudorange errors were then processed through a Housholder transformation to eliminate the network clock errors. Finally, a least squares filter was used to estimate the satellite clock errors.

It was found in that study that the radial component of the satellite orbit position error is not separately observable from the satellite clock error. Hence, they were estimated together under the WWDGPS study.

5.1.6 WADGPS Network Clock Model

Network clock synchronization is a critical issue in all but the simplest network implementation. Because of the unique structure of GPS, with so many satellites visible at any time, synchronization is relatively easy. Atomic frequency standards are helpful at the reference receivers to maintain synchronization once it has been established. Hence, the network would not need to be constantly resynchronized. However, the network can

function quite adequately without atomic frequency standards by continuous synchronization through double-differenced measurements, as discussed in Section 5.1.4.

First, we shall describe the condition that qualifies a network to avoid synchronization. Typically, a correction is generated as a combination of corrections from a set of participating reference stations. The basic condition is that each reference station clock error due to mis-synchronization creates an equal error in each of the pseudorange corrections at the user. This situation is actually quite common when the user is interpolating correction signals over a relatively small network of two or more reference stations a few hundred miles in diameter. The typical "common view" network, using a Partial Derivative Algorithm, will create the user correction PRC_j for the j 'th satellite as a linear combination of the set of reference station corrections, PRC_{ij} :

$$PRC_j = \sum a_i PRC_{ij}$$

Since all satellites use the same linear coefficients in the generation of the correction, the effect of a set of reference station clock biases, b_i , on the correction is to create an effective network clock bias, $\sum a_i b_i$. This effectively biases each correction equally as if a "virtual reference station" with that clock bias existed at the user location. This bias falls into the user clock error domain, leaving the user position and velocity navigation accuracy unaffected.

If any of the user corrections include data from a reference station that does not participate in one of the other corrections, then the effective network clock biases, present in each correction, will be slightly different. Unless the reference clocks are synchronized to each other, the navigation accuracy will be affected. This might occur for the Minimum Variance Algorithm network (Section 5.1.1) when corrections are generated using different coefficients.

Network self-synchronization, or inter-node time transfer, was first described by Fliegel [32] and concurrently developed during the WWDGPS study [5,6,7]. The central concept is that the number of unknown parameters in a system of m reference stations and n satellites being observed satisfy the requirement that $(m-1)$ clock synchronization parameters times $4n$ satellite position and time bias errors (or $3n$ if the radial and clock errors are combined) is less than the total number of measurements, mn , if m and n are large enough:

$$mn \geq 4n(m-1)$$

With more measurements than unknowns, the system is completely solvable via least-squares techniques.

For simulation purposes, TAU maintains a variety of clock models covering a range of crystal oscillators and atomic frequency standards. These are principally random walk or random run models that imitate the medium term and long term stability of the frequency generators. TAU also uses a null clock model with no assumed dynamics for study of self-synchronizing networks.

Time transfer applications are sensitive to orbit error. Correspondingly, if a network is performing self-synchronization and orbit estimation at the same time, error estimates of satellite position and network clock

synchronization will be heavily correlated. This correlation extends from position states of one satellite, through the network clocks, to other satellite position states. Consequently, the estimation processes of the satellite positions are not separable on a satellite-by-satellite basis, unless the network clock dynamics are much lower than the modeled orbit dynamics. This is a further argument in favor of using atomic clocks for large, self-synchronizing networks.

5.1.7 Multipath and Other Non-Common Mode Models

Receiver unique pseudorange errors can be divided into: receiver thermal noise, interchannel bias, and multipath as well as survey errors. With the current state of the art receiver technology, raw C/A-code noise levels can be found in the vicinity of 20-70 cm. After code/carrier filtering, the accuracy of the C/A-code approaches the accuracy of the P-code generated pseudorange measurements. Using the same technology and digital sampling techniques, the interchannel bias is inherently removed from the L1 pseudorange measurement.

Multipath is the most serious threat to the DGPS service accuracy. Multipath can be modeled as an error that consists of a bias and noise with magnitudes ranging from 0.5-15 m. Over the past few years, a number of techniques have been proposed to combat multipath, such as:

- Low-pass filtering
- Calibration with a second GPS antenna at a nearby low-multipath location
- Day-to-day correlation
- Use of antenna with a well calibrated gain pattern
- Calibration relative to differential carrier phase advance measurements
- Narrow correlator spacing
- Signal diffraction, and so on

Most of these methods reduce the magnitude of the multipath error component, but do not eliminate it completely.

Multipath errors on carrier-phase measurements are negligible when compared to the multipath induced code-phase errors. Thus, carrier-phase smoothing with a large enough time constant (not less than 5 minutes) will reduce the magnitude of the code-phase multipath. The difficulty lies in the fact that, to a receiver's navigation processor, group delay, interchannel bias, and multipath all look the same. The other problem is the code-carrier divergence caused by the opposite effect of the ionospheric delay on the code and carrier signal derived measurements. As a result, only a receiver capable of generating measurements with negligible inter-channel bias and capable of measuring the absolute ionospheric delay (L1/L2 processing) will allow the calculation of multipath-free pseudorange corrections.

In our work with multipath characterization, three facts were established. Multipath induced code error is 1) directly proportional to the strength of the reflected signal; 2) non-linearly dependent upon the relative time delay

between direct and reflected signals; and 3) oscillatory between positive and negative values based on the relative phase of the reflected signal. Two more features of multipath are that, in most of the cases, multipath error exhibits sinusoidal behavior and has a non-zero mean.

5.1.8 Selective Availability Effects

DoD has agreed to constrain the statistics of the horizontal error of a GPS-derived position to 100 m, 2 drms (roughly the 95th percentile). There are two independent error sources that contribute to SA error, satellite clock dither and orbit epsilon. Clock dither allows unpredictable clock synchronization wander of a few tens of nanoseconds. Hence, a stationary receiver will find its position wandering a few tens of meters over a couple of minutes. Almost all of the SA experienced to date appears to have been clock dither. Since clock dither is another satellite clock error source, it will be seen identically by all receivers tracking the same satellite. Hence, DGPS will correct it as well as it is able to correct the nominal satellite clock error, as discussed in Section 5.1.4.

Under Selective Availability (SA), the GPS orbit parameters broadcast by the DoD are purposely misreported to cause a controlled navigation error for the user—the so-called epsilon error. With incorrect orbit parameters, both the reference and the user will compute an incorrect satellite position. Although user and reference will have identical errors in computed satellite position, they will have slightly different errors in their respective computed pseudoranges because of differences in viewing angles. As the separation between reference and user becomes larger, so does the difference in viewing angles and the difference between the computed pseudorange corrections. The navigation error caused by satellite position error is highly correlated between viewers and very linear in nature, i.e., the error is roughly proportional to the distance from the reference station.

Since there are two independent error sources used to obtain the SA error, the satellite clock dither and satellite orbit epsilon errors, it was assumed in [8] that each would contribute 70 m of error at the 95th percentile level. Furthermore, it was assumed that maximum spatial decorrelation would be achieved by the DoD if the epsilon error primarily introduced this error in the along and cross-track orbit position components.

Specifically, if 190 m position error is introduced into both the orbit along and cross-track directions, a stand-alone horizontal navigation error of 71 m (2 drms) results, which is roughly the desired level. The horizontal navigation error after differential correction is 1.3 cm (2 drms) over a one kilometer baseline, or 13 ppm. Using an average HDOP of 1.5, this error translates into a UERE of 4.33 ppm (rms). At this level, epsilon becomes a significant error contributor in DGPS. For a separation distance of 100 km between reference and user, we can expect errors of 1.3 meters horizontal 5% of the time if the broadcast orbit parameters with the above described epsilon are used in conjunction with DGPS.

5.2 EVALUATION METHODOLOGY

The implicit filter performance can be evaluated with a Monte Carlo simulation as shown in Figure 19. The explicit filter performance can be evaluated with a similar Monte Carlo simulation as shown in Figure 20. Due to the close similarity between the two filters, it is possible to develop a Monte Carlo simulation that is flexible enough to handle both cases. This simulation will be developed under the option period of this contract (Section 6.1.2).

Briefly, the WADGPS network filter attempts to estimate the GPS error state vector, p , either in the measurement domain, z'_p , or the state domain, p' . It performs this in the presence of residual survey, reference receiver clock, and multipath errors, δx_w . The user, in turn, tries to estimate his position, x'_u , in the presence of the GPS error, p , by using the network filter corrections, z'_p or p' .

Instead of waiting until the option period to determine the performance of the three network DGPS filters, an error budget approach was used, as summarized in Table 26. Starting out with an error budget for both the standalone GPS and the DGPS errors, a composite DGPS spatial decorrelation function was derived using the single reference station minimum variance methodology shown in that table. Next, the Minimum Variance Algorithm Performance estimates were computed for a generic FLA-DGPS and EC/WCA-DGPS network using the covariance equations shown in Table 27. The numerical calculations were performed using MathCad 4.0. For comparison, the same covariance methodology was also used to evaluate the Partial Derivative Algorithm performance for the generic FLA-DGPS network. The network DGPS errors were then combined with the user errors to obtain the corresponding user navigation errors. For the explicit filter of the CONUS DGPS network, an error budget approach was also used, as it was for deriving the GPS and DGPS errors. The error estimates are based on the individual error sources discussed in Section 5.3.

5.3 WADGPS ERROR MODEL ASSESSMENT

The candidate error models were evaluated to determine their effect on WADGPS system accuracy. The two important selection criteria for the candidate error models were how well do they improve system accuracy, and at what burden on the data link or complexity to the user.

5.3.1 WADGPS Network Models

A scenario was selected to assess the performance of the Partial Derivative Algorithm and the Minimum Variance Algorithm as candidate network DGPS algorithms for the FLA-DGPS and EC/WCA-DGPS networks. This scenario, illustrated in Figure 21, consists of a generic five-reference station network (ABMCD or A'BMCD)

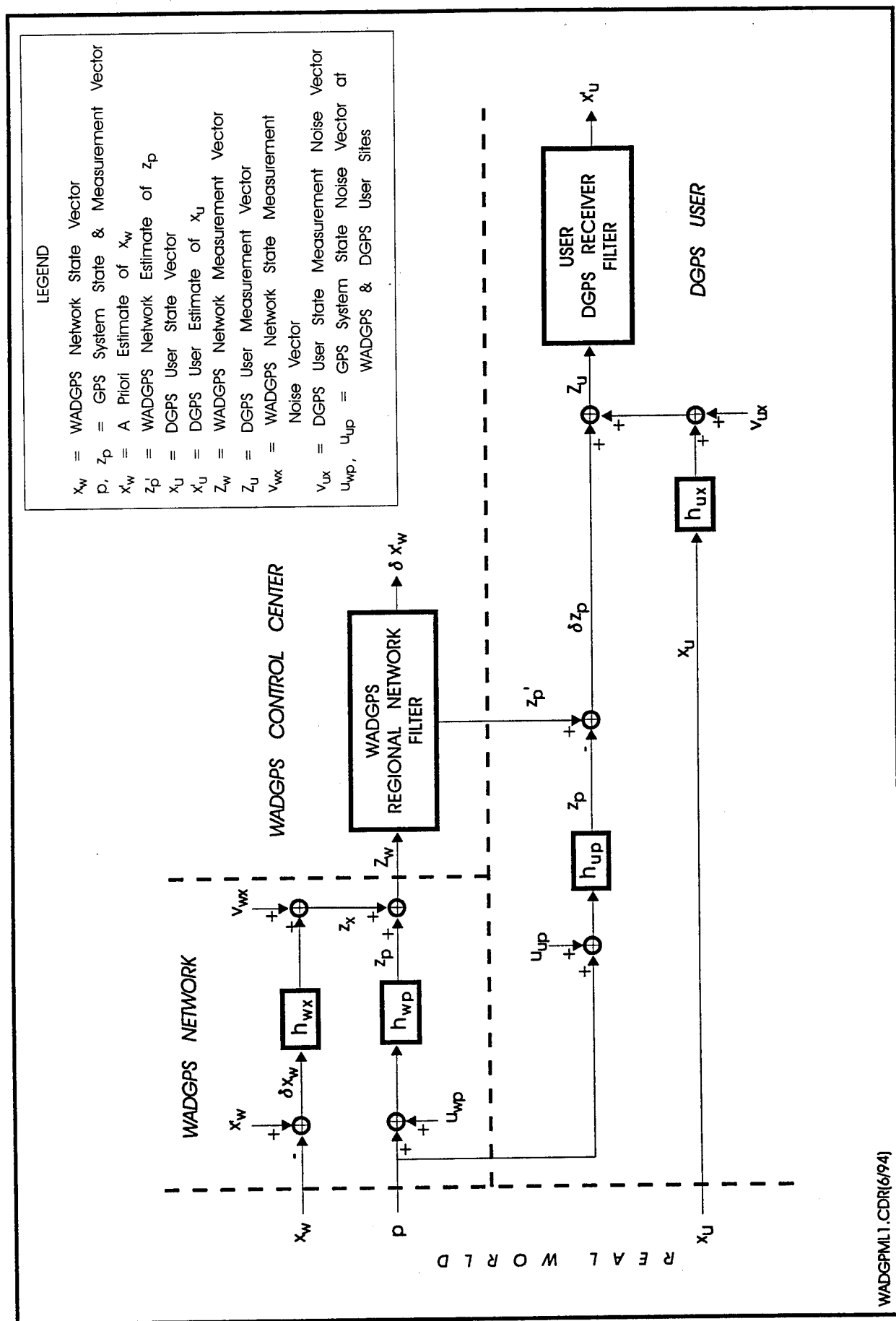


FIGURE 19. WADGPS (REGIONAL) NETWORK SYSTEM MODEL

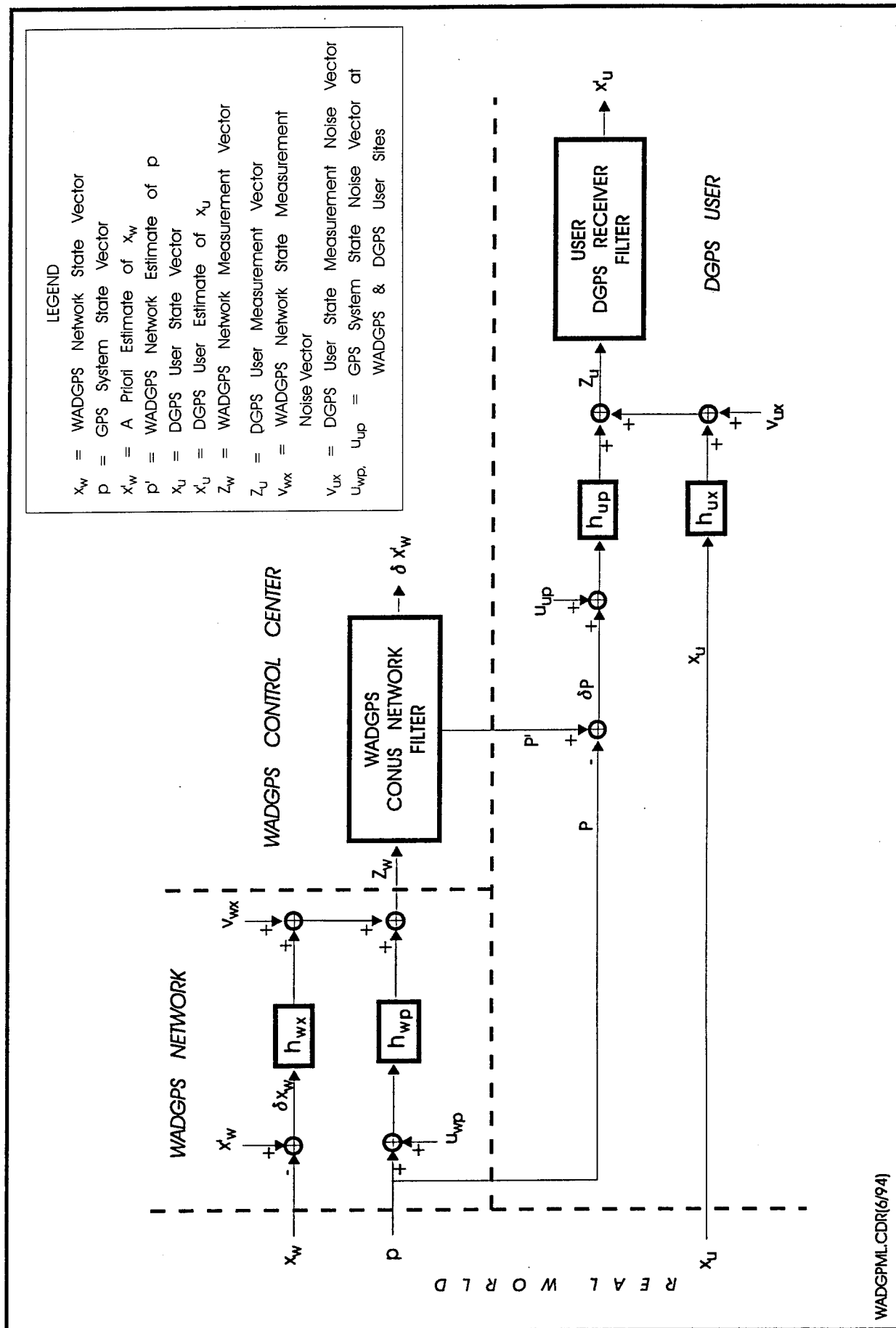


FIGURE 20. WADGPS (CONUS) NETWORK SYSTEM MODEL

TABLE 26. GPS ERROR BUDGET METHODOLOGY

ERROR	SOURCE
GPS Error	<ul style="list-style-type: none"> • Compile individual error statistics
DGPS Error	<ul style="list-style-type: none"> • Compile individual error statistics • For spatially correlated errors, obtain minimum variance solution
DGPS Spatial Decorrelation Function	<p>If $\sigma_{\text{DGPS}} = \sigma_{\text{GPS}} \sqrt{1 - \rho^2}$, then $\rho = \sqrt{1 - (\sigma_{\text{DGPS}} / \sigma_{\text{GPS}})^2}$, Minimum Variance</p>
FLA-DGPS Network or EC/WCA-DGPS Network	<ul style="list-style-type: none"> • Select generic scenarios • Solve for network coefficients using DGPS Minimum Variance spatial decorrelation function • Compute network DGPS error statistics
CONUS WADGPS	<ul style="list-style-type: none"> • Compile individual error statistics

TABLE 27. NETWORK DGPS ERROR COVARIANCE METHODOLOGY

If the <u>network DGPS Error</u> , Z, is:		$Z = X - X'$
and where	X'	$= aY_A + bY_B + cY_C + dY_D + mY_M$
and where	X, X'	$= \text{User GPS Error \& Network Estimate of User GPS Error}$
	Y	$= \text{Reference and Master Station GPS Errors}$
	a, \dots, m	$= \text{Network Weighting Coefficients}$ (Partial Derivative or Minimum Variance)
then the <u>network DGPS Error Statistics</u> , s_z , are:		
	σ_z^2	$= E\{Z^2\} = E\{[X - aY_A - bY_B - cY_C - dY_D - mY_M]^2\}$
or	σ_z	$= \{\sigma_x^2 + [a^2 + b^2 + c^2 + d^2 + m^2] \sigma_y^2 - 2[ap_{AX} + bp_{BX} + cp_{CX} + dp_{DX} + mp_{MX}] \sigma_x \sigma_y$ $+ 2[abp_{AB} + acp_{AC} + adp_{AD} + amp_{AM} + bcp_{BC} + bdp_{BD} + bmp_{BM} + cdp_{CD} + cmp_{CM}$ $+ dmp_{DM}] \sigma_y^2\}^{0.5}$
where	$\sigma_{Y_A} = \sigma_{Y_B} = \sigma_{Y_C} = \sigma_{Y_D} = \sigma_{Y_M} = \sigma_Y$	Reference Site GPS Sigmas
and	σ_X	User GPS Sigma
	ρ_{IJ}	DGPS Spatial Decorrelation functions between locations I and J

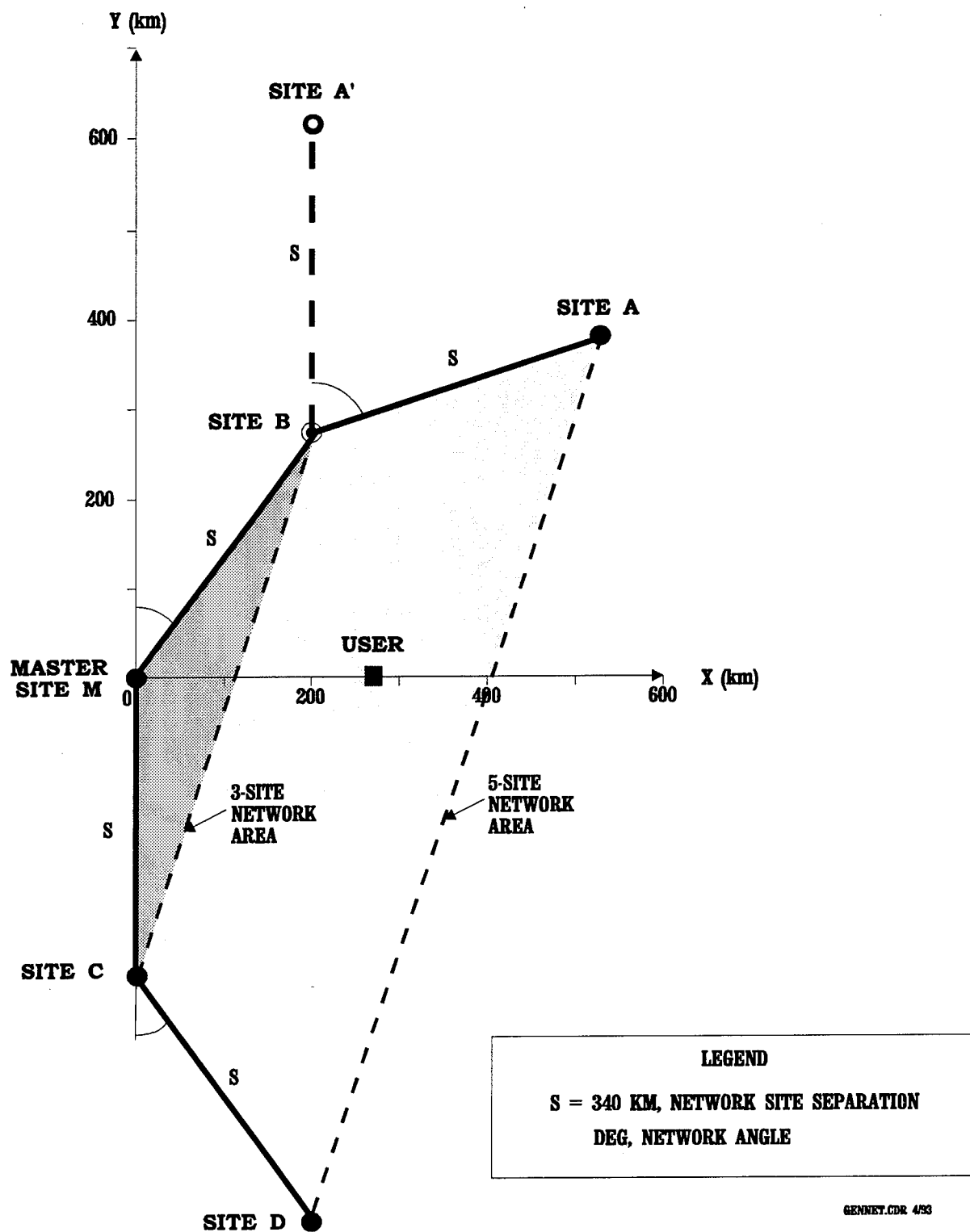


FIGURE 21. GENERIC DGPS NETWORK

or a subset thereof (e.g., BMC). The user is located along the x-axis of this figure directly opposite Station M, which is designated the master station. Average values of 340 kilometers for the inter-site separation (legs) and average network angles of 36 degrees were used based on the location of the DGPS service sites (Table 4) on the East Coast, Gulf Coast, and West Coast. A user is inside the network if his position is within the area enclosed by the network sites.

To evaluate the Partial Derivative Algorithm (PDA) and the Minimum Variance Algorithm (MVA), their respective network weighting coefficients were computed. For the MVA algorithm, this required a spatial decorrelation function for the total DGPS error. From the spatial decorrelation functions presented in Table 28, the spatial decorrelation function for the composite DGPS error in the latitude direction was selected. Examples of the weighting coefficients are presented in Appendix B.

With the PDA and MVA weighting coefficients and the DGPS spatial decorrelation function, the network DGPS error standard deviation for both algorithms was computed for a user at various baseline distances from the master station using the methodology of Table 27. Figure 22 presents the DGPS accuracy as a function of the baseline from the master station for standalone DGPS (Station M only), for the PDA and MVA algorithms and a three-site network (sites: BMC), and for the MVA algorithm for the five-site network (sites: ABMCD). Using the DGPS case as a reference, it can be seen that both the MVA cases perform much better, particularly at the longer baselines. The average maximum beacon coverage range for the same DGPS service sites previously used in obtaining the generic scenario, is 300 kilometers.

The PDA case results were very disappointing. A closer examination of these results and the scenario shows that the PDA case performance is as good as the DGPS case when the user is inside the network, corresponding to baselines less than 120 kilometers. For the baselines outside the network, the PDA algorithm has to extrapolate and thus does this very poorly. Figures 23 and 24 explore this further by extending the legs of the same (three-site) network from 340 to 680 and 1000 kilometers, respectively, in order to "enclose" the user baselines "within" the network. As these figures show, the PDA case results do improve with the longer baselines. It should be noted that the scenario selected is a difficult, although realistic, DGPS service network and that the user is positioned in nearly the worst-case direction for that scenario.

Replotting the results of the last three figures for the PDA and the MVA three-site network leads to Figures 25 and 26, respectively. Figure 25 shows the accuracy of the PDA algorithm when the user location is fixed (baselines: 100, 300, or 500 km), while the network spacing is varied. This figure shows the considerable improvement in the PDA accuracy at the longer user baseline for the longer network spacing. Examination of the comparable cases for the MVA algorithm in Figure 26, also shows an improvement in the accuracy for the longer user baselines and the longer network spacing. This, however, is achieved at the cost of slightly poorer accuracy for the shorter user baselines.

TABLE 28. SPATIAL DECORRELATION FUNCTIONS

ERROR	SPATIAL FUNCTION	COMMENT
General	$\rho_{\text{DGPS}} = \left[1 - 0.5 \left(\sigma_{\text{DGPS}} / \sigma_{\text{GPS}} \right)^2 \right]^{0.5}$	Single Difference
	$\rho_{\text{DGPS}} = \left[1 - \left(\sigma_{\text{DGPS}} / \sigma_{\text{GPS}} \right)^2 \right]^{0.5}$	Minimum Variance
Satellite Ephemeris	$\rho_{\text{EPHM}} = \left[1 - (b/5500 \text{ Km})^2 \right]^{0.5}$	Standard or Epsilon (Min. Var.) based on Loomis, et al. [8]
Ionosphere	$\rho_{\text{IONO}} = \left[1 - (b/6000 \text{ Km}) \right]$	Klobuchar [33]
	$\rho_{\text{IONO}} = \left[1 - (b/9700 \text{ Km}) \right]$	Latitude Separation
		Longitude Separation
Troposphere	$\rho_{\text{TROPO}} = e^{-(b/50 \text{ Km})}$	
Composite DGPS	$\rho_{\text{DGPS}} = \left[1 - (0.01715 + 0.0001926 b_{\text{Km}}^{0.9338})^2 \right]^{0.5}$	Based on GPS and DGPS statistics of Table 10 (Min. Var.)
	$\rho_{\text{DGPS}} = \left[1 - (0.01715 + 0.0001384 b_{\text{Km}}^{0.9714})^2 \right]^{0.5}$	Latitude Longitude

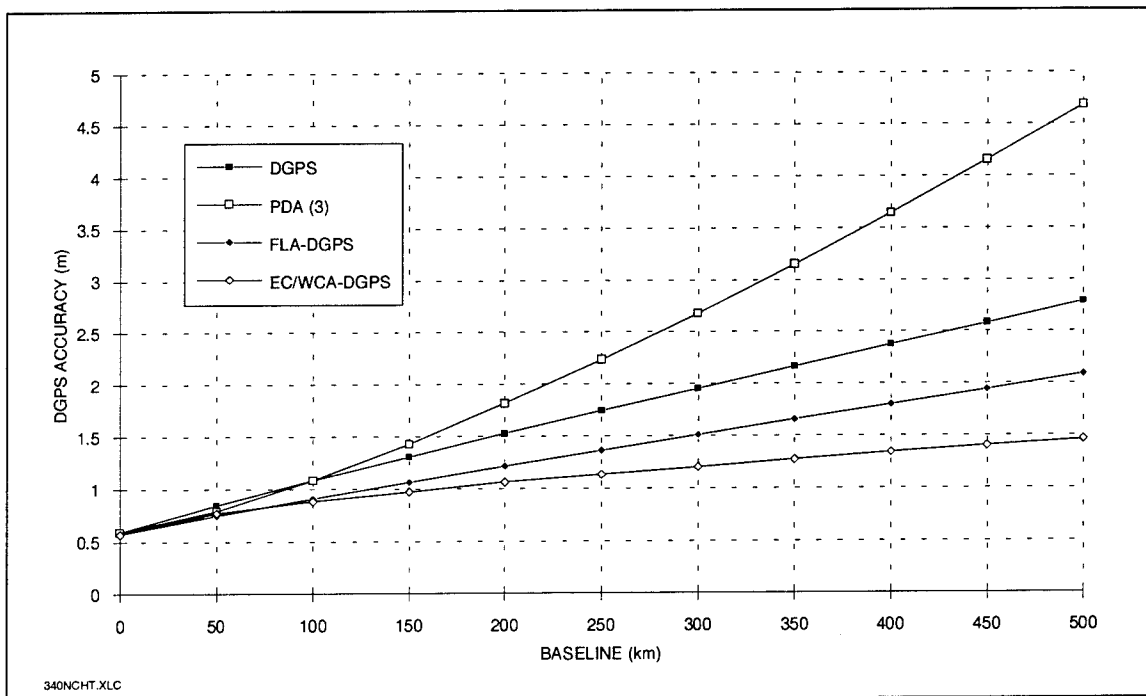


FIGURE 22. 340 KM NETWORK DGPS ACCURACY VS BASELINE

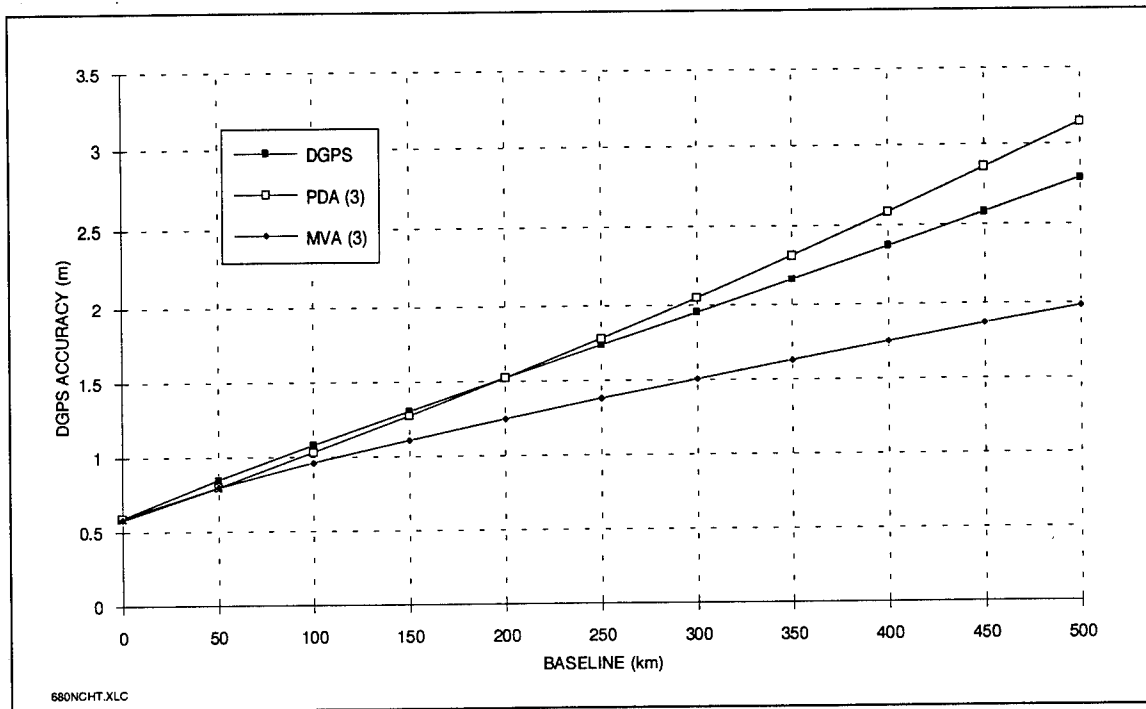


FIGURE 23. 680 KM NETWORK DGPS ACCURACY VS BASELINE

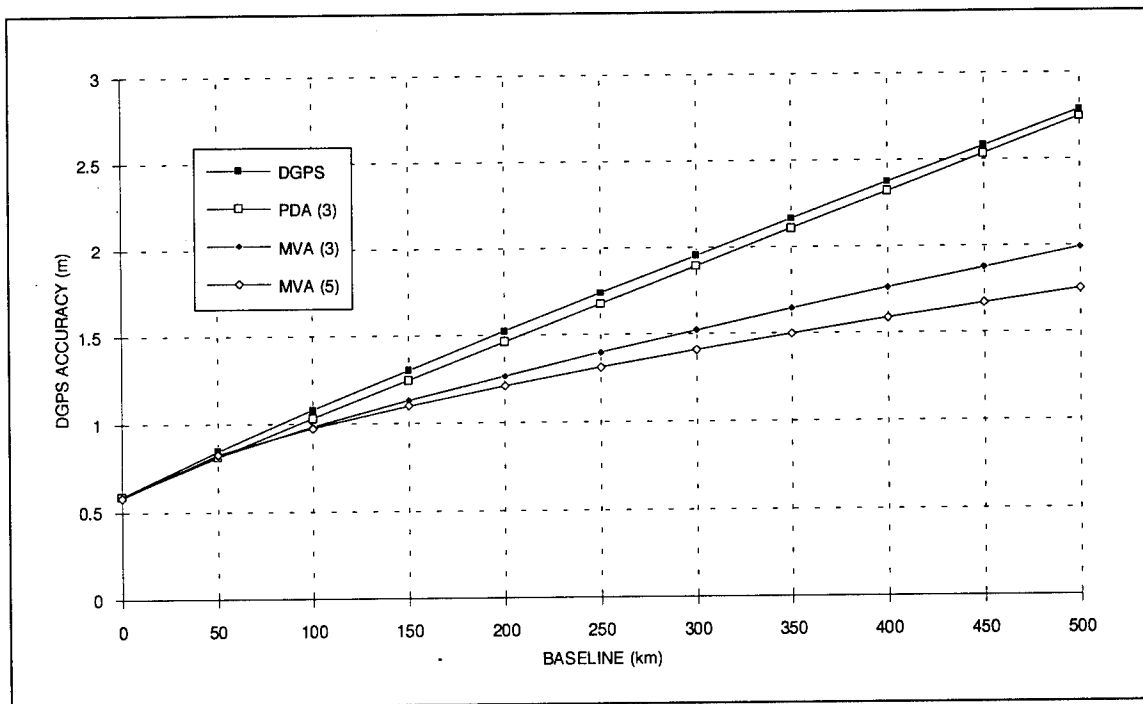


FIGURE 24. 1000 KM NETWORK DGPS ACCURACY VS BASELINE

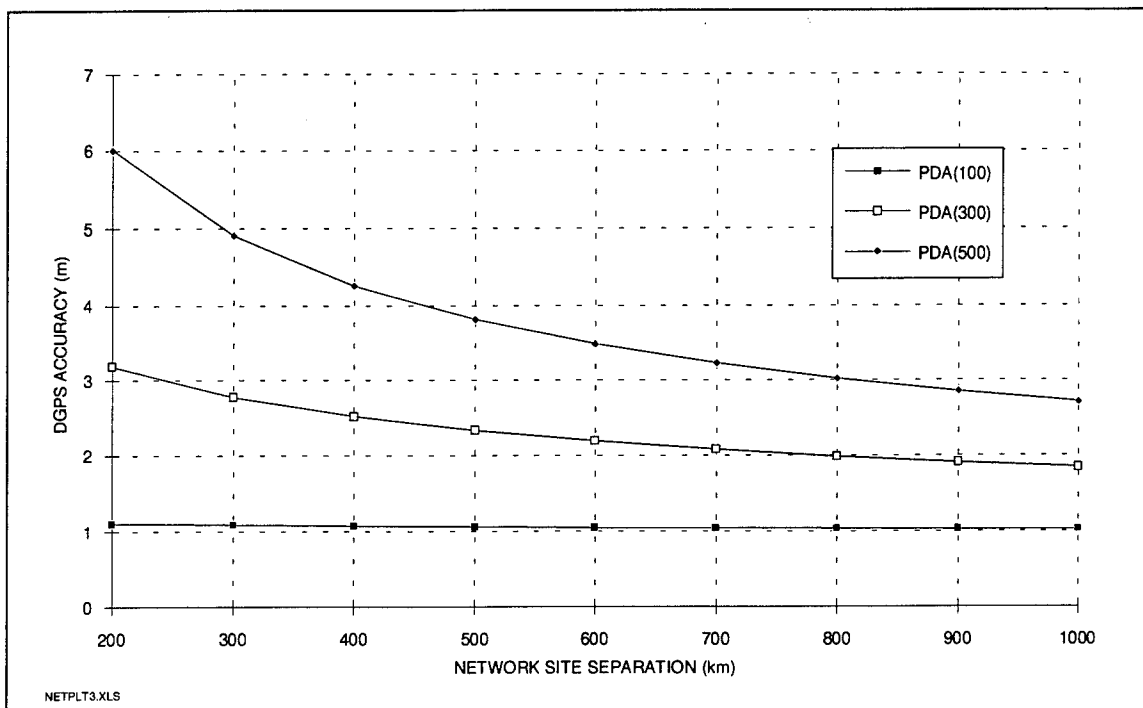


FIGURE 25. THREE-SITE NETWORK PARTIAL DERIVATIVE ALGORITHM DGPS ACCURACY VS SITE SEPARATION

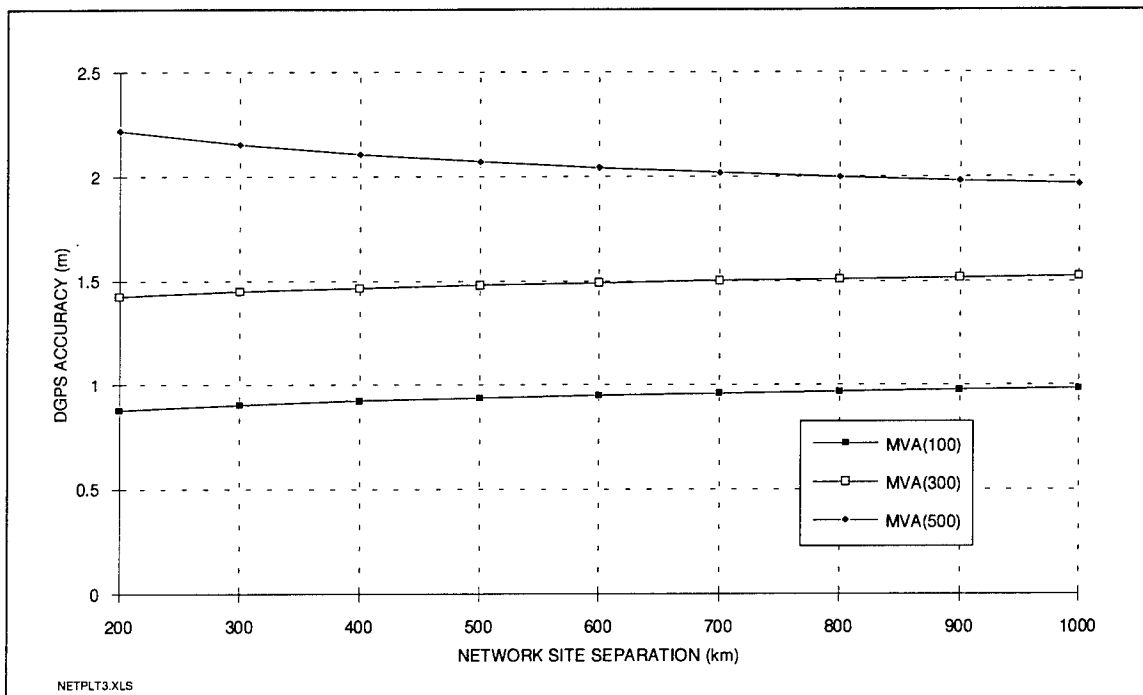


FIGURE 26. THREE-SITE NETWORK MINIMUM VARIANCE ALGORITHM DGPS ACCURACY VS SITE SEPARATION

As a representative network DGPS accuracy, the MVA three and five-site cases of Figure 22 were designated as the FLA-DGPS and EC/WCA-DGPS accuracies in Figure 13. Additional cases were computed and are presented in Appendix B.

The performance of the explicit filter of the CONUS DGPS network was determined from the individual error sources, as previously summarized in Table 10. Based on this table, the CONUS DGPS performance was estimated to be 2.1 meters, irrespective of the baseline. Examining Figure 22 indicates that with this performance the user benefits from using the CONUS DGPS corrections only for baselines greater than 330 kilometers. The user can get better accuracies from using the DGPS corrections from a local reference station if it is less than 330 kilometers away. Since these estimates are based on an error budget approach, rather than a simulation or field data, these conclusions are very tentative.

5.3.2 Ionospheric Model

Table 29 summarizes some of the statistics which describe the ionosphere for the DGPS user. Klobuchar [33] compiled ionospheric delay measurements from a set of 17 stations which were aligned approximately along a north-south baseline, with baselines varying between 1030 and 4000 kilometers, to obtain an ionospheric latitude decorrelation function. He repeated this analysis for a set of 17 stations which were approximately aligned along an east-west baseline, with baselines varying between 1450 and 5210 kilometers, to obtain an ionospheric longitude decorrelation function. As shown in this table, both decorrelation functions are linear with different characteristic distances.

Coco, et al. [34] compiled single difference ionospheric delays measured at five reference stations with predominately east-west baselines varying between 140 and 2300 kilometers. They performed this for both raw and broadcast ionospheric delay model corrected measurements to obtain the statistics of that table. As can be seen, the ionospheric spatial decorrelation function tends to be more nonlinear than the Klobuchar results, particularly for the uncorrected results. The Klobuchar results do involve a larger data base of measurements and these do tend to be at the longer baselines. Also, the DGPS curve fits for the data from Coco, which were made by the authors of this report, are only approximate.

The ionospheric models that exist for stand-alone navigation, such as the GPS broadcast model due to Klobuchar, the Bent model, and the newest version of the International Reference Ionosphere (IRI) 90, generally use monthly averages for prediction and are reported to remove 50-80% of the ionospheric delay. This is illustrated in Table 30 [35] for a comparison of the Bent and IRI 86 (predecessor to IRI 90) models with field measurements at three different latitudes for three levels of solar activity. Performance of the AFSFC PRISM model, which is under development (Section 3.3.1), is not known.

TABLE 29. IONOSPHERIC STATISTICS

GPS (m)	DGPS (m)	SPATIAL DECORRELATION, ρ	SOURCE
	$\sigma_{\text{DGPS}} = \sigma_{\text{GPS}} [1 - \rho^2]^{0.5}$	$[1 - (\Delta\text{Lat}/6000 \text{ km})]$	Klobuchar [33]: 17 <u>N-S Data Sets</u> (1030 - 4000 km)
	$\sigma_{\text{DGPS}} = \sigma_{\text{GPS}} [1 - \rho^2]^{0.5}$	$[1 - (\Delta\text{Lon}/9700 \text{ km})]$	17 <u>E-W Data Sets</u> (1450-5210 km)
8.1 m (rms)	$[B/1750 \text{ km}]^{0.78}$, (rms)	$[1 - 0.5(\sigma_{\text{DGPS}}/\sigma_{\text{GPS}})^2]$	Coco, et al. [34]: (Single Diff. Data) Five Sites (140-2300 km)
1.9 m (rms)	$[B/4960 \text{ km}]^{0.62}$, (rms)	$[1 - 0.5(\sigma_{\text{DGPS}}/\sigma_{\text{GPS}})^2]$	<u>Uncorrected</u> <u>Broadcast Model</u> <u>Corrected</u>

TABLE 30. COMPARISON OF BENT AND IRI-86 IONOSPHERIC DELAY MODELS [35]

Station	Latitude (Deg)	Level of Solar Activity (Sunspot Cycle)					
		High (Jan 80, R=163.9)		Medium (Nov 82, R=94.7)		Low (Jun 86, R=13.8)	
		<u>BENT</u>	<u>IRI-86</u>	<u>BENT</u>	<u>IRI86</u>	<u>BENT</u>	<u>IRI-86</u>
Goose Bay	47	56.6% (1.23m)	53.3% (1.92 m)	49.9% (1.35 m)	47.7% (1.22 m)	76.3% (0.19 m)	71.4% (0.20 m)
Sagamore	38	73.8% (1.12 m)	64.6% (1.42 m)	69.5% (1.38 m)	68.9% (1.34 m)	77.4% (0.24 m)	82.2% (0.21 m)
Patrick	26	79.6% (1.08 m)	78.6% (0.98 m)	77.7% (1.27 m)	82.9% (1.15 m)	69.6% (0.41 m)	69.5% (0.37 m)

- Note:
- Measurements were taken every hour for each month and compared to the monthly averages for the respective models
 - Percentages shown are the rms percentage of the measured vertical ionospheric delay the respective models were able to remove
 - The numbers in parentheses are the rms differences, in meters, between the measured and model-derived delays
 - R is the 12-month running average solar sunspot activity

A comparison between the broadcast model and the Bent model is presented in Figure 27 [23]. This figure explores the variability of the broadcast model nighttime D.C. bias and the daytime amplitude phase and period as a function of geomagnetic latitude, season, and level of solar activity. Note the geomagnetic latitude region which the Continental U.S. encompasses. This region was the basis for the four-term polynomial fits for the period and amplitude and for the bias terms for the phase (14.0 hrs) and D.C. (5 nsec) terms in the broadcast model.

The following general observations can be made about these ionospheric models: (1) all models predict quiet ionospheric conditions only; (2) the mid-latitude trough, which exhibits large horizontal gradients in electron density, is not incorporated in these models; and finally, (3) the models are good for latitudes ± 20 to ± 60 degrees and are poor predictors for the equatorial and high-latitude regions.

5.3.3 Tropospheric Model

A comparison of tropospheric delay models relative to ray-trace tropospheric delay estimates was performed in [36]. Generally, it was concluded that global models can predict tropospheric delay to an accuracy of 10-20 cm for elevation angles down to 10-20 degrees. Direct surface refractometry is the alternate method for dealing with tropospheric delays, where delays are measured directly along the line-of-sight.

Table 31 presents an error budget for the Davis Tropospheric Delay Model [28]. It is representative of the best tropospheric delay models available and was the model selected for the WWDGPS network contract [6,7].

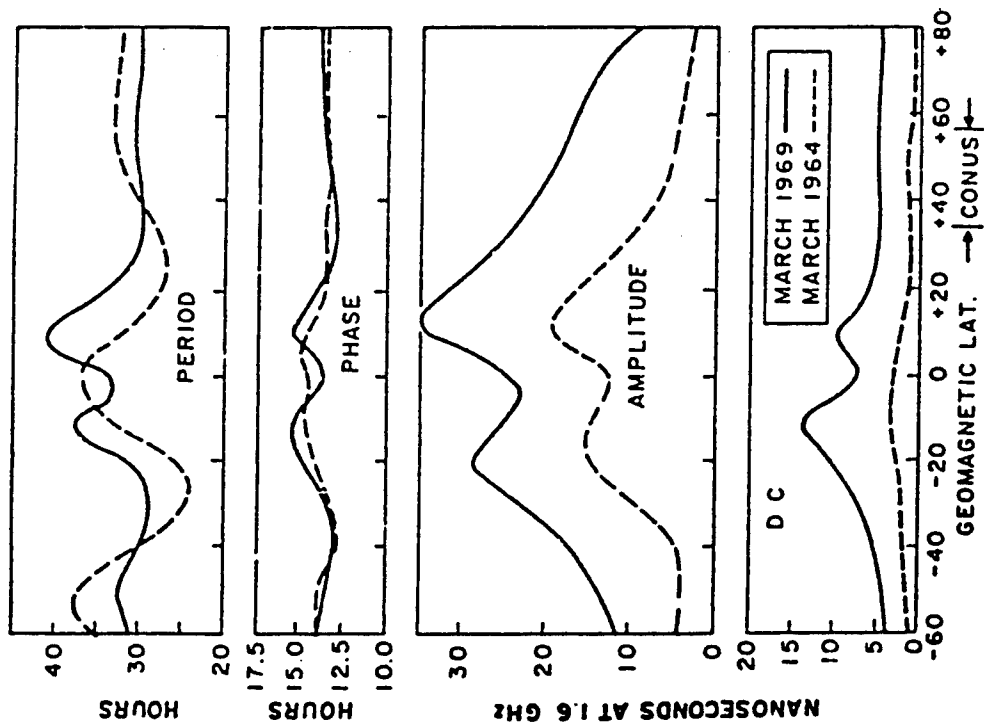
5.3.4 Satellite Ephemeris Model

Networked Differential GPS has a somewhat different outlook on orbit errors than does local DGPS. Rather than the absolute orbit error, networked Differential GPS concerns itself with how accurately the variation with distance can be measured and corrected.

For convenience in the following discussion, orbital bias errors are resolved in the frame formed naturally by the orbit plane: radial, along-track, and cross-track. The character of radial error is considerably different from the others.

Radial errors are very much along the line-of-sight for a satellite for all terrestrial viewers. The line-of-sight is parallel to the satellite radial axis when the user is directly below the satellite, and separated by roughly 15 degrees when the satellite is on the horizon. A radial error of 1 meter will be observed as a 1 meter range error when the satellite is at zenith. When the satellite is on the horizon, the same radial error (1 meter) will be observed as an approximately 97-cm range error (1 meter multiplied by cosine of 15 degrees).

Solar Minimum Year (1964) vs
Maximum Year (1969)



Four Seasons of 1969

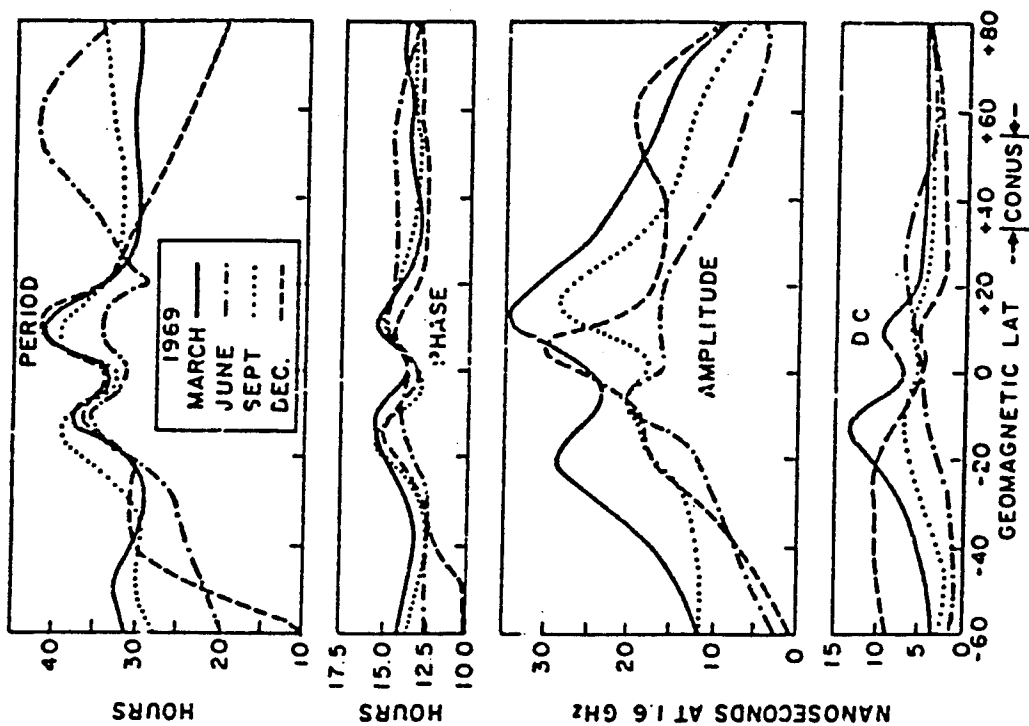


FIGURE 27. IONOSPHERIC DELAY COSINE MODEL COEFFICIENTS (BENT MODEL VS. GEOMAGNETIC LATITUDE)

TABLE 31. DAVIS TROPOSPHERIC DELAY MODEL ERROR BUDGET

Error Source	Error Model	Error Value	Tropo Delay Accuracy (rms-m)	Comments
Zenith Model				Saastamoinen Standard Model
Dry Component	δD_{D}	0.002 - 0.003 m	0.002 - 0.003	
Wet Component	δD_{W}	0.03 - 0.05 m	0.03 - 0.05	
Mapping Function	$\delta D_{\text{MF}} = k_{\text{MF}} D_{\text{T}}$	$k_{\text{MF}} = 1\text{-}2\%$ ($D_{\text{T}} = 2.3\text{-}25$ m)	0.02 - 0.05 (Zenith) 0.25 - 0.50 (5°)	Marini & Murray
Pressure Sensor	$\delta D_{\text{P}} = 2.31 k_{\text{P}} \text{ MF}$	$k_{\text{P}} = 1\%$ ($\text{MF}=1.0\text{-}10.2$)	0.02 - 0.24	Zenith to 5° elev.
Temperature Sensor	$\delta D_{\text{T}} = 3.03 \text{ RH } k_{\text{T}} \text{ MF}$	$k_{\text{T}} = 1\%$ ($\text{RH} = 0\text{-}1.0$)	0.008 - 0.077 0.023 - 0.23	RH=25%, Zenith to 5° RH=75%, Zenith to 5°
Relative Humidity Sensor	$\delta D_{\text{RH}} = 0.17 \text{ RH } k_{\text{RH}} \text{ MF}$	$k_{\text{RH}} = 5\%$	0.002 - 0.022 0.006 - 0.064	RH=25%, Zenith to 5° RH=75%, Zenith to 5°
TOTAL DELAY ACCURACY (rss-m):			0.04 - 0.60	

Note: $D_{\text{T}} = D_{\text{Z}} \text{ MF}$, the total tropospheric delay (D_{T}) is equal to the product of the zenith delay (D_{Z}) times the mapping function (MF).

Figure 28 shows the effect of radial orbit error on range error as a function of distance from the terminator (the point directly below the satellite). For typical maximum user/reference baselines of three hundred kilometers, local differential techniques remove virtually all of the radial error. Thus, the signature of the radial orbit error is nearly identical to that of a satellite clock bias.

The only practical method of distinguishing radial orbit error from clock error is observation over long periods and comparison to complex orbit models. Even then a radial orbit error due to eccentricity (no change in period) can be mimicked by a carefully constructed, slowly moving clock bias with a 12-hour cycle. In return for not being observable, radial error is quickly and completely removed by differential means with little or no spatial decorrelation.

This is not true of cross-track and along-track errors, however. As reported by Loomis, et al. [8], under normal Selective Availability conditions, the differential range error effect due to orbit error can be much larger than ionospheric model error or any other differential error, perhaps 1.3 meters (2 drms) per 100 km baseline separation. Modeling of this error becomes quite important. Because it causes so much difficulty with long baselines in local differential systems, it is observable using the long baselines of the networked GPS system.

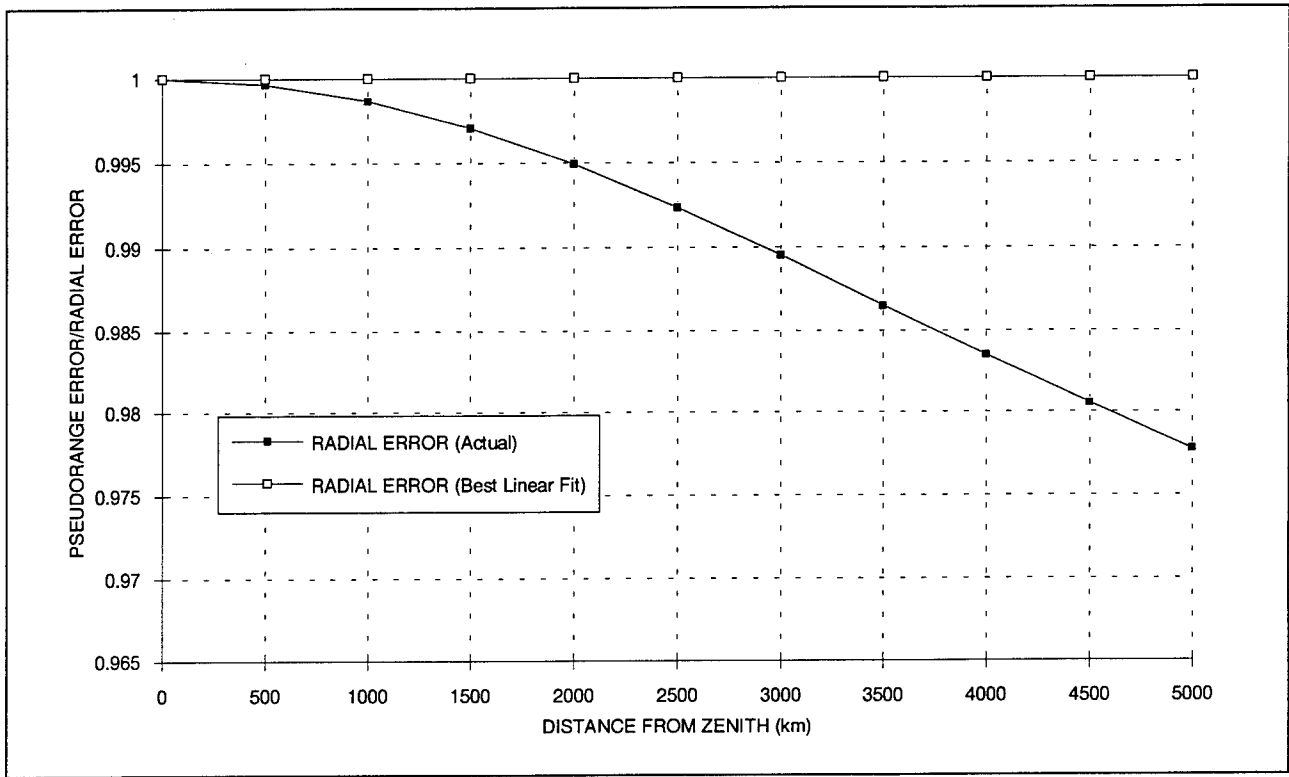


FIGURE 28. LINEARITY OF PSEUDORANGE ERROR DUE TO RADIAL ERROR

The propagation model is an equally important issue. Over short periods of time, a constant position offset bias model is appropriate, while over longer periods of time, a constant rate of change is. Finally, over even longer periods of time, a constant acceleration model is appropriate. As a rough rule, one can expect the differential range error to have an amplitude of no more than 10 meters on a 500 km baseline with sinusoidal behavior of a six-hour period (the period of the broadcast orbital parameters). This translates to maximum velocities of 3×10^{-3} m/s and acceleration of 10^{-6} m/s/s. To maintain accuracies on the order of 0.1 meter at 500 km baseline separation the update rate for a constant bias model would be less than 30 seconds, and for the constant bias rate model, roughly 400 seconds. A constant acceleration model would effectively last for an hour over the same baseline.

The gradient approach is not appropriate for large scale networks because of slight non-linearity over large baselines. Although the equation:

$$\delta\rho = (\underline{u} - \underline{r}) \cdot \left[\frac{\underline{R} \times (\delta\underline{S} \times \underline{R})}{|\underline{R}|^3} \right]$$

may look to be linear in $(\underline{u} - \underline{r})$, the term $\underline{R} = (\underline{S} - (\underline{r} + \underline{u})/2)$ is also dependent on \underline{u} , which creates a small but non-negligible second-order effect. The second-order effect only becomes evident over long distances.

Figure 29 shows the effect of non-radial satellite position on range error as a function of distance from the terminator. Satellite position error has been assumed to be parallel to the baseline to show maximum effect, and the range error has been computed using the cross-track/along-track offset method. The linear best fit shown on the

plot is a linear function describing the pseudorange error as a function of the two-dimensional Cartesian coordinates of the user position projected into the plane orthogonal to the satellite radial axis. This is effectively the two-dimensional gradient approach extended to a global scale.

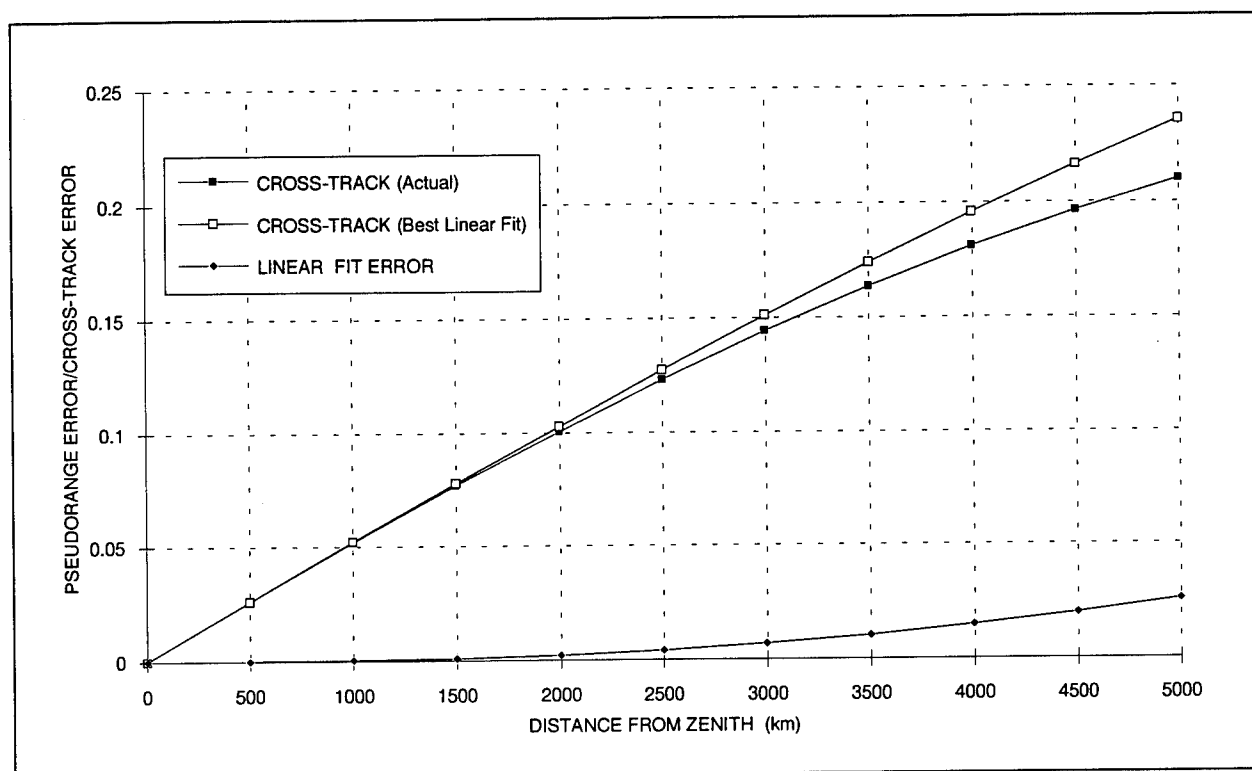


FIGURE 29. LINEARITY OF PSEUDORANGE ERROR DUE TO CROSS-TRACK ERROR

The gradient is accurate near the terminator, but it does not extrapolate well over long distances. The gradient estimate is two-dimensional, just as the cross-track/along-track satellite position offset estimate, and is no easier to compute. The cross-track/along track offset approach, however, gives a true account of the range error for its two dimensions and is preferable over any but the shortest baselines. The gradient approach is perhaps more robust for common-view networks with short baselines that combine atmospheric errors and orbit errors in a common pseudorange error function.

The question remains whether more complicated orbit methods using Kepler parameters or complex gravity and force models provide better estimates. In general, these methods search for the radial component and attempt to propagate the orbits for very long time periods, which may be helpful in case of a network outage. The radial component is not readily available from direct measurement.

To illustrate, a typical orbital radius error of thirty meters will cause a thirty meter offset for users directly below and a twenty-nine meter offset for users on the horizon. The one-meter difference can technically be used to

solve for the radial error. However, the horizon user's pseudorange measurement accuracy is poor because of slant range error effects. Hence, there is little likelihood of recovering a direct measurement of radial error. Consequently, the orbital radius must be observed by recording the start and end of an orbit over twelve hours, or more likely a two-orbit sequence over twenty-four hours, and relating the orbital period to the orbital radius through a gravity model. Even this approach gives only the period, and as noted above, the eccentricity can be hidden by a well-constructed clock bias.

In TAU's study with Worldwide DGPS, the radial element of the orbit was found to be so unobservable with pseudoranges over short orbit arcs that the orbital radius value in the estimator was initialized to the broadcast value, with corrections for radial error migrating into the pseudorange correction as a bias. Thus, the Worldwide DGPS estimator was weighted heavily, although not completely, in the direction of a two-dimensional estimator as described in the paragraph above.

Research has developed long-term orbit prediction models, but these use long baseline data sets and complex orbit models (e.g., Ashkenazi [19,20]). Table 32 summarizes the various forces that determine the orbit. Also shown is the impact of ignoring the major forces in a detailed propagation model. Clearly, the earth's gravity field (up to 4 x 4 term harmonics), the sun and moon point mass gravity, and the solar radiation pressure on the satellite need to be considered for a one hour orbit. The same accuracy for a real-time system can be achieved more simply with less data transfer by using the cross-track/along-track model.

TABLE 32. GPS ORBIT DETERMINATION ACCURACY

BROADCAST ORBIT SPECIFICATION ACCURACY [38]: 1.5 - 3.6 m UERE (Phase III - I GPS)

ORBIT FORCES	Acceleration [39] (m/sec ²)	1-Hour Orbit Error [38] (m)	1-Day Orbit Error [39] (m)
Earth Gravity			
Central Body	0.59		
Oblateness	5 E-5	300	10 ⁴
Nonsphericity	3 E-7	0.6	200
Moon Gravity	5 E-6	40	3 E+3
Sun Gravity	2 E-6	20	800
Solid Earth Tides	1 E-9		0.3
Ocean Tides	5 E-10		0.04
Solar Radiation Pressure ⁺	6 E-8	0.6	200
Albedo Pressure ⁺	4 E-10		0.03

⁺The GPS Satellite Area-to-Mass Ratio: 1.24 E-2 m²/kg, P_{sun} = 1367 w/m², P_{alb} = 10 w/m²

5.3.5 Satellite Clock Model

The satellite clock model currently in use by RTCM matches the presumed Selective Availability character of clock dither: a clock bias with frequency offset, with most of the latency error coming from frequency drift with a maximum magnitude equivalent to 0.01m/sec^2 . Considering that the major cause of accuracy failure is the latency added by missed messages at distances far from the reference station, the clock model in the RTCM message should be re-assessed to determine if extra terms are appropriate to allow propagation. Adding extra terms to the message becomes a trade-off study in bandwidth, missed messages, robustness and latency, and retrofitting.

An acceleration field, in the message, sufficient to propagate through a single missed message with accuracy equivalent to the case where the message has not been missed, would allow an increase in maximum latency from two message cycles to three. (One cycle to send a complete message A, and another to receive a new complete message B before A is discarded, at which time the data in A is two cycles old. If B is missed, another cycle is added until C is received.) Because error rises roughly with the square of the time, the current acceleration error would need to be halved, requiring at least four bits of acceleration data per satellite.

The simplest method is to infer acceleration by backwards differencing the rate terms in the pseudorange correction message, provided that they are direct measurements of range rate error. The range rate correction field must be specified to support this operation; otherwise, the inference is a straight-forward user function.

5.3.6 WADGPS Network Clock Model

For simulation purposes, TAU maintains a variety of clock models covering a range of crystal oscillators and atomic frequency standards. These are principally random walk/random run models that imitate the medium term and long-term stability of the frequency generators. TAU also uses a "null" clock model with almost no assumed dynamics for study of self-synchronizing networks.

Clock synchronization is performed using the standard least-squares approach. If atomic frequency standards are used, the effects of performing synchronization intermittently, as opposed to continuously, should be examined. Continuous synchronization has the effect of removing one measurement from each reference station for double-differencing, reducing the power of the measurement set. It also prevents the satellite position estimators from being separated, since all satellite ranges are inter-correlated through the reference station errors. With intermittent synchronization, the satellite estimators can be separated, resulting in a number of small efficient estimators rather than one large unwieldy one.

The proposed Coast Guard DGPS network will have atomic frequencies as an option. Hence, intermittent synchronization can be applied.

5.3.7 Multipath and Other Non-Common Mode Error Models

The following paragraphs illustrate multipath behavior in the GPS measurements and demonstrate how it can be minimized.

Figure 30 demonstrates the systematic error in the code-carrier differenced measurement. The period of this particular multipath signature is about 100 seconds. The solid line shows the difference between raw pseudorange and integrated Doppler (later referred to as code-carrier difference). The dashed line shows carrier smoothed pseudorange with a 100 second time constant Low Pass Filter (LPF). It is evident that the 100-second filter is not enough to remove this extreme multipath error.

Figure 31 contains three curves: the solid line represents the adjusted code-carrier difference, the dotted line represents the estimated multipath in the original code measurements, and the dashed line is the carrier-smoothed code. The carrier-smoothed code is used by the reference stations to generate differential pseudorange corrections, and by the mobile users to calculate code residuals for the navigation processor.

The multipath estimate is derived by real-time parallel processing of the code-carrier linear combinations. By filtering code-carrier measurements with different time constants, it is possible to identify the multipath signature. By passing the adjusted code measurements through a LPF, multipath and receiver noise are reduced to a level sufficiently low to maintain an external accuracy of less than 5 meters (95% confidence level).

The systematic effects seen in Figure 30 for the static case are not expected to be present in the kinematic case of the user, due to the motion of the antenna (i.e., roll, pitch, and yaw). As the motion of the antenna decreases, the multipath is likely to become a significant error source. Thus, calm water represents a higher multipath environment to the marine user than agitated water. In that case, a similar parallel measurement processing approach can be performed at the mobile user to decrease the effect of the multipath errors.

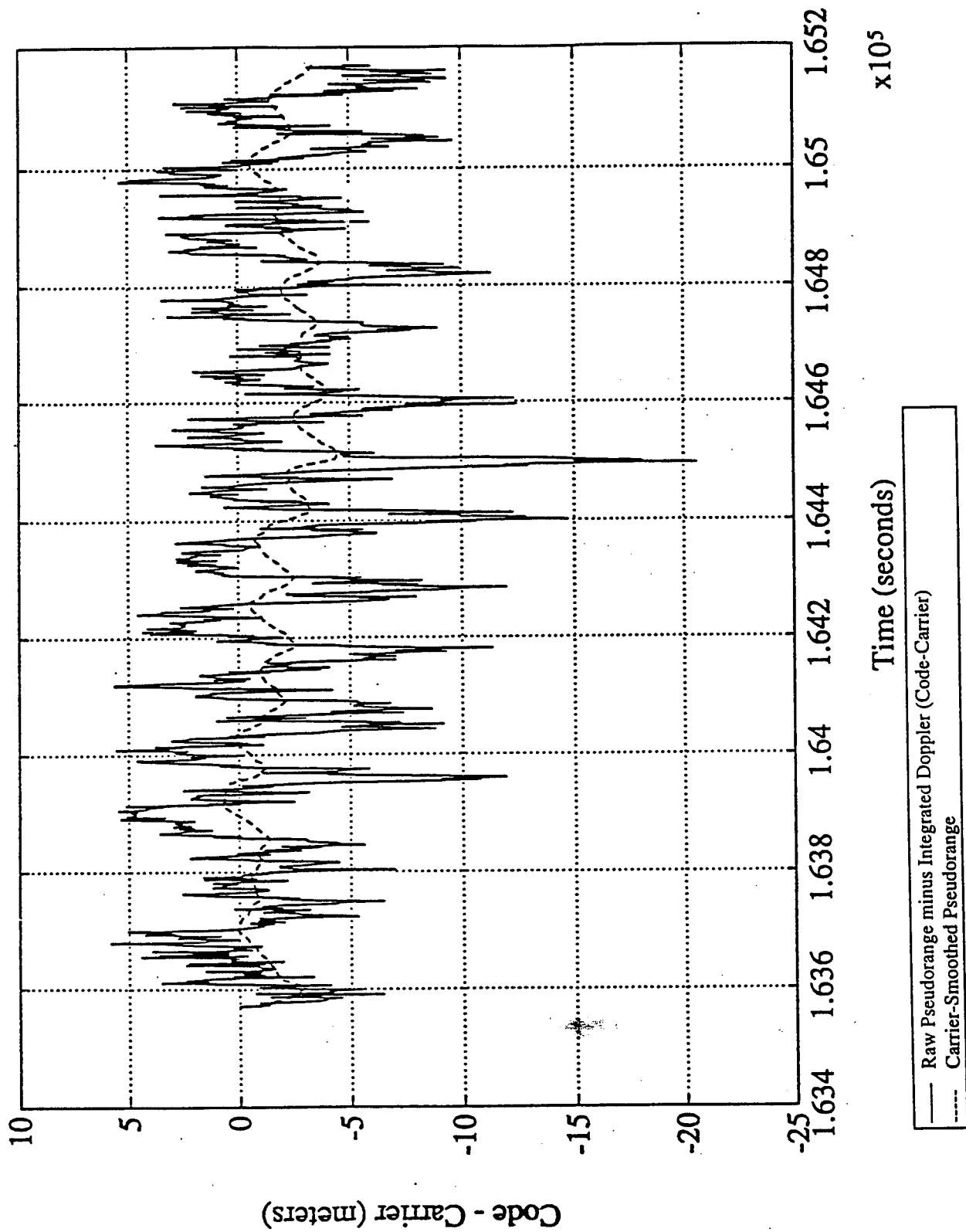


FIGURE 30. EXTREME MULTIPATH CONDITIONS

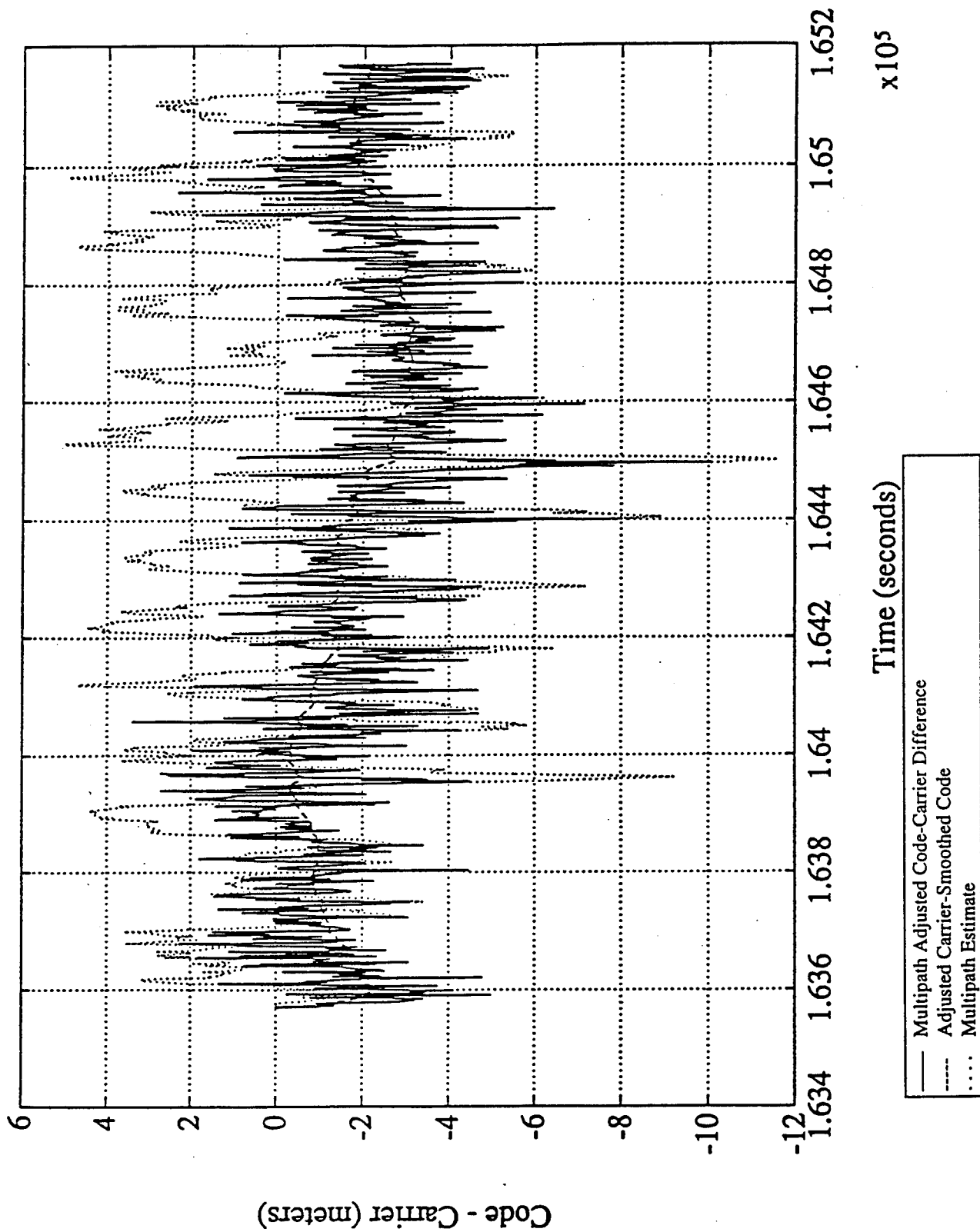


FIGURE 31. REDUCED MULTIPATH

6. REMAINING WORK

This section summarizes additional work that is required to address any concerns about the feasibility of upgrading the Coast Guard Local Area DGPS architecture to a WADGPS architecture. This additional work will be separated into WADGPS architecture and WADGPS model-related tasks.

6.1 WADGPS ARCHITECTURE

The following architecture related issues should be addressed during the option period of this contract.

6.1.1 Establish WADGPS Network Time Transfer and Synchronization Requirements

For each of the three architectures, the unique network time transfer and synchronization requirements would be examined. This would include such techniques as using the clock of the satellite in common view to all stations in the local or regional network to perform the time transfer. It would also explore using the control center or local master station clock as the reference clock. As a baseline for comparison, the use of atomic clocks at each reference station would be considered. The output from this task would be an algorithm or recommended methodology for performing the network clock time transfer and synchronization for each of the three WADGPS architectures.

6.1.2 WADGPS Network Performance Simulation

A Monte Carlo performance simulation would be developed to allow a fair comparison of the proposed WADGPS network software algorithms for the three candidate WADGPS architectures. It would have the general structure of the performance models shown in Figures 19 and 20, and would be able to model both. Specifically, it would include a simulation of the satellite orbits, ionospheric delays, and tropospheric delays. It would include the actual location of the WADGPS network reference stations and would randomly select the user's location within the beacon coverage area. Initially, the results would be kept "realistic" by the use of both state and measurement noise statistics.

If practical, a more sophisticated version of the performance model would be coded. This version would include separate "real" world and "filter" world state and measurement equations. This performance simulation would be used to compare the performance of the network software for the three WADGPS architectures.

6.1.3 Obtain Availability of Accuracy Estimates

The COAST methodology, developed by The Analytic Sciences Corporation (TASC) for the USCG, provides a sophisticated approach to obtain Availability of Accuracy Estimates for each of the three WADGPS architectures. By providing performance results from Task 6.1.2 to the Coast Guard, the USCG would be able to obtain the Availability of Accuracy Estimates using the COAST methodology. The output of the TAU effort would be accuracy statistics for each of the three WADGPS architectures.

6.1.4 Perform Cost-Benefit Analysis

A cost-benefit analysis would be performed to assess which, if any, of the three WADGPS architectures should be implemented. This would incorporate estimates of Availability of Accuracy, reliability, integrity, and cost, as well as qualitative factors. While the Availability of Accuracy Estimates would come from Task 6.1.3, the remaining factors would come from Section 4.0. A weighting scheme would be selected to combine the separate factors in order to obtain a weighted score for each architecture. The output from this task would be a summary of the individual factors as well as the weighted cost-benefit score for each of the three architectures.

6.1.5 Develop a WADGPS Integrity Network

The current DGPS service integrity monitor architecture and the three WADGPS network integrity monitor architectures differ only in that permanent beacon coverage monitors have been added to the latter. Hence, the three WADGPS architectures are essentially using a DGPS integrity architecture. Under this task, the WADGPS integrity monitors would be considered the elements of a WADGPS integrity network. This is the analogue of the WADGPS reference stations forming the elements of the WADGPS accuracy network.

Due to the finite range of the broadcast beacons, which limits the monitors to typically covering only one beacon, there may be limitations to the extent to which such a WADGPS integrity network can be realized. Hence, alternate integrity architectures would be derived and compared. Also, candidate integrity software algorithms best suited to this integrity network would be identified in the literature. The output from this task would be candidate WADGPS integrity network architectures and a comparison of these architectures.

6.1.6 Investigate Alternate WADGPS Network Communications Systems

For the DGPS service, all the critical components of this system are hardwire connected. Only the control function, which is not in the critical data path, uses the AT&T FTS 2000, X.25 packet switching service, landline communications network. To minimize cost, this same X.25 communications network was selected to provide critical data communications for the three WADGPS network architectures. As was shown in Section 4.4, this resulted in unacceptably low ground system reliabilities.

Under this task, alternate WADGPS network communications system approaches would be explored. One approach, if feasible, would be to use a redundant FTS 2000 X.25 communications network. Alternately, redundancy could be achieved by relying on another communications system for backup. Finally, the option of selecting a single communications network with sufficient standalone reliability would be investigated. This evaluation would consider the joint goals of improved communications reliability with minimum communications costs.

6.2 WADGPS MODEL DEVELOPMENT AND ASSESSMENT

Based on the Model Assessment of Section 5.0, it became clear what the limitations in defining and implementing a practical WADGPS network error model are. A practical model satisfies the USCG accuracy requirements and conveniently disseminates this information to marine users. As the various authors who have previously defined network filters have found (Table 14), the issue is not how complex a network error model one can formulate, but how accurately (if at all) the unknown coefficients in the model can be determined. The scope of this section will be to identify the mathematical models that need to be developed for those WADGPS error sources for which no satisfactory model exists.

The following tasks address the additional model development and analysis that should be performed during the option period of this contract.

6.2.1 Evaluate High Frequency (Spatial and Temporal) Ionospheric Effects

The well-known ionospheric delay models, such as the broadcast (Klobuchar), Bent, and IRI-90 models, provide 24-hour global coverage for the C/A-code user. These models are limited in describing local ionospheric conditions that are beyond the normally expected behavior and which may only be temporary. The proposed 16 dual-frequency reference stations of the CONUS DGPS network provide a relatively dense real-time ionospheric delay measurement network with which to determine the real-time ionospheric delays for the CONUS DGPS network user.

By reviewing the available literature, the nature of the high frequency ionospheric effects data would be summarized. Based on this data and the 16 dual-frequency station CONUS network (which includes an iono model estimator), an assessment would be made of the net impact of these high frequency ionospheric effects on the user. Outputs from this task would be a summary of high frequency ionospheric effects data and an assessment of the net impact on the CONUS DGPS network, since it includes an iono model estimator.

6.2.2 Refine the Minimum Variance Algorithm for the EC/WCA-DGPS Network

This task would focus on the complexity of the Minimum Variance Algorithm when the network increases, such as in the case of the East-Coast/West-Coast area DGPS network, which includes 33 sites on the East Coast and 17 sites on the West Coast. Alternate formulations would be investigated which would retain the high accuracy of this algorithm but would reduce the number or frequency of the terms that would have to be broadcast. Also, alternate forms would be investigated which would be more practical to solve by the user.

One of the alternate approaches that would be investigated is the use of the Minimum Variance Algorithm to compute a DGPS "correction surface" based on evaluating the corrections for a matrix of possible user locations in the beacon coverage area. Using this "correction surface," practical fits would be identified. These would be characterized by minimized complexity for the user with the highest accuracy possible. The output from this task would be a recommended optimum formulation of the Minimum Variance Algorithm for the user under the EC/WCA-DGPS network architecture.

6.2.3 Evaluate Minimum Variance Algorithm with Field Data

Under this task, DGPS network field data would be obtained and used to evaluate the performance of the Minimum Variance Algorithm. The field data set should consist of DGPS data from a minimum of three C/A-code reference stations, preferably with legs (spacing) of 200-300 kilometers. The data should, as a minimum, cover a period of two hours for nominal daytime ionospheric conditions as well as good HDOP visibility conditions. In addition, data from "user" sites both inside and outside the network would be required.

This analysis would evaluate the performance of both the Minimum Variance Algorithm and the Partial Derivative Algorithm. Truth would be provided by the known locations of the user. The software used to perform this analysis might be a modified version of the performance simulation of Section 6.1.2.

6.2.4 Evaluate RAIM Integrity Software Performance

When the WADGPS network is tracking more than four satellites, it is possible to detect failures of one or more satellites using Receiver Autonomous Integrity Monitoring (RAIM) software. This same software given more than 5 satellites can, under most circumstances, identify which satellite has failed. This is accomplished using a parity vector concept originally developed by Sturza and others [41,42]. Since this concept is being considered for both the integrity monitors and the marine beacon users, its performance should be investigated.

The performance simulation of Task 6.1.2 would be modified. This would involve adding the measurement parity logic to this simulation and using it with the measurement matrix of the monitor or user. A Monte Carlo evaluation could then be performed with varying HDOPs and user locations to determine the potential benefits of such an algorithm. The simulation would focus on a single RAIM algorithm selected from the literature.

The output from this task would be the performance simulation results for one RAIM algorithm for a WADGPS architecture.

7. CONCLUSIONS AND RECOMMENDATIONS

Under the base period of this contract, three candidate WADGPS architectures have been postulated and evaluated. These are the Federated Local Area DGPS (FLA-DGPS) network, the East Coast/West Coast Area DGPS (EC/WCA-DGPS) network, and the Continental US DGPS (CONUS-DGPS) network.

7.1 WADGPS ARCHITECTURES

The FLA-DGPS network is formed by designating each DGPS reference station as its own master station and using the reference stations on either side to form a three-station Local Area DGPS network. At the master station, the DGPS spatial decorrelation function and an inverse network spatial decorrelation matrix would be computed and broadcast to the user, together with the DGPS corrections from the three stations of the network. The user would compute the Minimum Variance Algorithm weighting coefficients for combining the individual reference station DGPS corrections in order to obtain a network DGPS correction valid for his location.

The EC/WCA-DGPS network nets all of the East Coast (including Great Lakes, Gulf Coast, and Puerto Rico) DGPS stations into a 33-station East Coast network. It also nets all of the West Coast (including Alaska and Hawaii) DGPS stations into a 17-station West Coast network. The DGPS corrections from each site of the respective Coast networks would be sent to the control centers for that coast. The control centers would use Minimum Variance Algorithms to compute DGPS correction "surfaces" for the beacon coverage area of that Coast by calculating the corrections for a matrix of possible user locations. The control center would reformulate these corrections for the local beacon site so as to provide the maximum accuracy for the user with a minimum of communication burden and minimum user complexity.

The CONUS DGPS network would place dual-frequency DGPS reference receivers at 16 of the 50 DGPS beacon sites. These receivers would compute the ionospherically corrected DGPS corrections and send them, together with the iono corrections, to the redundant control centers. The control centers would use an explicit filter model to estimate the user's ionospheric delays, the satellite clock and ephemeris errors, and the network clock errors. These would be reformulated into a practical user algorithm and sent back to each of the 50 beacon sites for transmission to the user.

All three architectures would be implemented with fault-tolerant network software. Hence, the architectures would be able to provide network DGPS corrections to the user even if some of the individual reference site DGPS corrections become unavailable to the network DGPS algorithm. Also, a capability would be incorporated to always broadcast, as a minimum, the basic DGPS service corrections, in case the network DGPS corrections are not available due to network communication outages or other reasons.

Table 33 summarizes the physical assets for the three network architectures. As can be seen in this table, these network architectures use the DGPS service architecture as the fundamental building block. The FLA-DGPS network adds permanent coverage monitors and the AT&T FTS 2000, X.25 digital landline communications links between these and the beacon site. In addition, X.25 communications between the beacon sites is introduced.

The EC/WCA-DGPS network eliminates the need for intersite X.25 communications, except as a backup. It does place the responsibility for computing the network DGPS corrections at the two control centers. Finally, the CONUS network architecture eliminates the need for the 50 dual-redundant single-frequency DGPS reference receivers, except for backup. Instead, 16 dual-redundant, dual-frequency DGPS reference receivers are introduced at 16 of the 50 beacon sites.

The network hardware and software are presented in Table 34. This table shows that the baseline DGPS reference receiver for the DGPS service, and hence for the FLA-DGPS and EC/WCA-DGPS networks, is a 12-channel C/A-code receiver. For the CONUS DGPS network, a 24-channel P-code receiver is baselined. This receiver will be a non-military P-code receiver which will be able to revert to a full-wavelength codeless tracking capability in the presence of Y-code (encrypted P-code).

The FLA-DGPS network has baselined a separate processor to host the master station network software. For the EC/WCA-DGPS networks, the control centers will have separate workstations for hosting the network DGPS software.

The beacon site DGPS correction software will always compute the local DGPS corrections, except that for the CONUS 16-site network these corrections will be ionospherically corrected. These corrections will be the basic input into the three network DGPS filters, whether at the local master station or at the control center. In all three cases, the network DGPS corrections that are broadcast to the user will form a local network solution valid for that beacon site.

The architectures for the FLA-DGPS, EC/WCA-DGPS, and CONUS DGPS networks were presented in Figures 5, 7, and 9, respectively. The functional data flows for these same three WADGPS networks were presented in Figures 6, 8, and 10, respectively.

7.2 WADGPS MAJOR ISSUES

Estimates of the performance for these three architectures were presented in Table 10 and Figure 13 of Section 4.2. It was shown that for a baseline of 300 kilometers, the FLA-DGPS network navigation accuracy was 20% better than for the DGPS service. For the EC/WCA-DGPS network, the navigation accuracy was 29% better than for the DGPS service. For both of these network cases, the results were computed for a near-worst case location of the user relative to the network. Therefore, the results are conservative.

TABLE 33. WADGPS NETWORK PHYSICAL ASSETS

ASSETS	DGPS SERVICE [3]	FLA-DGPS	EC/WCA-DGPS	CONUS DGPS	COMMENTS
DGPS Beacon Sites	50	50	50	50	See Figure 2 & Table 2
Control Centers	2	2	2	2	Alexandria, VA & Petaluma, CA
DGPS Reference Stations	2/Site	2/Site	2/Site	2/Site (16 Sites)	Collocated with Beacon
MSK Transmitters	2/Site	2/Site	2/Site	2/Site	
MSK Beacons	1/Site	1/Site	1/Site	1/Site	
<u>Integrity Monitoring:</u> Monitor Stations	2/Site	2/Site	2/Site	2/Site	Collocated with Beacon
Beacon Coverage Monitors	10	2/Site	2/Site	2/Site	DGPS coverage monitors-movable WADGPS coverage monitors-fixed, at coverage limit
DGPS Receiver Data Logger	2/Site	2/Site	2/Site	2/Site	Option
Integrity Monitor Data Logger	2/Site	2/Site	2/Site	2/Site	
Coverage Monitor Data Logger	None	2/Site	2/Site	2/Site	
Communications:					Underlined cases in critical path - Navigation Data
Beacon - Control Center	X.25 PSS	X.25 PSS	<u>X.25 PSS</u>	<u>X.25 PSS</u>	
Beacon - Beacon	None	<u>X.25 PSS</u>	None	None	
Beacon - Coverage Monitor	None	X.25 PSS	X.25 PSS	X.25 PSS	
NGS Dual-Frequency Receivers	15	15	15	15	Not used for real-time DGPS corrections except for CONUS (Option)

TABLE 34. WADGPS NETWORK HARDWARE AND SOFTWARE

HARDWARE	DGPS SERVICE [3]	FLA-DGPS	EC/WCA-DGPS	CONUS DGPS	COMMENTS
DGPS Receiver with MSK Modulator	12 Channel C/A Code	12 Channel C/A Code	12 Channel C/A Code	24 Channel P-code (Codeless)	
Beacon Site DGPS Processor	None	386/486 PC or Receiver Processor	None	None	
Control Center DGPS Processor	None	None	Workstation	Workstation	
DGPS Monitor with MSK Receiver	C/A Code	C/A Code	C/A Code	C/A Code	
Coverage Monitor with MSK Receiver	C/A Code	C/A Code	C/A Code	C/A Code	
DGPS Receiver Data Recorder	8 mm Tape (Bernoulli) Recorder	8 mm Tape (Bernoulli) Recorder	8 mm Tape (Bernoulli) Recorder	8 mm Tape (Bernoulli) Recorder	Option
Integrity Monitor Data Recorder	8 mm Tape (Bernoulli) Recorder	8 mm Tape (Bernoulli) Recorder	8 mm Tape (Bernoulli) Recorder	8 mm Tape (Bernoulli) Recorder	
Coverage Monitor Data Recorder	None	8 mm Tape (Bernoulli) Recorder	8 mm Tape (Bernoulli) Recorder	8 mm Tape (Bernoulli) Recorder	
SOFTWARE	DGPS SERVICE	FLA-DGPS	EC/WCA-DGPS	CONUS DGPS	COMMENTS
Beacon Site	DGPS Corrections	DGPS Corrections	DGPS Corrections	DGPS Corrections & Iono Data	
Master Station	None	3-Station DGPS Network Corrections	None	None	For FLA-DGPS, each beacon site is its own master station
Control Center	None	None	EC/WCA DGPS Corrections & Fit For each b Beacon Site	CONUS DGPS Error Estimates & Beacon Site Corrections Formulation	

The estimated navigation accuracy under the CONUS DGPS network, which is baseline independent, is approximately 5% worse than the accuracy with the DGPS service at a baseline of 300 kilometers. The results for the CONUS DGPS network are very preliminary and should be verified with a performance simulation or field data.

It was determined that the Availability of Accuracy for an HHA navigation accuracy requirement of 8 meters (2 drms) with an availability of 0.997 cannot be satisfied by the DGPS service out to a baseline of 300 kilometers, assuming no broadcast signal loss (Figure 14). Using a fault-tolerant approach for the FLA-DGPS network, this Availability of Accuracy requirement also cannot be satisfied for baselines out to 300 kilometers using the same assumptions and for the generic scenario used above. Finally, with the EC/WCA-DGPS network, the Availability of Accuracy requirement also cannot be satisfied for baselines out to 300 kilometers under the same assumptions and for the generic scenario used above. When the probability of broadcast signal loss is factored in, the Availability of Accuracy estimates will be further reduced.

Evaluation of the integrity focused primarily on changes to the basic DGPS service integrity architecture and a summary of the probability that the integrity ground system is available. The specific hardware changes involved adding a permanent dual-redundant integrity coverage monitor at the outer coverage limit of each beacon site, in addition to the existing beacon co-located dual-redundant integrity monitors. Since these coverage monitors would provide a check of the network DGPS corrections at non-zero baselines, they were considered to be an essential part of the network integrity architecture. For the DGPS service, which does not factor in the non-permanent coverage monitors currently included under this service, the probability of integrity ground system availability is estimated by TASC to be 0.9985 (Table 13). For the three network architectures, which all three use the same integrity architecture, the probability of integrity ground system availability is 0.9925.

Evaluation of the reliability of the architectures was also performed for the DGPS service and the first two network DGPS architectures as summarized in Table 14. For the DGPS service, TASC estimated that 121.1 outages per million hours of operation would occur. Using the same component reliabilities and factoring in the fault-tolerant approach for the FLA-DGPS and EC/WCA-DGPS network architectures, reliabilities of 2918 and 8191 outages per million hours of operation were obtained, respectively. These low reliabilities arise from the use of the X.25 communications network in the critical data path for these network architectures. While the use of the X.25 communications network minimizes the communications cost, the resulting reliability is not high enough. Hence, possible redundant communications networks or a more reliable communications network need to be considered for these architectures.

Finally, estimates were made of the incremental costs required to upgrade from the DGPS service architecture to any of the three WADGPS architectures. As summarized in Table 9, it was determined that while the DGPS service acquisition costs as estimated by TASC are \$5.4 million, the incremental acquisition costs for the FLA-DGPS, EC/WCA-DGPS, and CONUS DGPS networks are, respectively: \$2.3 million, \$2.3 million, and \$3.4 million. The annual operations costs for the DGPS service are estimated to be \$1.0 million by TASC, while the incremental operations costs for the FLA-DGPS, EC/WCA-DGPS, and CONUS DGPS networks are, respectively:

\$0.5 million, \$0.6 million, and \$0.6 million. While the annual maintenance costs for the DGPS service are estimated to be \$0.4 million by TASC, the incremental maintenance costs for the FLA-DGPS, EC/WCA-DGPS, and CONUS DGPS networks are \$0.04 million each. Finally, TASC has estimated the total life cycle costs to be \$15.4 million for the DGPS service. The incremental life cycle costs for the FLA-DGPS EC/WCA-DGPS and CONUS DGPS networks are, respectively: \$6.1 million, \$7.1 million, and \$8.3 million.

7.3 MODEL ASSESSMENT

The highlight of the model assessment effort was the derivation of a new network DGPS algorithm—the Minimum Variance Algorithm. It was motivated by the poor performance of the well-known Partial Derivative Algorithm under the difficult local area and regional network geometries of the FLA-DGPS and EC/WCA-DGPS networks. The Minimum Variance Algorithm differs from the Partial Derivative Algorithm in that it determines the weighting coefficients for the reference station DGPS corrections using a minimum variance approach that incorporates the spatial decorrelation functions of the DGPS corrections. It is also versatile in that it can be used with any number of reference stations. One drawback is that the calculation of the coefficients, which must be done with the users position, rapidly becomes complex for networks with more than three reference stations.

7.4 RECOMMENDATIONS

Based on the work completed to date, both the FLA-DGPS and ECWCA-DGPS network architectures look very promising as candidate architectures for a WADGPS service. These systems could be formulated and implemented as a two-phase WADGPS upgrade of the basic DGPS service. The principal drawback to all three WADGPS architectures, as currently postulated, is the use of the AT&T X.25 landline communications network in the critical data flow path. While the CONUS DGPS network results are very preliminary, they do suggest that the benefits of this architecture would be realized only at the outer regions of the coverage area.

Additional work should be performed to resolve issues raised under the base period of this contract. These issues were presented in Section 6. The specific additional tasks are summarized below:

WADGPS Architecture:

- Establish WADGPS Network Time Transfer and Synchronization Requirements
- Perform WADGPS Network Performance Simulation
- Obtain Availability of Accuracy Estimates
- Perform Cost-Benefit Analysis
- Develop a WADGPS Integrity Network
- Investigate Alternate WADGPS Network Communications Systems

WADGPS Model Development and Assessment:

- Evaluate High Frequency (Spatial and Temporal) Ionospheric Effects
- Refine the Minimum Variance Algorithm for the EC/WCA-DGPS Network
- Evaluate Minimum Variance Algorithm with Field Data

REFERENCES

1. *1992 Federal Radionavigation Plan*. Department of Transportation and Department of Defense. January 1993.
2. Alsip, D.H., et al. "Implementation of the U.S. Coast Guard's Differential GPS Navigation Service." USCG Headquarters, ION 49th Annual Meeting, Cambridge, MA, 23 June 1993.
3. Creamer, P.M., et al. *DGPS Architectures Analysis*. TASC, April 1993.
4. Creamer, P.M., et al. *DGPS Operational Requirements Definition*. TASC, October 1992.
5. Loomis, P.V.W., et al. "Worldwide Differential GPS for Space Shuttle Landing Operations." IEEE PLANS '90, Las Vegas, March 1990.
6. Mueller, T., et al. *NASA SBIR Phase II Worldwide Differential GPS System Specification*. TAU Corporation, May 1991.
7. Loomis, P., et al. *NASA SBIR Phase II, Worldwide Differential GPS Final Report*. Trimble Navigation, November 1992.
8. Loomis, P., et al. *Differential GPS Network Design*. Trimble Navigation, ION GPS-91, September 1991.
9. Geier, G.J., et al. *System Analysis for a Kinematic Positioning System Based on the Global Positioning System*. Trimble Navigation, U.S. Army Corp of Engineers, 1990.
10. Hartberger II, A.W., et al. *Introduction to the U.S. Coast Guard Differential GPS Program*. USCG Headquarters, November 1991.
11. Spalding, J.W., et al. *Status of Prototype USCG DGPS Broadcasts*. USCG R&D Center, ION GPS-91, September 1991.
12. Bishop, G.J. "Specification of Trans-Ionospheric Effects for Space Surveillance." Space Surveillance Workshop, MIT Lincoln Laboratory, 7-9 April 1992.
13. Creamer, P.M., et al. *Methodologies for DGPS Architecture Analysis*. TASC, May 1992.
14. Tang, W., et al. "Differential GPS Operation with Multiple Reference Stations." ION '89, Colorado Springs, Colorado, 27-29 September 1989.
15. Mueller, T. *DGPS System Design Issues Study, Interim Briefing*. TAU Corporation, 10 March 1993.
16. McBurney, P.W. *Documentation of Differential and Integrity Monitoring Network Design and Simulation*. Trimble Navigation, 27 June 1990.
17. Brown, A. "Extended Differential GPS." *Navigation, Journal of The Institute of Navigation*, Vol. 36, No. 3, Fall 1989.
18. Kee, C., et al. *Algorithms and Implementation of Wide Area Differential GPS*. Stanford University, 1992.
19. Ashkenazi, V., et al. *Wide Area Differential Corrections R&D Study, Project Report*. University of Nottingham, 18 June 1992.
20. Ashkenazi, V., et al. "Wide Area Differential GPS: A Performance Study." University of Nottingham, ION-GPS 92, Albuquerque, New Mexico, 16-18 September 1992.
21. Klobuchar, J.A. *Ionospheric Effects on Earth-Space Propagation*. AFGL-TR-84-0004, Air Force Geophysical Laboratory, 27 December 1983.
22. Klobuchar, J.A., et al. "Design and Characteristics of the GPS Ionospheric Time Delay Algorithm for Single Frequency Users." Air Force Geophysical Laboratory, IEEE PLANS '86, Las Vegas, 4-7 November 1986.
23. Klobuchar, J.A. *A First-Order, Worldwide, Ionospheric Time-Delay Algorithm*. Air Force Cambridge Research Laboratories, AFSC, 25 September 1975.

24. Klobuchar, J.A. "Ionospheric Time-Delay Algorithm for Single-Frequency GPS Users." *IEEE Transactions on Aerospace and Electronic Systems*, Vol. AES-23, No. 3, May 1987.
25. Llewellyn, S.K., et al. *Documentation and Description of the Bent Ionospheric Model*. AD-772 733, Atlantic Science Corporation, July 1973.
26. Bilitza, D. *International Reference Ionosphere 1990*. NSSDC/WDC-A-R&S 90-20, National Space Science Data Center, Greenbelt, Maryland.
27. Mueller, T. *Preliminary WWDGPS Software Specification*. Trimble Navigation, 11 September 1991.
28. Davis, J.L. *Atmospheric Propagation Effects on Radio Interferometry*. AFGL Technical Report 86-0243, Air Force Geophysical Laboratory, Hanscom AFB, MA, 1986.
29. NAVSTAR GPS Space Segment/Navigation User Interfaces. ICD-GPS-200, Rockwell International Corporation, 30 November 1987.
30. Delikaraoglou, D. *On Principles, Methods, and Recent Advances in Studies Towards a GPS-Based Control System for Geodesy and Geodynamics*. NASA TM-100716, NASA/Goddard Space Flight Center, 1989.
31. Chou, H.T. "An Anti-SA Filter for Non-Differential GPS Users." ION GPS-90, Colorado Springs, Colorado, 19-21 September 1990.
32. Fliegel, H.F., et al. "An Alternative Common View Method for Time Transfer with GPS." *Navigation, Journal of The Institute of Navigation*, Vol. 37, No. 3, Fall 1990.
33. Klobuchar, J.A., et al. *Correlation Distance of Mean Daytime Electron Content*. AFGL-TR-77-0185, Air Force Geophysics Laboratory, AFSC, 22 August 1977.
34. Coco, D.S., et al. *Mitigation of Ionospheric Effects for Single Frequency GPS Users*. Applied Research Laboratories, The University of Texas at Austin.
35. Newby, S.P., et al. *Ionospheric Modeling for Single Frequency Users of the Global Positioning System, A Status Report*. ION-GPS-90, September 1990.
36. Van Dierendonck, A.J., et al. "The GPS Navigation Message." *Global Positioning System*, Volume I, The Institute of Navigation, 1980.
37. Jones, H.W., et al. "Analysis of Tropospheric Delay Prediction Models: Comparisons with Ray-Tracing and Implications for GPS Relative Positioning (A Summary)." *GPS '90 Proceedings*, Ottawa, Canada, 1990.
38. Landau, H., et al. "Preliminary Results of a Feasibility Study for a European GPS-Tracking Network." *Proceedings of the Fourth International Geodetic Symposium on Satellite Positioning*, The University of Texas at Austin, 28 April-2 May 1986.
39. Russell, S.S., et al. "Control Segment and User Performance." *Global Positioning System*, Volume I, The Institute of Navigation, 1980.
40. Kremer, G.T., et al. "The Effect of Selective Availability on Differential GPS Corrections." *Navigation, Journal of The Institute of Navigation*, Vol. 37, No. 1, Spring 1990.
41. Sturza, M.A. "Navigation System Integrity Monitoring Using Redundant Measurements." *Navigation Journal of the Institute of Navigation*, Vol. 35, No. 4, Winter 1988-89.
42. Brown, A., et al. "Differential GPS Autonomous Failure Detection." ION GPS-91, Albuquerque, NM, 11-13 September 1991.

APPENDIX A: ERROR BUDGET ASSUMPTIONS

The following appendix summarizes the assumptions and sources used to obtain the GPS error budget of Table 10, in Section 4.2. Table A-1 presents the individual error contributors to the GPS and DGPS accuracy. Using these, the spatial decorrelation functions can be derived for each of the DGPS error sources.

With a knowledge of the composite DGPS spatial decorrelation function, the FLA-DGPS and EC/WCA-DGPS network accuracy can be derived. It was assumed that the Minimum Variance Algorithm Network accuracy for a generic three-station and five-station DGPS network would be representative of the expected FLA-DGPS and EC/WCA-DGPS network accuracy, respectively, as previously discussed in Sections 4.2 and 5.3.1.

The statistics for the User Horizontal Dilution of Precision (HDOP), are summarized in Figure A-1. Specifically, it was assumed that a full operational 24-satellite constellation was available and that the user was using an all-in-view GPS receiver with either a 10 or 15 degree mask angle. Hence, the mean HDOP for the 10 and 15 degree mask angle is respectively: 1.10 and 1.47.

A plot of the spatial decorrelation functions of Table A-1 is presented in Figure A-2.

TABLE A-1. DGPS ERROR STATISTICS NOTES

ERROR	GPS (m)	DGPS (m)	SPATIAL DECORRELATION, r	FOOT- NOTE
SV Clock	3.0	0	1.0	(1)
SV Ephemeris	2.4	$(0.433\text{E-}4) B_{\text{km}}$	$[1 - (\sigma_{\text{DGPS}}/\sigma_{\text{GPS}})^2]^{0.5}$	(2)
SA Dither	24	$(0.5)a_{\text{SA}}t_{\text{DELAY}}^2$ $a_{\text{SA}} = 0.005 \text{ m/s}^2$ $t_{\text{DELAY}} = 10 \text{ sec}$	1.0	(3)
SA Epsilon	24	$(4.33\text{E-}3) B_{\text{km}}$	$[1 - (\sigma_{\text{DGPS}}/\sigma_{\text{GPS}})^2]^{0.5}$	(4)
Ionosphere	$[2.0/\sin(\text{Elev})]$	$\sigma_{\text{DGPS}} = \sigma_{\text{GPS}} [1 - \rho^2]^{0.5}$	$[1 - (\Delta\text{Lat}/6000 \text{ km})]$ $[1 - (\Delta\text{Lon}/9700 \text{ km})]$	(5)
Troposphere	$[0.2/\sin(\text{Elev})]$	$\sigma_{\text{DGPS}} = \sigma_{\text{GPS}} [1 - \rho^2]^{0.5}$	$e^{-(B/50 \text{ km})}$	(6)
User Receiver Noise & Multipath	1.0	N/A	N/A	(7)
Reference Receiver Noise & Multipath	N/A	0.5	N/A	(8)
Reference Receiver Survey	N/A	0.2	N/A	(9)
User HDOP	1.5			(10)

Footnotes:

- (1) GPS Error consistent with: SS-GPS-300B.
- (2) GPS Error consistent with Russell, et al [39], and assumes elevation angle = 30 deg. DGPS error based on scaled SA epsilon results which are based on Monte Carlo results (Loomis et al [8]).
- (3) GPS Error assumes equal partitioning of SA error between dither and epsilon to obtain UERE = 34 m. DGPS latency error based on SA acceleration from Kremer, et al [40], and time delays expected to range: 5 - 15 sec.
- (4) GPS Error assumes equal partitioning of SA error between dither and epsilon to obtain UERE = 34 m. DGPS error based on SA Epsilon Monte Carlo analysis and assuming an HDOP = 1.5 (Loomis, et al [8]).
- (5) GPS Error, net error after broadcast model correction (Coco, et al [34]). Spatial Decorrelation Function based on Klobuchar [33].
- (6) GPS Error based on Trimble experience. Spatial Decorrelation Function - reasonable.
- (7) GPS Error based on Trimble experience.
- (8) DGPS Error assumes accuracy after 5 minutes of tracking for satellites >15 degrees elevation.
- (9) DGPS Error based on Trimble experience.
- (10) HDOP is average value for all-in-view tracking of 24-satellite constellation and elevation angles >15 degrees, based on a Monte Carlo simulation (Figure A-1).

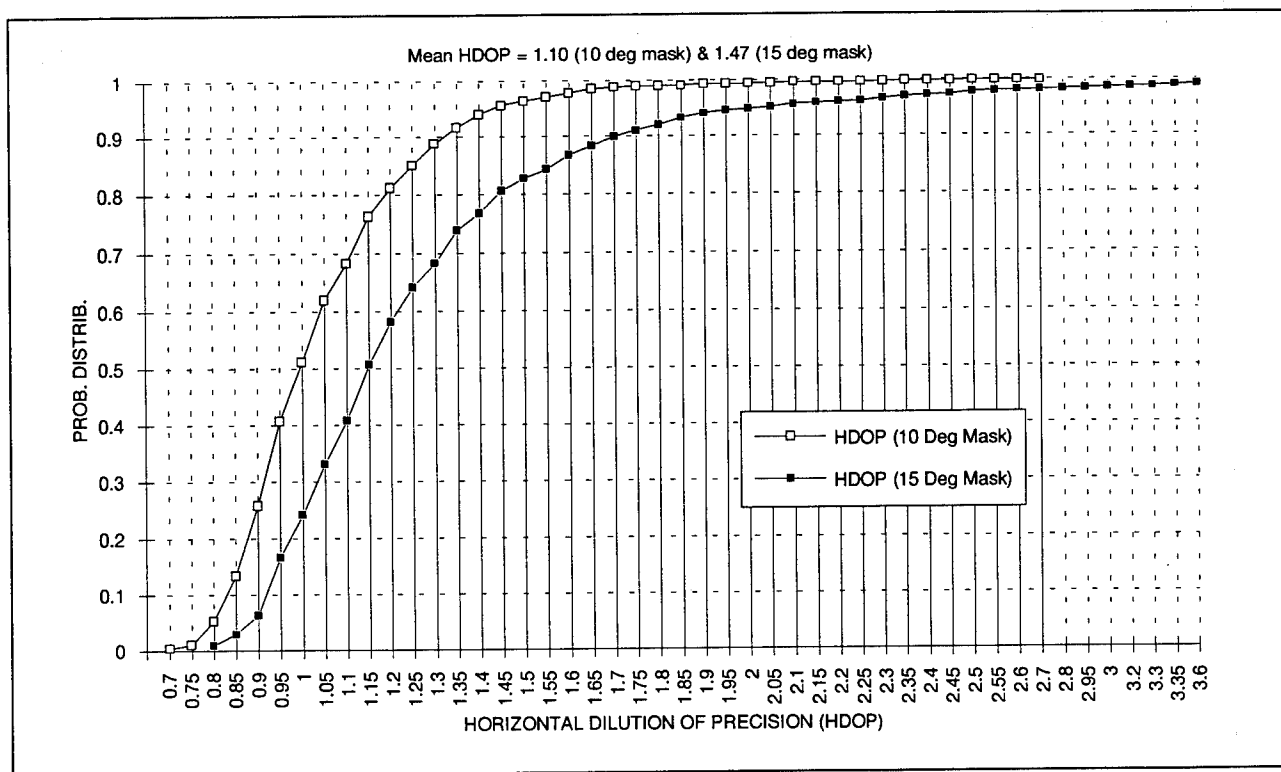


FIGURE A-1. CUMULATIVE HDOP DISTRIBUTION FOR ALL-IN-VIEW (24 SATELLITES)

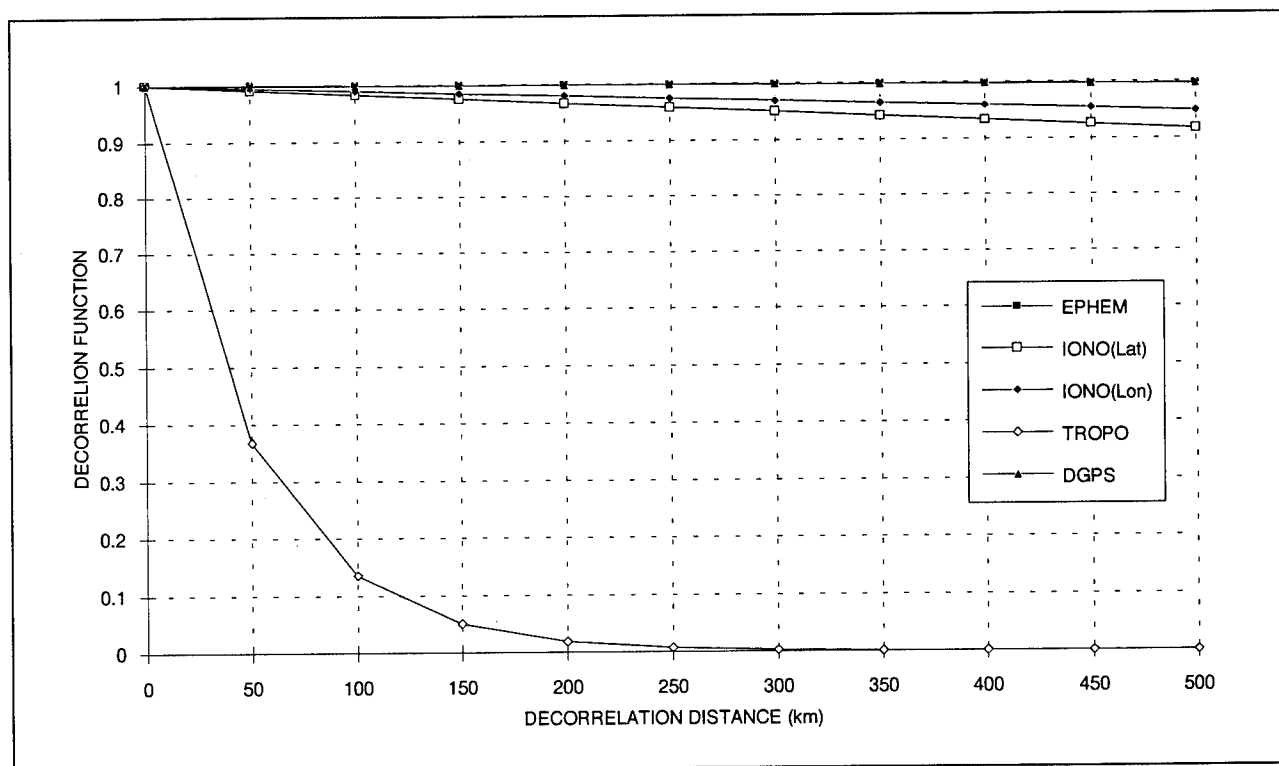


FIGURE A-2. SPATIAL DECORRELATION FUNCTIONS

APPENDIX B: NETWORK DGPS ACCURACY TEST CASES

This appendix presents a more detailed discussion of the DGPS, FLA-DGPS network, and EC/WCA-DGPS network accuracy results presented in Sections 4.2 and 5.3.1. It also presents a more detailed look at the performance of the Minimum Variance Algorithm (MVA) and contrasts its performance to that of the Partial Derivative Algorithm (PDA).

Table B-1 summarizes the test cases which were run. MathCad 4.0 was used to perform the calculations while the generic scenario used is presented in Figure B-1. The major distinguishing features which contrasted the different cases were: the DGPS sites used in the network, the separation (leg) between the sites, the corresponding central angle between the Master Site (M) and the outer sites, and the network algorithm used. The results are presented in terms of the network DGPS, rather than the navigation, accuracy relative to the DGPS (single site) accuracy for four baselines.

Case 1 is the DGPS case which is the reference case for all the network DGPS cases (Cases 2 - 12). Cases 2 - 9 are the 3-site network cases while the remaining three cases are 5-site network cases. Cases 2 and 3 show the performance for the standard 3-Site Network when the PDA and MVA algorithms are used, respectively. As can be seen, the MVA outperforms the PDA and DGPS case (Case 1) for all 4 baselines. The PDA algorithm performs as good as the DGPS case for the first two baselines, which correspond to a user inside the Network, and performs much worse than the DGPS case at the longer baselines.

Cases 6-9 explored the performance sensitivity to the separation between the (3) Sites, effectively increasing the Network area. Comparing Cases 2, 6, and 8, which correspond to the PDA software cases, we see that the performance improves with the longer separation distances and the longer baselines. Comparing Cases 3, 7, and 9, which correspond to the MVA software cases, we see some improvement at the longer baselines for the longer separation distances at some decreased accuracy for the intermediate baselines. As before, the MVA cases outperform the PDA cases for the same scenario.

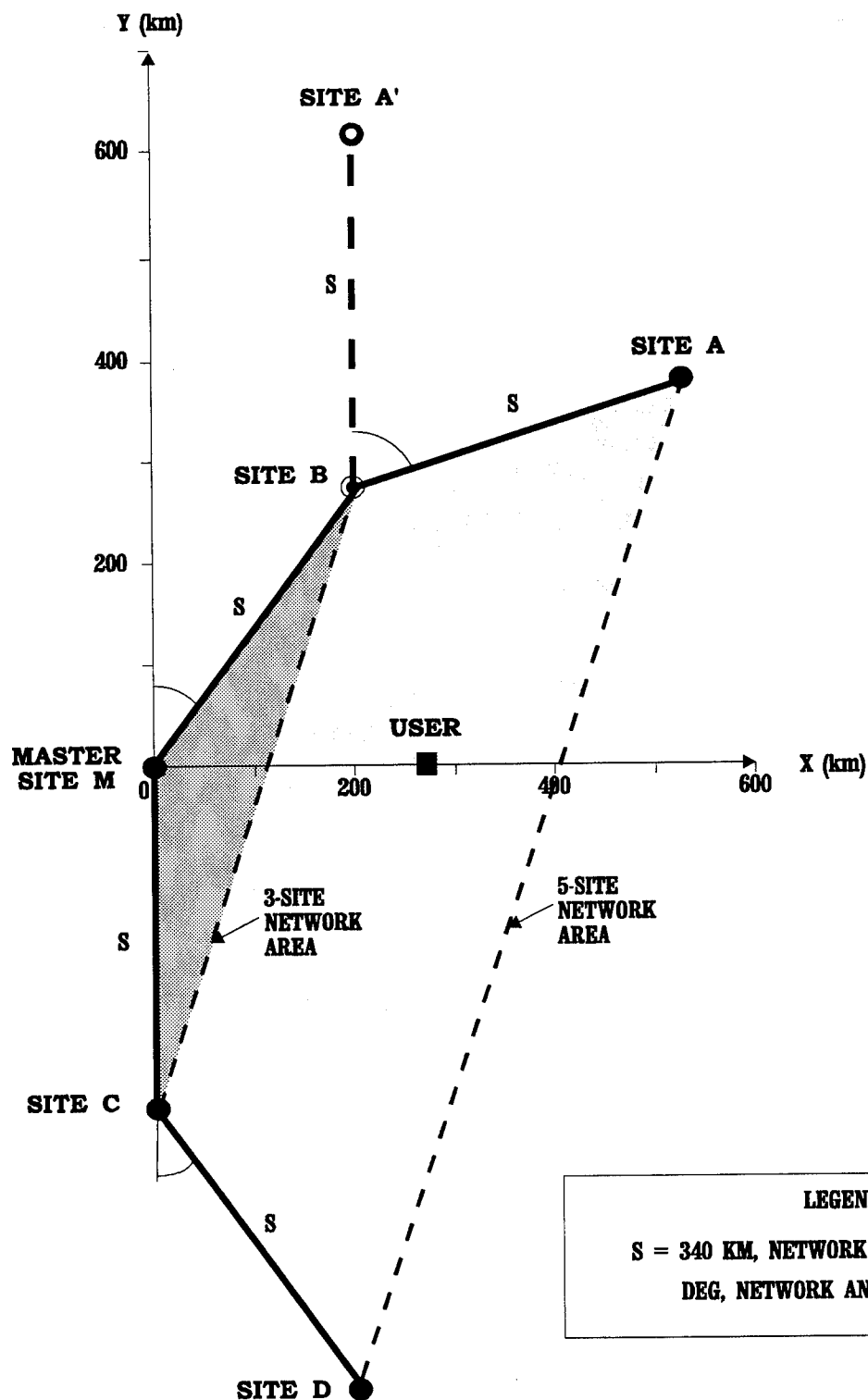
Cases 4 and 5 explore an alternate form of extending the site separation which is to use alternate (every second) sites to form a 3-site network. As can be seen, this is the best 3-site network case for both algorithms.

When we examine the 5-site network Case 10 and compare it to the 3-site network Case 5, with both cases using the MVA software, we obtain very nearly the same answer at the longer baselines, relative to Case 3. This suggests that the central angle, which is reduced from 144 degrees for Case 3 to 108 degrees for Cases 5 and 10, is a factor in determining the performance of the network. Alternately, both Cases 5 and 10 have similar network areas which are considerably larger than the network area of Case 3.

TABLE B-1. NETWORK ACCURACY RESULTS

CASE	NETWORK SITES							NETWORK VARIABLES			DGPS ACCURACY (M)			
	A'	A	B	C	D	M	X	LEG	CENTRAL ANGLE*	ALGO	BASELINE (KM)			
											(KM)	(DEG)	0	100
1							X	—	—	—	0.59	1.08	1.94	2.80
2			X	X		X	X	340	144	PDA	0.59	1.08	2.69	4.67
3			X	X		X	X	340	144	MVA	0.57	0.91	1.46	2.14
4		X			X	X	X	(647)	(108)	PDA	0.59	0.92	1.27	1.60
5		X			X	X	X	(647)	(108)	MVA	0.59	0.92	1.24	1.47
6			X	X		X	X	680	144	PDA	0.59	1.03	2.02	3.17
7			X	X		X	X	680	144	MVA	0.58	0.96	1.49	2.00
8			X	X		X	X	1000	144	PDA	0.59	1.03	1.88	2.76
9			X	X		X	X	1000	144	MVA	0.59	0.98	1.53	1.98
10		X	X	X	X	X	X	340	108	MVA	0.57	0.88	1.20	1.46
11	X		X	X	X	X	X	340	144	MVA	0.59	0.98	1.40	1.93
12		X	X	X	X	X	X	1000	108	MVA	0.58	0.97	1.43	1.73

*Central Angle - Angle between master site (M) and outer sites of network.



GENNET.CDR 4/93

FIGURE B-1. GENERIC DGPS NETWORK

Case 11 considers a less-favorable 5-site network by replacing Site A with Site A'. This case clearly exhibits lower performance than Case 10, although it outperforms the 3-site network Case 3 at the longer baselines.

Finally comparing the 1000 kilometer separation distance 3-site and 5-site network cases, Cases 9 and 12, we observe better performance for the 5-site network at the longer baselines.

Table B-2 summarizes the PDA and MVA weighting coefficients for some of the cases from Table B-1. Any arbitrary set of coefficients could be selected, with the PDA and MVA approaches providing just two examples of the strategies which could be used. When the selected coefficients are used in evaluating the network DGPS error covariance (Table 26), the best strategy can be established. Since the MVA strategy is optimum if the problem is reasonably linear, it will outperform all other strategies.

Examining Table B-2 more closely and comparing the PDA cases to the corresponding MVA cases, we see that the former tend to have larger coefficients, in a root-sum-square sense, than the latter for baselines outside the network. Also, the MVA cases will always assign a non-zero weight to all of the sites in the network, even at a null baseline—corresponding to the case where the user is right next to the Master Station. While the PDA coefficients sum to unity, the MVA coefficients do so only approximately for the cases evaluated.

TABLE B-2. NETWORK WEIGHTING COEFFICIENTS

CASE	BASELINE (KM)	SITES & COEFFICIENTS						COMMENT
		A†	A	B	C	D	M	
1	0-500						1	BASLINE CASE
2	0			0	0		1	PDA, 340 KM LEG
	100			0.500	0.404		0.095	
	300			1.500	1.213		-1.713	
	500			2.500	2.022		-3.524	
3	0			0.053	0.053		0.894	MVA, 340 KM LEG
	100			0.266	0.173		0.561	
	300			0.607	0.341		0.050	
	500			0.842	0.445		-0.287	
8	0			0	0		1	PDA, 1000 KM LEG
	100			0.170	0.138		0.692	
	300			0.510	0.413		0.077	
	500			0.851	0.688		-0.539	
9	0			0.015	0.015		0.970	MVA, 1000 KM LEG
	100			0.107	0.075		0.818	
	300			0.288	0.190		0.522	
	500			0.467	0.301		0.232	
10	0		-0.010	-0.065	0.065	-0.010	0.888	MVA, 340 KM LEG
	100		0.068	0.179	0.095	0.061	0.597	
	300		0.298	0.225	0.060	0.219	0.199	
	500		0.596	0.080	-0.026	0.366	-0.015	